Agnes G. Oomen

Determinants of oral bioavailability of soil-borne contaminants

diffusion
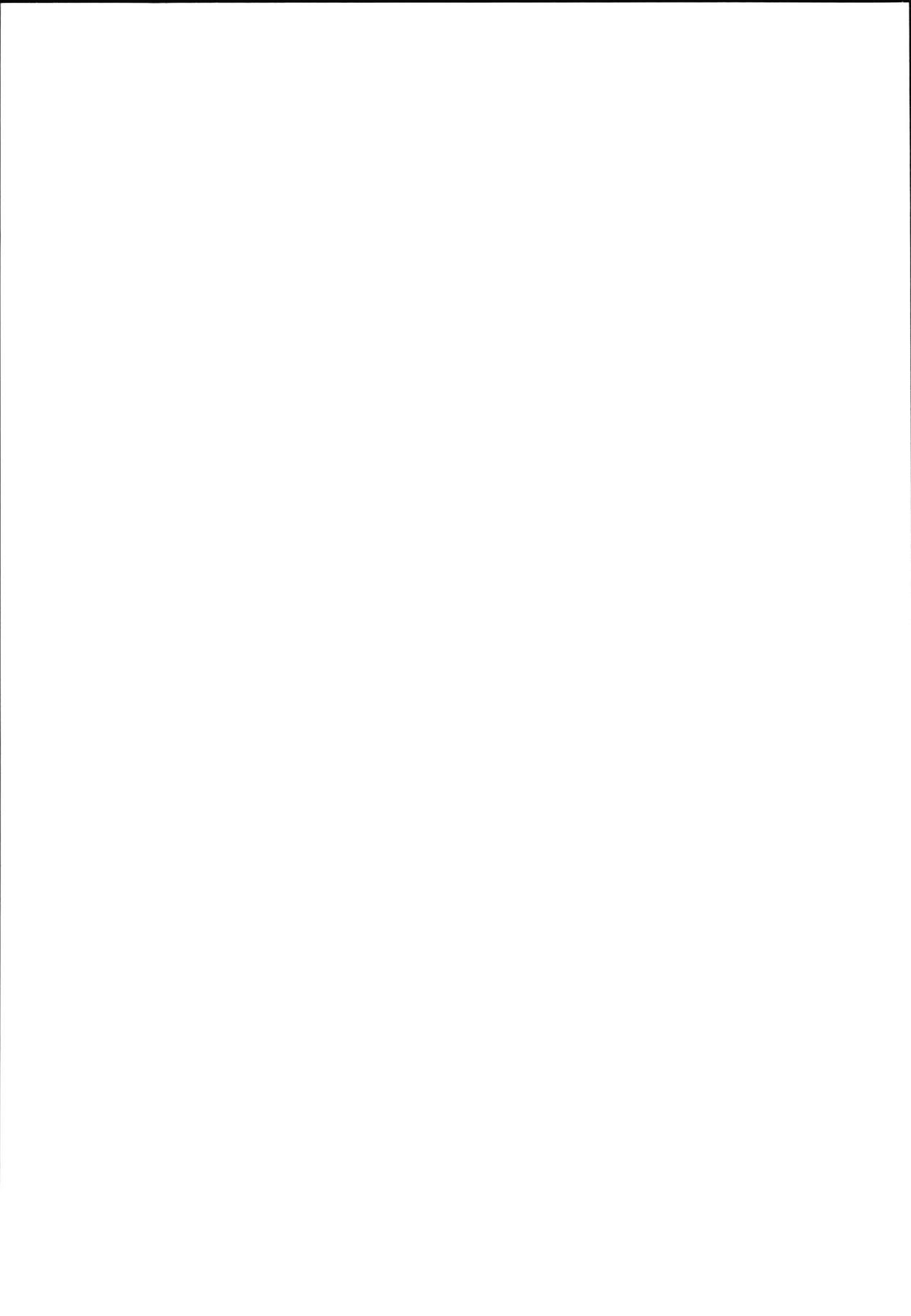
Determinants of oral bioavailability of soil-borne contaminants

Determinanten van orale biobeschikbaarheid van
contaminanten in de bodem

(met een samenvatting in het Nederlands)

Proefschrift

Ter verkrijging van de graad van doctor aan de Universiteit Utrecht
op gezag van de Rector Magnificus Prof. Dr. H.O. Voorma
ingevolge het besluit van het College voor Promoties
in het openbaar te verdedigen op

donderdag 23 november 2000 des namiddags om 12.45 uur

door

Agnes Guadalupe Oomen

geboren op 12 juni 1973 te Valles SLP, Mexico

i

Promotor: Prof. Dr. W. Seinen

Co-promotors: Dr. J.P. Groten
Dr. A.J.A.M. Sips
Dr. J. Tolls

Cover design: Femke Bulten and Agnes Oomen.
Photographer's model: Miriam R. E. Tolls

Voor Gijsbert,
mijn lieve broer.

Abbreviations

BSA	Bovine serum albumine
Caco-2 cells	Type of *in vitro* intestinal cells originating from a colon cancer
DMEM	Dulbecco's modified Eagle's medium
DPASV	Differential pulse anodic stripping voltammetry
FCS	Fetal calf serum
GC-ECD	Gas chromatograph with an electron capture detector
HCH	Hexachlorocyclohexane
γ-HCH	γ-isomer of hexachlorocyclohexane = lindane
HOC	Hydrophobic organic compound
ICP-MS	Inductively coupled plasma/mass spectrometry
ISE	Ion selective electrode
LDH	Lactate dehydrogenase
NEAA	Non essential amino acids
OECD	Organization for Economic Cooperation and Development, Paris
OECD-medium	Artificial soil prepared according to guidelines developed by the OECD
Pb	Lead
PBS	Phosphate buffered saline
PCB	Polychlorinated biphenyls
PDMS	Polydimethylsiloxane, coating material for SPME fiber
SPMD	Semipermeable membrane devices
SPME	Solid phase microextraction
TEER	Transepithelial electric resistance
UWL	Unstirred water layer
VLDL	Very low density lipoproteins

Contents

Chapter 1

Introduction

In human risk assessment, ingestion of soil is considered a major route of exposure to many soil-borne contaminants (*1-6*). For that reason, absorption and toxicity of ingested contaminants have been studied extensively. It appears that less absorption and toxicity in test animals is observed when contaminants are ingested with soil compared to contaminants that are ingested with food or liquid (*7-14*). Furthermore, the chemical form of the ingested contaminant (*13,15-18*), the physicochemical conditions in the gastro-intestinal tract (*18-23*), and the nature of the matrix, i.e. type of soil, food, liquid etc. (*18,24,25*), may affect the amount absorbed and, consequently, toxicity. The conditions in the gastro-intestinal tract can be altered by factors such as the ingestion matrix, time after a meal, malnutrition and diseases.

The differences in absorption and toxicity between the presence and absence of soil during ingestion, and between different soils, show that soil and its characteristics should be taken into account in order to perform accurate risk assessment of soil-borne contaminants. However, it is not feasible to perform *in vivo* studies for each specific soil of a contaminated site. Furthermore, discrepancies between an *in vivo* test animal study and the actual situation in humans can occur since the biochemistry and physiology of the gastro-intestinal tract may be different. Therefore, insight into processes determining oral bioavailability of soil-borne contaminants is required as foundation for a proper approach to estimate the exposure via this route, and to establish critical factors in the exposure to soil-borne contaminants. The objective

of the present thesis is to gain insight into determinants of oral bioavailability of several soil-borne hydrophobic organic compounds (HOCs) and a heavy metal (lead). Oral bioavailability of soil-borne contaminants is defined as the contaminant fraction that reaches the systemic circulation.

This chapter will start with an introduction of the test compounds. Prerequisite for understanding of oral bioavailability of soil-borne contaminants is knowledge on the functioning of the gastro-intestinal tract. Hence, some background information on the physiology of the gastro-intestinal tract is given. Important differences between the fed and the fasted state are mentioned. Extra attention is paid to the anatomy of the small intestine and the possible routes of absorption. In the following section the reader is familiarized with the different processes that can be distinguished for oral bioavailability of soil-borne contaminants. Finally, the scope of this thesis is presented.

Test compounds

Lead (Pb), arsenic (As), polycyclic aromatic hydrocarbons (PAHs), polychlorinated biphenyls (PCBs), and to a lesser extent lindane, are contaminants that are frequently present in soil at levels above the present intervention value. Of this series, lead, PCBs and lindane are chosen as test compounds. In addition, the PCBs and lindane are chosen as they cover a range of hydrophobicity, and more practical, these compounds can be studied simultaneously since the use of gas chromatography with electron capture detector (GC-ECD) allows for specific and sensitive analysis of these compounds. Hence, it is possible to generate data for a broad range of hydrophobicity with a limited number of experiments. Furthermore, an inorganic contaminant, lead, is examined. It is to be expected that organic and inorganic compounds are affected by different factors during digestion and absorption. The different physicochemical properties of the contaminants can be employed to extend our understanding of the processes that dominate oral bioavailability for different chemical classes.

PCBs. PCBs contain two phenyl rings substituted with different numbers of chlorine atoms at various positions, see Figure 1. Hence, 209 different PCB congeners exist that each have specific physicochemical properties, which are determined by their degree and position of chlorination. Their hydrophobicity is represented by the high octanol-water partition coefficient, K_{ow}, which, depending on the congener, ranges between $10^{3.9}$ and $10^{8.3}$ (*26*).

PCBs have been widely used as plasticizer, flame retardant, and as dielectric fluid in transformers and capacitors. PCB production in Europe increased from the latter half of the 1950s, peaked at the end of the 1960s, and ceased by the 1970s after the discovery of the presence of PCBs in all compartments of the environment (*27-29*). Due to their chemical stability, high levels of PCBs are still found all through the environment (*30-34*). Studies in

mammals have shown that these may compounds cause weight loss, reproductive impairment, thymus atrophy, immune disorders, teratogenesis and Ah receptor binding (*35*). Carcinogenic effects have also been shown (*36*). The current Dutch intervention value for the sum of PCBs is 1.0 mg/kg dry matter soil (*37*), which is based on potential risks to humans and ecosystems.

Lindane. Lindane is the γ-isomer of hexachlorocyclohexane, and its structure is presented in Figure 1. Lindane has a K_{ow} of $10^{3.8}$ (*38*), indicating the hydrophobic nature of the compound. Eight isomers of hexachlorocyclohexane exist, but the γ-isomer is the active compound due to its insecticidal activity. It has widely been used in veterinary medicine and as a household, agricultural and gardening pesticide. In the Netherlands lindane is presently almost abolished, with a few exceptions for crop protection. Lindane is degraded rapidly relative to PCBs, both in soil by action of microorganisms (*39,40*), and by the liver of higher organisms (*41-43*). Interconversion to other isomers can take place (*39*). Toxicity exerted by the hexachlorocyclohexane isomers has been related to interference with GABA receptors in the central nervous system (*44*). Lindane may act as a convulsant agent, and may cause both acute and chronic neurotoxic effects (*45-48*). In addition, hepatotoxic (*47,49*) and uterotoxic (*47,50*) effects have been observed. The β-isomer of hexachlorocyclohexane is known for its endocrine activity (*51*), and lindane might also act as an endocrine disrupter (*52*). The current Dutch ecotoxicological and human toxicological intervention value for lindane are 2.0 and 21.1 mg/kg dry matter soil, respectively (*37*).

PCB   **Lindane**
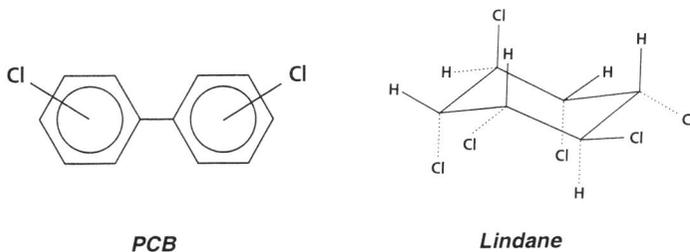
Figure 1. The general structure of PCBs and the structure of lindane.

Lead. Many locations in the Netherlands contain relatively high levels of the heavy metal lead, mostly due to historic input (*53*). Several major sources of lead contamination can be identified, including leaded gasoline, leaded paint, shooting and stationary sources such as mining. Leaded gasoline represents the dominant diffuse source (*54,55*). The alkyl lead addition to gasoline was reduced from the 1970s throughout the 1980s and 1990s, and presently is ongoing in many countries all over the world (*55*). Although the anthropogenic lead emission

is declining, lead is still a high priority hazardous substance. Lead may elicit symptoms of the peripheral and central nervous system (2,56), while also the kidneys and gastro-intestinal tract may be affected (56). Lead is an animal carcinogen, but conclusive evidence for carcinogenesis in humans is lacking (56). In human subjects without obvious clinical signs, nonspecific symptoms such as fatigue, impaired concentration, loss of memory etc. may occur (2,56). Of main concern is mental retardation of children caused by chronic lead exposure (1,2). The current Dutch intervention value based on potential risks to humans and ecosystems is 530 mg/kg dry matter soil (37).

Physiology of gastro-intestinal tract

The gastro-intestinal tract is evolved in order to digest and absorb food, and can be divided into compartments with different functions. In the mouth the food is chewed to smaller pieces and homogenized with saliva, while also the enzyme α-amylase is excreted. This already starts the degradation process of starch. Subsequently, the homogenate is transported through the esophagus to the stomach. Here, it is acidified and enzymatic protein and fat digestion begins due to the action of pepsine and gastric lipase. The food homogenate is stored in the stomach until, depending on the size of the food particles, it is delivered to the small intestine. Bicarbonate secretions, both from the pancreas and from the gall bladder, neutralize the contents. These secretions are addressed in the present thesis as duodenal juice and bile, respectively. The resulting fluid in the small intestine is referred to as chyme. The enzymatic degradation process is continued, while the small intestine is also the site where absorption mainly takes place (23,57,58). Fat absorption is facilitated by accumulation of its degradation products, i.e. fatty acids, glycerol etc, in the interior of mixed micelles. The interface of mixed micelles is formed by bile salts, as these are amphipathic molecules. In this manner, fat is solubilized and its flux towards the intestinal cells is increased (23,58). The small intestine merges into the large intestine. The role of the large intestine is primarily to reabsorb water and to store unabsorbed material, while further degradation of remaining food components can take place due to microbial activity.

The presence of food can markedly alter the physicochemical conditions in the gastro-intestinal tract (22,23,57,59-62). An important difference is that the gastric pH is low for the fasted state and much higher for the fed state, the pH can be as low as 1 and as high as 6 for the respective conditions. Furthermore, the secretions of the gastric juice, duodenal juice and bile increase for the fed state, while the presence of food also delays the gastric emptying. To the contrary, both the human small intestinal pH of 5.5 to 7.5 and the intestinal transit time of about 2 to 5 h are hardly affected by the presence of food (57,59-62).
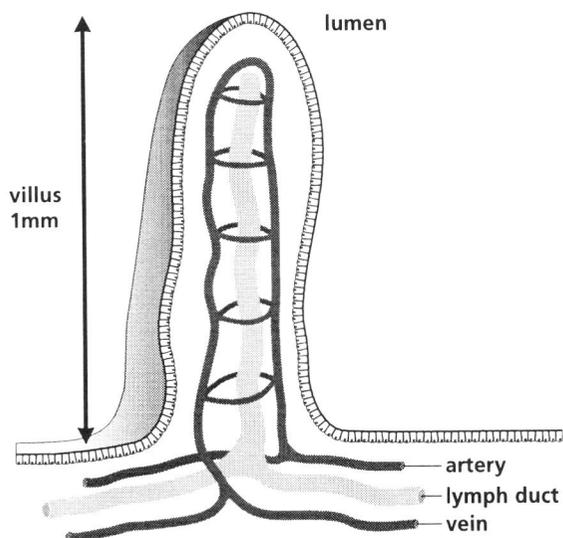
Figure 2. Schematic representation of the organization of an intestinal villus.

Small intestinal anatomy. The small intestine requires some further attention, since absorption occurs mainly here. The small intestinal epithelium is composed of an enormous number of small, fingerlike projections, which are directed into the lumen, see Figure 2. These projections, which are about one millimeter long, are called villi. Inside each villus are blood and lymphatic capillaries. The capillaries provide the routes by which compounds are transported to the rest of the body. The surface of each villus consists of a heterogeneous population of cells, which include enterocytes or absorptive cells, goblet cells, which secrete mucin, endocrine cells and several more cell types.

The enterocyte is the most common cell and is predominantly responsible for intestinal absorption. The luminal membrane of each enterocyte contains microvilli, each about 1 μm long and 0.1 μm in diameter. The microvilli, villi and large ridges in the intestinal tissue called *plicae circularis* attribute to an enormous magnification of the total surface area of the small intestine, of up to 200 m^2 for adults. This large surface area facilitates mass transfer from the intestinal lumen to enterocytes and thereby to the blood and lymph flow.

Intestinal absorption routes. Compounds can be absorbed across the intestinal epithelium either along the cells, i.e. the paracellular route, or through the cells, the transcellular route (*63*), see Figure 3. Transport via the paracellular route is reserved for small hydrophilic molecules only, due to the presence of tight junctions between the cells. Transcellular transport of a molecule can take place by passive diffusion, or by a specific carrier, either active or facilitated. Another possibility is that compounds are absorbed via transcytosis, which means

that a small volume of the intestinal fluid is invaginated by the cell membrane to form an endocytotic vesicle. This route is also referred to as pinocytosis.
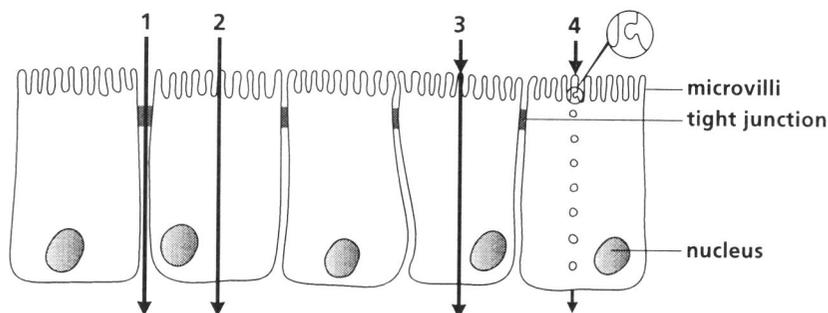
paracellular route 1
transcellular: passive diffusive route 2
    carrier-mediated route 3
    transcytosis route 4

Figure 3. Schematic representation of the transepithelial permeation routes in the intestine.

ORAL BIOAVAILABILITY OF SOIL-BORNE CONTAMINANTS

ingestion	bioaccessibility	absorption	first-pass effect

In the present thesis oral bioavailability is defined as the fraction of an orally administered dose that reaches the systemic circulation. The flow chart describes the different steps of oral bioavailability of soil-borne contaminants. After soil ingestion, contaminants can be partially or totally released from soil during digestion in the gastro-intestinal tract. The fraction of contaminant that is mobilized from soil into chyme is defined as the bioaccessible fraction. This fraction is considered to represent the maximum amount of contaminant available for intestinal absorption. Bioaccessible contaminants can subsequently be absorbed, i.e. transported across the intestinal wall, and transferred into the blood or lymph stream. The compounds may be biotransformed and excreted in the intestinal epithelium or liver. This is referred to as first-pass effect. After these steps, the contaminants reach the systemic circulation and thereby the rest of the body, and may exert system toxicity. Consequently, oral bioavailability of soil-borne contaminants is the resultant of the four steps of the flow chart: soil ingestion, bioaccessibility, absorption, and first-pass effect.

The different steps of exposure to soil-borne contaminants are discussed in more detail below.

Soil ingestion

| ingestion | → | bioaccessibility | → | absorption | → | first-pass effect |
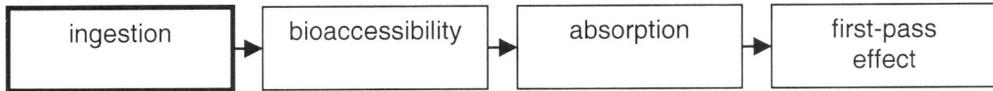
Obviously, the amount of soil that is ingested largely determines the exposure to soil-borne contaminants. Both children and adults ingest soil via food. Sheppard and Evenden estimated the soil loads for leafy tissues after normal washing at 20 mg soil/kg dry weight, and for fruits at 2 mg soil/kg dry weight (*64*). Furthermore, soil is also ingested via hand-to-mouth behavior. Thereby, soil and dust particles that stick to an object or fingers are put into the mouth and are ingested. This is of special importance for children as they typically play outside and display hand-to-mouth behavior (*65*). Several studies have been performed to estimate the amount of soil that is ingested by children. These studies indicate that, in general, between 50 and 200 mg soil per day is ingested (*66-70*). Besides this normal hand-to-mouth behavior, some children deliberately ingest soil. Via this so-called pica behavior ingestion of several grams of soil on a single day, up to 60 g, has been observed (*67,70,71*).

For risk assessment purposes, the Dutch "National Institute of Public Health and the Environment" assumes that the daily intake of soil is 150 mg for children and 50 mg for adults (*1*). Other countries use similar values (*1*). For example, the U.S. Environmental Protection Agency (U.S. EPA) has assumed that 95 percent of children ingest 200 mg of soil per day or less, references in (*1,67,71*).

Bioaccessibility

| ingestion | → | bioaccessibility | → | absorption | → | first-pass effect |
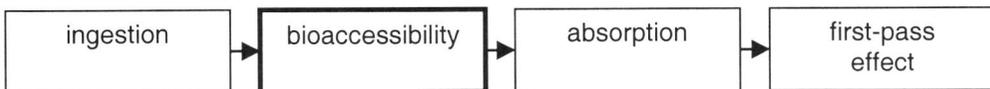
After soil ingestion, contaminants can be mobilized from soil during digestion. This bioaccessible fraction of soil-borne contaminants is considered the fraction that is at maximum available for intestinal absorption. Different factors can affect bioaccessibility. For example, the bioaccessibility of metals and ionizable contaminants (acids and bases) from soil is expected to be highly dependent on the pH values in the different compartments of the gastro-intestinal tract (*22,72,73*).

Another factor that may affect bioaccessibility is the presence of food, which increases the transit time of the stomach. Therefore, the period in which mobilization can take place is increased, which may be important for compounds for which dissolution is rate limiting (*23*). Also an increased solubilizing capacity of the digestive mixture, due to an increased flow of the digestive juices or to the presence of food particles, may cause an increase in the mobilization of contaminants from soil (*22,23*). Especially bile is known to increase the solubilizing capacity for poorly water-soluble compounds, as bile salts form micelles that have an apolar interior (*22,23*). Furthermore, since bile salts have surfactant properties, they may increase the wetting and thereby the rate of mobilization from soil (*22,23*).

Absorption

ingestion		bioaccessibility		absorption		first-pass effect

It is generally accepted that at least the freely dissolved form is available for transport across a biological membrane (*74-77*), which is the case for the transcellular intestinal permeation route. Therefore, the freely dissolved contaminant concentration seems to be an important determinant for absorption. Besides this freely dissolved form, contaminants are present in the small intestine in other physicochemical forms. The distribution of compounds among different physicochemical species is referred to as speciation. The physicochemical properties of each form determine, together with properties of the intestinal cells, whether and to what extent a form can be absorbed. As precipitation and complexation reactions in the small intestine determine the contaminant speciation, they may affect absorption and oral bioavailability. Also, the flows of digestive juices determine the concentration of sorbing constituents and thereby influence the speciation, which in turn may change the absorption.

Extremely hydrophobic compounds such as PCBs are assumed to join the pathway for lipid transport. In line with fatty acid absorption, HOCs may accumulate in bile salt micelles, which can act as a transport vehicle towards the intestinal membrane. After dissociation from or degradation of the micelles, the PCBs probably traverse the luminal membrane by passive diffusion. The mechanism of HOC transport across the cells is not fully known, but this process is probably also comparable to the lipid pathway. Lipids are transported through the cells via very low density lipoproteins (*78,79*), and subsequently enter the lymph flow. Also highly hydrophobic compounds such as PCBs are almost exclusively transported to the lymph (*23,78-80*). As lipid assimilation is enhanced in the presence of food in the gastro-intestinal tract, transport of compounds following the lipid pathway may also be enhanced. Lindane can either follow the same route as the PCBs or cross the intestinal cells by passive diffusion only.

The exact mechanisms of absorption for lead are unknown and may follow the calcium pathway (*18,81-84*). Lead absorption is assumed to involve active and passive transport, both via the transcellular and paracellular permeation route (*18,82*). Transcellular metal uptake may first involve a binding step to the luminal membrane followed by internalization into the cell (*82,85-88*). Lead is mainly transported to the blood flow (*80,82*). Children are known to absorb more lead than adults do (*2,82,89*). Children have higher calcium absorption efficiencies than adults, which is induced by their elevated calcium demands for bone formation (*90*). Probably, for this reason is the efficiency of lead absorption higher for children than for adults.

It should be noted that the properties of the gastro-intestinal tract and the constituents that are present during digestion can affect both bioaccessibility and absorption.

First-pass effect

ingestion	→	bioaccessibility	→	absorption	→	first-pass effect
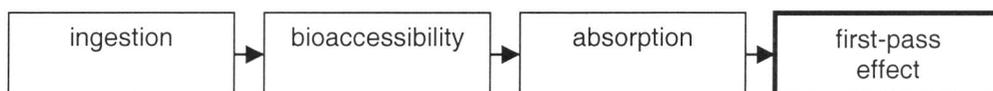
After absorption, the contaminants may be biotransformed and excreted by enzymes such as the cytochrome P-450s and P-glycoprotein pump in the intestinal cells (*91-94*). Contaminants that are transported from the intestine via the portal vein to the liver may be extracted and excreted into bile, or biotransformed by the liver, before the systemic circulation is reached. Consequently, less than the absorbed fraction of contaminants may pass the liver unchanged. This phenomenon of removing chemicals after oral absorption and before entering the systemic circulation is referred to as first-pass effect (*95*).

Lindane can be biotransformed in the liver (*41-43*). Lead is not biotransformed, but may undergo some biliary secretion (*18,96*). PCBs can be excreted into the bile and are biotransformed to a small extent (*95*). However, most absorbed PCBs circumvent first-pass liver metabolism and excretion, since they almost completely enter the lymph flow (*78,97*), which joins the systemic circulation without first being transported towards the liver.

SCOPE OF THIS THESIS

The objective of the present thesis is to gain insight into determinants of oral bioavailability of soil-borne PCBs, lindane and lead for children. Children are the group at risk as they are exposed to higher contaminant doses than adults, especially in relation to body weight. Furthermore, children may display increased oral bioavailability due to their high demand of

specific compounds, and they may also be more vulnerable to contaminants as vital organs are growing.

We consider soil ingestion as a given fact, and first-pass effect is not relevant or has been studied extensively for the presently used contaminants. Therefore, we will focus on several aspects of the second and the third step of the flow chart, bioaccessibility and absorption.

ingestion	→	bioaccessibility	→	absorption	→	first-pass effect
		Chapter 2: HOCs		Chapter 4: HOCs		
		Chapter 5: lead		Chapter 6: lead		
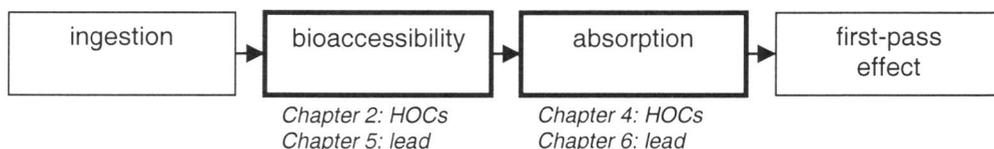
In the present thesis, we aimed at employing reproducible methods and conditions in order to investigate mechanistic aspects of oral bioavailability of soil-borne contaminants. To that end, artificial soil, i.e. OECD-medium (98), was used to obtain comparable ingestion conditions. Furthermore, *in vitro* models were employed to obtain reproducible digestion and absorption conditions that also allow for specific variations. An *in vitro* digestion model based on the physiology of children simulated gastro-intestinal digestion. This model was applied to investigate the bioaccessibility of the soil-borne contaminants. Subsequently, *in vitro* differentiated intestinal cells were employed to mimic intestinal absorption. This model was employed to investigate the absorption of bioaccessible contaminants, and to explore the effects of the different physicochemical forms on the intestinal absorption.

The research approach to investigate several aspects of oral bioavailability of the soil-borne HOCs and lead was similar. Therefore, the present thesis consists of two parallel research lines. *Chapter 2, 3* and *4* apply for the HOCs, *Chapter 5* and *6* apply for lead.

PCBs and lindane

In *Chapter 2*, mobilization of PCBs and lindane from an artificial standard soil, i.e. OECD-medium, during *in vitro* digestion is investigated. Furthermore, the effect of bile, digestive proteins and OECD-medium on the bioaccessibility is examined. A partitioning based model was developed and employed in order to estimate the distribution of the PCBs and lindane among bile salt micelles, proteins and OECD-medium. The impact of these constituents on the bioaccessibility of PCBs and lindane is discussed.

Non-equilibrium solid-phase microextraction (SPME) is applied in *Chapter 3* to artificial chyme in order to estimate the freely dissolved concentration of PCBs and lindane. The contribution of PCBs sorbed to digestive proteins to the accumulation into this passive

chemical sampling phase is discussed. The SPME fiber is a passive sampling phase for HOCs in chyme. The HOC accumulation into the SPME fiber can be compared to the active and biological HOC uptake by small intestinal cells from a chyme solution.

Chapter 4 describes the uptake of the PCBs and lindane into *in vitro* intestinal Caco-2 cells. The Caco-2 cells are exposed to HOCs in different apical exposure media to different concentrations of HOCs. In this way, the absorption by intestinal cells of the HOCs that are mobilized from the OECD-medium during artificial digestion is investigated.

Lead

In *Chapter 5*, the mobilization of lead from OECD-medium during artificial digestion is investigated. Furthermore, the fraction of the free metal ion, Pb^{2+}, is estimated. Main physicochemical forms of lead in chyme are determined and their dissociation and association kinetics are investigated and commented.

Chapter 6 describes the lead accumulation into and transport across a monolayer of *in vitro* intestinal Caco-2 cells. These results are related to lead speciation in the chyme solution and to human *in vivo* lead absorption. The contribution of different lead forms to lead absorption is considered.

General discussion

In *Chapter 7*, contaminant bioaccessibility, accumulation into a passive sampler and the intestinal cells, and transport across the cell monolayer, are interpreted in the perspective of mass transfer processes. With use of this interpretation the main factors that determine oral bioavailability of soil-borne PCBs, lindane and lead are discussed. Also, the effect of the physiological status on the oral bioavailability is considered. The differences and similarities between the different contaminants are commented and implications for exposure assessment for soil ingestion with these compounds are given.

Chapter 2

Mobilization of PCBs and lindane from soil during *in vitro* digestion and their distribution among bile salt micelles and proteins of human digestive fluid and the soil

Agnes G. Oomen, Adrienne J.A.M. Sips, John P. Groten, Dick T.H.M. Sijm, Johannes Tolls

Abstract

Children can take up contaminated soil via hand-to-mouth behavior. The contaminants can be mobilized from the soil by digestive juices and thus become available for intestinal absorption (i.e. become bioaccessible). In the present study components of an *in vitro* digestion model were varied to study their effect on the mobilization of several PCBs and lindane from surrogate soil (OECD-medium). Approximately 35% of the PCBs and 57% of lindane were bioaccessible after a default digestion. Since the mobilization was independent of the spiking level, a partitioning-based model could describe the distribution of the test compounds. Fitting the data to the model yielded a ratio of partitioning coefficients that indicated that approximately 60% of the PCBs were sorbed to the OECD-medium, 25% to bile salt micelles and 15% to proteins. The respective values for lindane were 40%, 23% and 32%. The relatively large fraction of the mobilized compounds that was sorbed to bile salt micelles indicates that micelles play a central role in making hydrophobic compounds bioaccessible. The distribution model is suitable for explaining the results reported in several literature studies and can be used to extrapolate the physiological parameters for the worst case situation and trends in the bioaccessible fraction.

INTRODUCTION

Children ingest on average 50-200 mg soil/day via hand-to-mouth behavior, although amounts of as much as 25-60 g/day have also been described (*66,67,69*). Hence, for children ingestion of soil can be a significant route of exposure to soil-borne contaminants such as hydrophobic organic compounds (HOCs). To assess the health risk of this exposure route, one needs to know the fraction of the HOCs that is absorbed from the gastro-intestinal tract. In addition, it is necessary to know the effect on the intestinal absorption of physiological factors and of the matrix in which the HOCs are ingested. At present, such factors are not taken into account for risk assessment of contaminated soils (*5,99*). However, the fraction of the contaminants which is accessible for absorption, and thus the actual intestinal absorption of the contaminants, may vary according to the type of matrix (i.e. soil, food, liquids) and the nature of the matrix (type of soil, food, liquid). For example, in rats intestinal absorption of PCBs administered via spiked soil has been shown to be lower than for PCBs ingested via corn oil (*9*), in which case the test compounds were almost completely absorbed (*9,100*). This indicates that the matrix in which the HOCs are ingested indeed influences the intestinal absorption. Other studies confirm that the toxicity exerted by several HOCs is lower when the test compounds are ingested in soil compared to ingestion in an oily matrix (*7,8,101*).

Digestion of food or other material starts in the mouth. It is continued in the stomach and the small and large intestines. Absorption takes place mainly in the small intestine (*58,102*). The digestive fluid in the small intestine is referred to as chyme. Leaving food particles aside, soil particles, bile and proteins in the chyme are assumed to sorb HOCs. Pinocytosis of soil particles in the gastro-intestinal tract is supposed to be negligible (*103-105*). Therefore, the fraction of HOCs that is sorbed to soil is considered to be unavailable for absorption. Bile salts form mixed micelles with fatty acids and compounds such as lecithin (*23*). HOCs can be incorporated into the apolar interior of these micelles (*23,58,102*). For fatty acids and HOCs, the bile salt micelles act as a transport vehicle that is able to traverse the unstirred water layer adjacent to the intestinal wall (*23,58,102*). Proteins are hydrolyzed and subsequently absorbed in the gastro-intestinal tract. Although a compound is generally absorbed in the freely dissolved form, it seems likely that HOCs sorbed to micelles and proteins are available for absorption after digestive degradation and disintegration. This fraction that is mobilized from the soil during the digestion, and that is considered to be available for absorption, is defined as the bioaccessible fraction.

In the present study, bioaccessibility of HOCs is studied using an *in vitro* digestion model. The model is based on synthetic saliva, gastric juice and intestinal juices and imitates human physiological pH-values, components and transit times for fasting conditions. Spiked OECD-

medium was used as surrogate soil. The digestion model can be manipulated and it is thus possible to investigate the effect of the composition of chyme and the amount of soil on the bioaccessibility of HOCs. A mathematical model describing the distribution of HOCs among sorbing components is developed and used to analyze and interpret the experimental results.

The aims of the present study are 1) to measure the fractions of several PCBs and lindane which are mobilized from OECD-medium, i.e. the bioaccessible fractions, 2) to determine the distribution of the HOCs among constituents of chyme and soil, 3) to distinguish components which are relevant for making the HOCs bioaccessible, and 4) to provide a tool to extrapolate trends, and the magnitude of the trend, in the bioaccessible fraction for other situations.

MATERIAL & METHODS

Chemicals

PCB congeners 2,2',5,5'-tetrachlorobiphenyl (IUPAC PCB #52), 2,3',4,4',5-pentachlorobiphenyl (IUPAC PCB #118), 2,2',4,4',5,5'-hexachlorobiphenyl (IUPAC PCB #153), 2,2',3,4,4',5,5'-heptachlorobiphenyl (IUPAC PCB #180) and lindane (γ-HCH) were used as test compounds. The logarithms of their octanol-water partition coefficients, log K_{ow}, are 6.1, 6.2-6.5, 6.9, 7.2 and 3.8, respectively (26,38). The internal standards for the PCBs and lindane were 2,2',4,4',6,6'-hexachlorobiphenyl (IUPAC PCB #155) and α-hexachlorocyclohexane (α-HCH), respectively. All chemicals were of analytical grade.

Dry OECD-medium consisting of 10% peat, 20% kaolin clay and 70% sand was prepared according to OECD-guideline 207 (98). The appropriate amounts of PCBs dissolved in hexane were added to dry, uncontaminated OECD-medium. The hexane was evaporated under continuous shaking. To prevent losses of lindane during spiking, lindane was added to the OECD-medium as an aqueous solution that was prepared using the generator column technique (106). Generally, the OECD-medium was spiked with a mixture of 7 mg PCB #52, 7 mg PCB #118, 14 mg PCB #153, 7 mg PCB #180 and 2 mg lindane per kg dry OECD-medium. The concentration of lindane of 2 mg/kg represents the current Dutch intervention value (37). PCB #153 is environmentally abundant. Therefore, its level was chosen higher than that of the other PCBs. The spiking levels of the PCBs are of environmental relevance (107), although relatively high in the perspective of the current Dutch intervention value of 1 mg PCB/kg dry soil (37). The final water content of the OECD-medium was measured by drying an aliquot of the OECD-medium for 24 h in an oven at 110 °C, and was approximately 50%. OECD-medium was freshly spiked for each series of experiments to prevent aging effects (108). The OECD-medium was left to equilibrate for two weeks at room temperature prior to digestion.
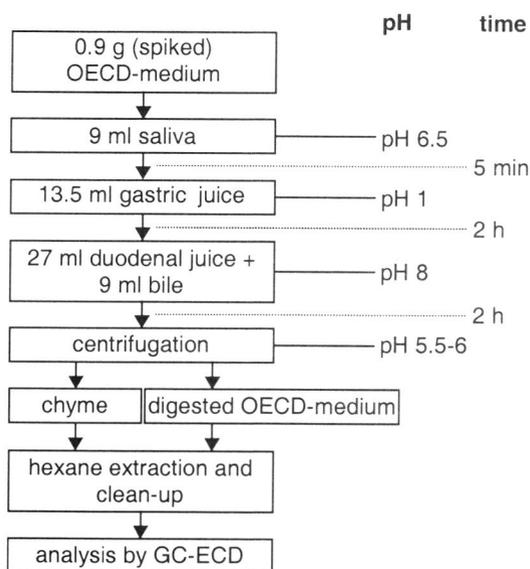
Figure 1. Schematic representation of the procedure of an artificial digestion and the subsequent sample treatment.

Digestion experiments

The physiologically based *in vitro* digestion model designed by Rotard *et al.* (*104*) was employed in this study in a modified version as described by Sips *et al.* (*109,110*). The essential differences from Rotard *et al.* were 1) the volume and the ratio of digestion juices were based on the daily human production, 2) more physiological transit times were applied and 3) the gastric pH was set to 1 to imitate fasting conditions. The digestion process is schematically presented in Figure 1. In short, synthetic saliva, gastric juice, duodenal juice and bile were prepared. Saliva was added to 0.9 gram of spiked OECD-medium and rotated at 60 rpm for 5 minutes at 37 °C. Subsequently, the gastric juice was added and the mixture was rotated at 60 rpm for 2 hours. In the last digestion step duodenal juice and bile were added and this mixture was rotated at 60 rpm for 2 more hours. Finally, the suspension was centrifuged for 5 minutes at 3000*g*, yielding a pellet (i.e. the digested OECD-medium) and 58.5 ml of supernatant (i.e. the artificial chyme), containing the proteins and bile. Important constituents of an artificial digestion were freeze-dried chicken bile, bovine serum albumin (BSA), mucine, pancreatine, pepsin and urea. After a default digestion, i.e. normal concentrations of chyme constituents and OECD-medium, 0.9 g/l bile, 15.4 g/l OECD-medium and 3.7 g/l protein were present in the system. The ionic strength of the chyme was 0.14 M and the pH was 5.5 (±0.2).

Table 1. Set-up for the experiments in which the spiking level of the OECD-medium and the additions of bile, protein and OECD-medium to an artificial digestion, were varied. When one factor was varied, the default amounts were used for the other factors. For each combination of components 4 or 5 artificial digestions were performed in separate tubes.

Experiment	Variation
Contamination level OECD-medium	The OECD-medium that was added to a digestion was spiked 0.5, 1, 3 or 5 times the default level of 2 mg lindane, 7 mg PCB #52, 7 mg PCB #118, 14 mg PCB #153 and 7 mg PCB #180 per kg dry OECD-medium.
Bile	The amount of bile added to a digestion was 0, 1, 2 or 4 times the default level. The concentration of bile after a default digestion was 0.9 g/l.
OECD-medium	The amount of OECD-medium added to a digestion was 0.5, 1, 2 or 4 times the default level of 0.9 gram per digestion. The contamination level of the OECD-medium was varied simultaneously, respectively to 2, 1, 0.5, 0.25 times the default level. Therefore, the same amounts of test compounds were present in every digestion in this experiment.
Protein	The amount of protein added to a digestion was 0, 0.25, 0.5, 1, 1.5 times the default level. The concentration of protein after a default digestion was 3.7 g/l.

Variations in the artificial digestion

In four series of experiments, the amounts of test compounds spiked to the OECD-medium and the amounts of bile, of protein and of OECD-medium added during the digestion were varied according to Table 1. After each digestion the concentrations of the HOCs in the digested OECD-medium and in the chyme were measured. The spiking level of the OECD-medium was varied in order to investigate the linearity of the distribution of the PCBs and lindane over the digested OECD-medium and the chyme. The bile, protein and OECD-medium were varied in order to determine the distribution of the HOCs among these components.

Since the addition of bile, OECD-medium or protein was varied in the artificial digestions, also the volume of each component was varied. The variation in the amounts of the components was expressed relative to their default amount that was added to a digestion. One of the components was varied, whereas the default amounts of the others were used. To obtain a complete mass balance (i.e. the summed amount of the test compounds sorbed to protein, to bile salt micelles, to OECD-medium and the freely dissolved amount is 100%) protein represents all constituents of an artificial digestion, excluding bile, OECD-medium and inorganic salts. This is referred to as protein since this is the main sorbing constituent. Four or five digestions in separate tubes were performed for each combination of bile, OECD-medium and protein. The replicates were used to determine standard deviations.

Analytical procedure

Approximately 25 ml of hexane were added to 35 ml chyme or to the digested OECD-medium, which was resuspended in 35 ml of water. All samples were reflux extracted after addition of internal standards, which were used to correct for losses of the PCBs and lindane during clean-up. In chyme samples a white protein layer between the water and the hexane layer disturbed phase separation. Addition of a few drops of methanol destabilized the white protein layer upon centrifugation (*103*). The hexane phase was collected and concentrated to 10 ml under a gentle nitrogen stream. Subsequently, the samples were analyzed by GC-ECD.

Mass balance

A new batch of spiked OECD-medium was prepared for each series of experiments. Therefore, the total amount of test compounds in each series of experiments was slightly different. The mass balance was calculated by summing up the amounts of test compounds measured in the digested OECD-medium (i.e. the pellet) and the chyme (i.e. the supernatant). These summed amounts were compared to the amounts of test compounds that were present in the spiked OECD-medium before digestion.

Bioaccessible fraction

The bioaccessible HOC-fractions were determined as the fractions, which were mobilized from the OECD-medium into the chyme during the *in vitro* digestion. The bioaccessible fractions were quantified by the partition coefficient, $K_{OECD-ch}$ (l/kg dry matter), which is the concentration of a test compound in the digested OECD-medium (mg/kg dry matter) divided by its concentration in the chyme (mg/l).
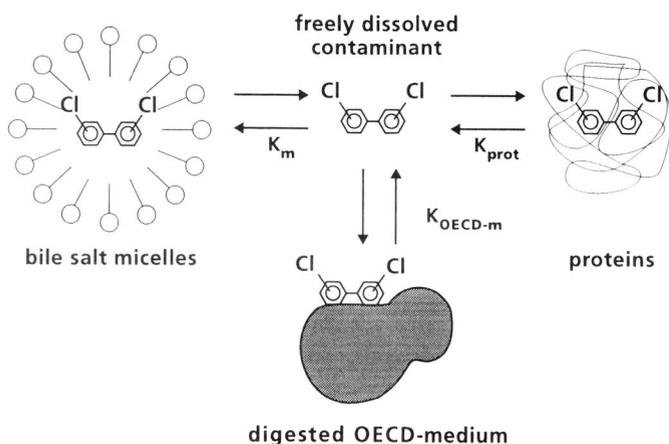
Figure 2. Schematic representation of the distribution of HOCs among bile salt micelles, proteins and OECD-medium, and the partition coefficients describing the equilibria between the freely dissolved HOCs and the sorbed compounds.

Distribution among bile salt micelles, proteins and OECD-medium

Partition coefficients are defined as the concentrations of test compounds sorbed to bile salt micelles (K_m), to digested OECD-medium (K_{OECD-m}) or to protein (K_{prot}) divided by the concentration of the freely dissolved test compounds in the chyme. In Figure 2 these partitioning coefficients are depicted schematically. A partition coefficient K_i, which can be K_m, K_{OECD-m} or K_{prot}, is defined as:

$$K_i = \frac{C_i}{C_{free}} = \frac{n_i/V_i}{n_{free}/V_{ch}} \tag{2.1}$$

"C", "n" and "V" denote concentration (mg/l), amount (mg) and volume (l), respectively. The subscript "free" stands for freely dissolved and "ch" for chyme. The subscript "i" represents any component. The different components are indicated with "prot" for protein, "m" for bile salt micelles, or "OECD-m" for digested OECD-medium. Eq 2.1 can be rewritten as:

$$n_i = \frac{K_i \times n_{free} \times V_i}{V_{ch}} \tag{2.2}$$

The amounts of a compound in the chyme, n_{ch} (mg), and in the digested OECD-medium, n_{OECD-m} (mg), can be described by:

$$n_{ch} = n_{free} + n_m + n_{prot} = n_{free} \times \left(1 + \frac{K_m \times V_m}{V_{ch}} + \frac{K_{prot} \times V_{prot}}{V_{ch}}\right) \tag{2.3}$$

$$n_{OECD-m} = n_{free} \times \frac{K_{OECD-m} \times V_{OECD-m}}{V_{ch}} \tag{2.4}$$

The absolute micellar volume and the absolute protein volume, V_m and V_{prot}, are unknown. We therefore normalize the volumes of the bile salt micelles, proteins and OECD-medium to the volume they have after a default digestion. Thus, the normalized volumes, which are denoted by the superscript "0", have a value of "1" after a default digestion. In the present calculation a linear relation is assumed between the amounts of bile, protein or OECD-medium added to the digestion and the volume of the component. We introduce f_i, the factor by which the amounts of bile, protein or OECD-medium are varied. When normalized values are used, the partition coefficients are also normalized to default digestion conditions, which are consequently referred to as K^0_i. Therefore, n_{ch} divided by n_{OECD-m} is:

$$\frac{n_{ch}}{n_{OECD-m}} = \frac{V_{ch} + \left(f_m \times K^0_m \times V^0_m\right) + \left(f_{prot} \times K^0_{prot} \times V^0_{prot}\right)}{f_{OECD-m} \times K^0_{OECD-m} \times V^0_{OECD-m}} \tag{2.5}$$

According to eq 2.5, a graph with $n_{ch}/n_{OECD\text{-}m}$ versus f_m, f_{prot} or $1/f_{OECD\text{-}m}$ should yield a straight line. This was checked by linear regression. Since n_{ch} and $n_{OECD\text{-}m}$ were measured with varying f_m, f_{prot} or $f_{OECD\text{-}m}$, V_{ch} is known and the normalized V^0_i-values are "1", the only unknowns in eq 2.5 are K^0_m, K^0_{prot} and $K^0_{OECD\text{-}m}$. The ratio of these K^0-values was fitted into the spreadsheet Microsoft Excel® using the solver routine. The fitting was performed by minimizing the squared sum of the difference between the experimentally obtained $n_{ch}/n_{OECD\text{-}m}$-value, and the $n_{ch}/n_{OECD\text{-}m}$-value according to eq 2.5. The ratio of K^0-values is a measure of the relative affinity of the HOCs for the bile salt micelles, proteins and OECD-medium.

The fraction that was sorbed to a component was calculated as the amount sorbed to that component, n_i, divided by the total amount of the compound brought into the system, n_{tot}:

$$\frac{n_i}{n_{tot}} = \frac{n_i}{n_{free} + n_m + n_{prot} + n_{OECD\text{-}m}} \tag{2.6}$$

Solid phase microextraction (SPME) measurements showed that the freely dissolved amount of the PCBs in chyme, n_{free}, was less than 1% of n_{tot} (*111*). Therefore, n_{free} can be neglected in eq 2.6. Upon inserting eq 2.2 into eq 2.6 an equation is obtained that expresses the percentage of a compound that is sorbed to a component:

$$\frac{n_i}{n_{tot}} \times 100\% = \frac{f_i \times K^0_i \times V^0_i \times 100\%}{f_m \times K^0_m \times V^0_m + f_{prot} \times K^0_{prot} \times V^0_{prot} + f_{OECD-m} \times K^0_{OECD\text{-}m} \times V^0_{OECD\text{-}m}} \tag{2.7}$$

For lindane n_{free} is between 0% and 10% of n_{tot} (*111*). Therefore, the K^0_i-values are determined for $n_{free}=0$ and $n_{free}=0.1\times(n_m+n_{prot}+n_{OECD\text{-}m})$. The latter case can be approximated as:

$$n_{free} = \frac{0.1 \times n_{free}}{V_{ch}} \times \left(f_m \times K^0_m \times V^0_m + f_{prot} \times K^0_{prot} \times V^0_{prot} + f_{OECD-m} \times K^0_{OECD\text{-}m} \times V^0_{OECD\text{-}m} \right) \tag{2.8}$$

which can be inserted into eq 2.6, divided by n_{free} and multiplied by V_{ch}.

The averages and the matching standard deviations of the percentages sorbed to bile salt micelles, protein and OECD-medium were determined from the three series of experiments in which f_m, f_{prot} and $f_{OECD\text{-}m}$ were varied.

RESULTS AND DISCUSSION

Mass Balance

On average 103% (standard deviation 16%) of the test compounds were recovered, indicating that no significant losses of compounds occurred during the artificial digestion and sample preparation. This is a prerequisite for the use of the mass-balance-based description of the test compounds in the *in vitro* digestion system.

Table 2. Percentages of the test compounds that were bioaccessible (± standard deviation) after a default digestion.

| Compound	% bioaccessible (± SD)
lindane	57 (± 5)
PCB #52	34 (± 10)
PCB #118	30 (± 7)
PCB #153	40 (± 7)
PCB #180	40 (± 9)

Partitioning-based model

As is shown in Table 2, 30-40% of the PCBs, and 57% of lindane were bioaccessible. The calculation includes all samples of default composition and the samples, in which the spiking level of OECD-medium was varied.

Figure 3a presents the mobilization of PCB #153 into chyme and the amount of PCB #153 in digested OECD-medium after the *in vitro* digestion at four different spiking levels of the OECD-medium. Similar curves were obtained for the other test compounds. In the remainder of this paper only data of PCB #153 are shown in graphs because this PCB congener is representative for all test compounds. The linear relationship between the concentrations of PCB #153 in the chyme and the digested OECD-medium is shown in Figure 3b. The slope of the regression yields the partition coefficients, the $K_{OECD-ch}$-values of 64, 83, 90, 107 and 48 l/kg dry OECD-medium for PCB #52, PCB #118, PCB #153, PCB #180 and lindane, respectively. The r^2-values of these regressions are between 0.96 and 1.00, and the intercepts are close to zero.

This concentration-independent mobilization from the OECD-medium into the chyme suggests that the sorbing components are unlikely to be saturated with HOCs. Therefore, describing the distribution of the test compounds among the different constituents of chyme and the OECD-medium with a partitioning-based model is justified.
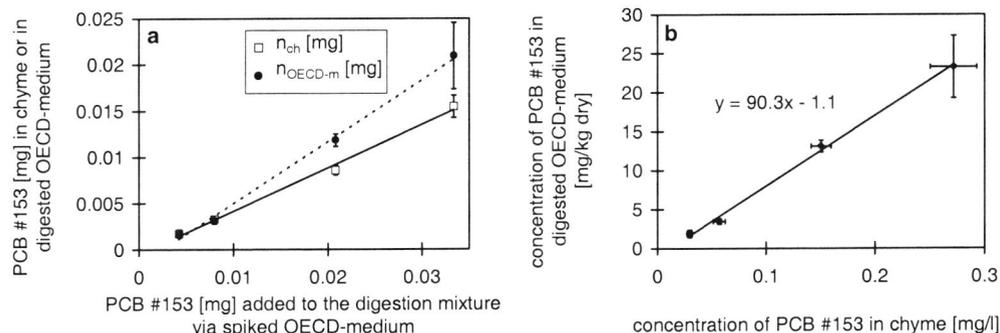
Figure 3. a) The amount of PCB #153 in chyme and in digested OECD-medium after *in vitro* digestions with OECD-medium that was spiked at four levels. b) The concentration of PCB #153 in the chyme versus the concentration in the digested OECD-medium, after *in vitro* digestions with OECD-medium that was spiked at four levels. The value of $K_{OECD-ch}$ is the slope of the line. The error bars represent 4 artificial digestions performed in separate tubes.

Variations in the artificial digestion

Figure 4a shows that the amount of PCB #153 in the chyme increased as increasing amounts of bile were added during an artificial digestion, whereas the amount of PCB #153 left in the digested OECD-medium decreased. A similar pattern was observed with increasing amounts of protein, see Figure 4c. In contrast, when the amount of spiked OECD-medium that was added at the start of the artificial digestion was increased, the amount of PCB #153 in the chyme decreased and the amount of the test compound left in the digested OECD-medium increased, see Figure 4b. Thus, the mobilization from OECD-medium is highly dependent on the composition of the chyme and the amount of OECD-medium added. As can be seen in Figure 4, the increase in f_{OECD-m} resulted in a strongly decreasing bioaccessibility whereas the increase in bioaccessibility with increasing f_m and f_{prot} was less pronounced.

Fitting results

To quantify the influence of the individual components, the data were fitted to the mathematical, partitioning-based model. Linear regression of n_{ch}/n_{OECD-m} versus f_m, f_{prot} or $1/f_{OECD-m}$ within one series of experiments yielded r^2-values of 0.95 (±0.05), indicating that the model is suitable for describing the data. The ratios of the K^0_i-values, which were determined by fitting, are presented in Table 3. The ratio of $K^0_m:K^0_{prot}:K^0_{OECD-m}$ for the PCBs is approximately 0.4 : 0.2 : 1. The corresponding ratio for lindane is 0.7 : 0.6 : 1. This ratio shows the relative affinity of the test compounds for the different components. The largest K^0-value is thus K^0_{OECD-m}. The K^0_m-value is the second largest. The K^0_{prot}-value is almost equal to the K^0_m-value for lindane and about half the K^0_m-value for the PCBs.

22
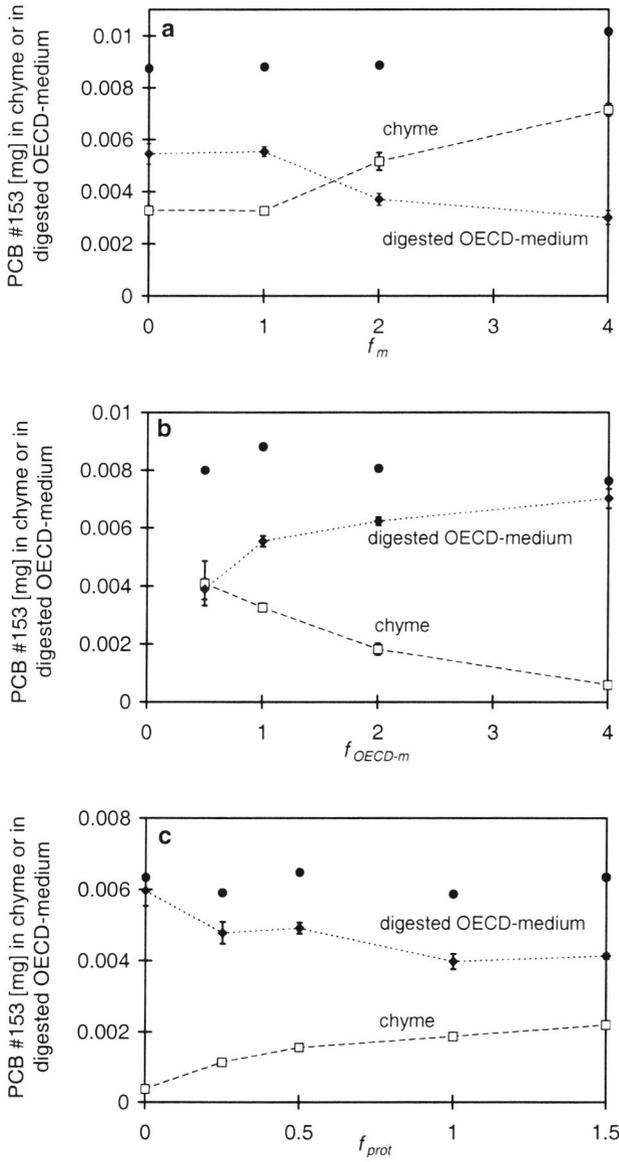
Figure 4. Effect of the variation of the amount of bile (a), OECD-medium (b) and protein (c) added to an artificial digestion on the distribution of PCB #153 over the chyme and the digested OECD-medium. The f_m, f_{OECD-m} and f_{prot} represent the factors, by which respectively the default amount of bile, OECD-medium and proteins added to a digestion is varied. For every experiment (a, b or c) one f_i-value was varied, whereas the other f_i-values were constant (i.e. were "1"). The error bars represent 4 or 5 artificial digestions performed in separate tubes.

Table 3. The ratio of the partitioning coefficients describing the relationship between the amount of freely dissolved test compounds and of the compounds sorbed to micelles (K^0_m), to proteins (K^0_{prot}) and to digested OECD-medium (K^0_{OECD-m}) after a default digestion.

Compound	K^0_m	K^0_{prot}	K^0_{OECD-m}
lindane	0.70	0.62	1
PCB #52	0.42	0.15	1
PCB #118	0.39	0.20	1
PCB #153	0.47	0.22	1
PCB #180	0.36	0.17	1

With the ratio of K^0-values, the percentages of the test compounds can be calculated which were freely dissolved (%free), sorbed to bile salt micelles (%micelle), to proteins (%protein) and to OECD-medium (%OECD-medium). These percentages are presented in Table 4 for a digestion with default amounts of bile, protein and OECD-medium (i.e. f_m, f_{prot} and f_{OECD-m}-values of "1"). About 40% of lindane were sorbed to OECD-medium, 23% to bile salt micelles, 32% to proteins and on average 5% was freely dissolved. The corresponding percentages for the PCBs are approximately 60%, 25%, 15% and <1%. The relatively large standard deviations reflect the inter-experiment variation. The effect on the standard deviation originating from other processes is negligible compared to the effect of the inter-experiment variation.

Table 4. The percentages of the test compounds (± SD) after a default digestion that were freely dissolved (%free), sorbed to bile salt micelles (%micelle), to digested OECD-medium (%OECD-medium) and to proteins (%protein).

Compound	%micelle [b]	%protein [b]	%OECD-medium [b]	%free [b]
Lindane ($n_{free}=0$)[a]	25 (± 17)	34 (± 21)	42 (± 4)	< 1
Lindane ($n_{free}=0.1 \times n_{tot}$)[a]	22 (± 16)	30 (± 19)	38 (± 4)	10 (± 0.6)
PCB #52	23 (± 15)	13 (± 7)	64 (± 11)	< 1
PCB #118	19 (± 17)	15 (± 6)	67 (± 11)	< 1
PCB #153	25 (± 14)	16 (± 7)	59 (± 11)	< 1
PCB #180	22 (± 13)	17 (± 10)	62 (± 12)	< 1

[a] For lindane, this distribution is calculated for the situation that the freely dissolved amount is negligible, $n_{free}=0$, and that the freely dissolved amount is 10% of the total amount present in the system, $n_{free}=0.1 \times n_{tot}$.

[b] The data represent the average and standard deviation over the three series of experiments in which the additions of bile, protein and OECD-medium to an artificial digestion were varied, so that the inter-experiment variation is included.

These percentages show that the PCBs and lindane were sorbed to a large extent to bile salt micelles, 20-25% of the total amount of HOCs, although the concentration of bile (0.9 g/l) was

small compared to the concentration of protein (3.7 g/l) and OECD-medium (15.4 g/l). This suggests that bile salt micelles play a central role in mobilizing HOCs from a matrix and in making the HOCs bioaccessible.

To the best of our knowledge a physiologically realistic *in vitro* model of human digestion has been used only once before, namely by Hack and Selenka (*103*), to investigate mobilization of PCBs from a matrix such as soil. Hack and Selenka employed a digestion model somewhat less complex than the model utilized in the present study. They found that 6-40% of the PCBs were mobilized into the supernatant (i.e. chyme) after the *in vitro* digestion of different types of soil (*103*). The range of percentages probably reflects differences in soil properties. Our values for the mobilization from OECD-medium for the PCBs ranged from 30-40%. The study by Hack and Selenka (*103*) highlights the need for experimentally determined bioaccessibility for different soil types, which can be normalized for example to its organic carbon content, to investigate extrapolation of the bioaccessible fraction to other soils (*112,113*).

Hack and Selenka found that addition of 56 g/l dry whole milk to the digestion model caused the bioaccessible fraction of PCBs to increase from 6-40% to 43-85% (*103*). This may be due to the milk fat and the milk proteins. Similarly, Dulfer *et al.* (*79*) observed that more test compounds were mobilized from PCB-coated chromosorb in the presence of bile salts and fatty acids in medium. This shows that bile salts and fatty acids increase the bioaccessibility of PCBs. The Caco-2 cell line, which is used as a model system to simulate human intestinal absorption, was exposed to the contaminated medium with bile salts and with or without fatty acids (*79*). The PCB uptake into and transport across the cells were increased when fatty acids were present in the medium.

In terms of the model presented here, the observations of Hack and Selenka (*103*) and Dulfer *et al.* (*79*) can be attributed to an increased V_m (and V_{prot}) due to the presence of fat (and protein). On the basis of the present study an increased V_m (and V_{prot}) leads to increased bioaccessible fractions of HOCs, indicating that more contaminants are available for absorption. In addition, the micelles and proteins may facilitate the HOCs to traverse the unstirred water layer next to the intestinal membrane (*23,58,102*). Both processes can lead to an enlarged absorption of HOCs.

It should be noted that the bioaccessible fraction of a compound does not provide information about the actual absorption of that compound. It merely indicates the fraction that is at maximum available for absorption. The distribution among constituents of chyme and the OECD-medium provides insight in the process of intestinal absorption and the model provides a tool to extrapolate the bioaccessible fraction of different situations.

The present *in vitro* study shows that the composition of synthetic chyme and the addition of OECD-medium influence the bioaccessibility of the HOCs. Probably these factors also influence the *in vivo* bioaccessibility and intestinal absorption. For example, a fatty administration matrix of HOCs increases V_m and thus the bioaccessible fraction of the HOCs, possibly leading to increased absorption, bioavailability and toxicity. As an illustration of the change in direction and the order of magnitude of the bioaccessible fraction in different situations, Figure 5 shows the percentage of PCB #153 that is bioaccessible at different f_i-values. The experimentally obtained ratio of the K^0-values of PCB #153 is used to calculate the percentages sorbed to micelles and to proteins according to eq 2.7, which added give the percentage that is bioaccessible. The default conditions ($f_m=f_{prot}=f_{OECD-m}=1$) represent the fasting situation as is used in the present study. Approximately 40% of PCB #153 ingested with OECD-medium is bioaccessible under these circumstances. Co-ingestion with food is likely to result in increased values of f_m and f_{prot}, which in turn lead to an increased bioaccessibility of PCB #153. Based on the model, it can thus be concluded that fasting conditions are not a worst case scenario for HOCs. The worst case situation is more likely to be ingestion of HOCs in small amounts of soil in combination with food of high fat content.
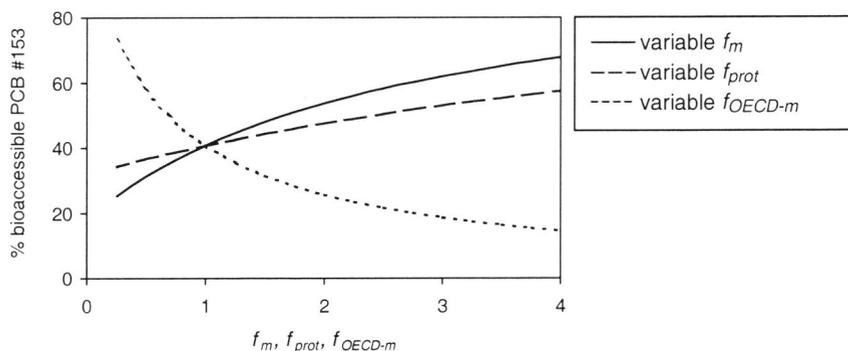
Figure 5. The percentage of PCB #153 that is bioaccessible at different levels of bile salt micelles, proteins or OECD-medium in an artificial digestion relative to their default amount, expressed as f_m, f_{prot} or f_{OECD-m}, respectively. For every line one f_i-value is varied, whereas the other f_i-values are constant (i.e. are "1").

Acknowledgments

Chapter **3**

Nonequilibrium solid phase microextraction (SPME) for determination of the freely dissolved concentration of hydrophobic organic compounds: matrix effects and limitations

Agnes G. Oomen, Philipp Mayer, Johannes Tolls

Abstract

Solid Phase MicroExtraction (SPME) has recently been applied to measure the freely dissolved concentration, as opposed to the total concentration, of hydrophobic substances in aqueous solutions. This requires that only the freely dissolved analytes contribute to the concentration in the SPME fiber coating. However, for nonequilibrium SPME the sorbed analytes that diffuse into the unstirred water layer (UWL) adjacent to the SPME fiber can desorb from the matrix and contribute to the flux into the fiber. These processes were described as a model. Experimentally, an equilibrated and disconnected headspace was used as a reference for the freely dissolved concentration. The expected contribution of desorbed analytes to the uptake flux was measured for PCB #52 in a protein rich solution, while it was not measured in a matrix containing artificial soil. The latter was possibly due to slow desorption of the analyte from the artificial soil. On the basis of the present study a contribution of desorbed analytes to the uptake flux is expected only if 1) the rate-limiting step of the uptake process is diffusion through the UWL, 2) the concentration of the sorbed analyte is high, and 3) desorption from the matrix is fast.

INTRODUCTION

The freely dissolved form of an organic compound is generally considered to be the only form that can cross membranes by passive diffusion (75,114). Therefore, quantitative determination of the freely dissolved concentration is interesting from a toxicological and pharmacological point of view. Recently, such concentrations have been measured with new techniques, which include SemiPermeable Membrane Devices (SPMD) (115,116), solvent microextraction (117) and Solid Phase MicroExtraction (SPME) (118-124).

SPME has been developed by Pawliszyn and co-workers (125). The SPME fiber consists of a silica rod with a polymer coating, into which analytes accumulate when exposed to a fluid or air sample. Subsequently, the extracted analytes are thermally desorbed in the injector of a gas chromatograph (GC) for analytical separation and quantification.

Determination of the freely dissolved concentration of an analyte by means of SPME requires two conditions to be met. First, the freely dissolved concentration should not be depleted by the SPME extraction (118,122,124). Second, a matrix in a sample may not interfere with the analyte uptake into the fiber. Matrix effects by nonequilibrium SPME have been theoretically considered by Vaes *et al.* (122), investigated and found to be absent for hexachlorobenzene and a PCB in samples containing dissolved organic carbon by Urrestarazu Ramos *et al.* (121), and shown and discussed for organotin compounds and fluoranthene in samples containing humic organic matter by Pörschmann *et al.* (118) and Kopinke *et al.* (126). Kopinke *et al.* suggested two mechanisms in order to explain the matrix effects, one of which was similar to the mechanism proposed here (126). This illustrates the need for further research on the mechanism that induces matrix effects and on the limitations of SPME, as is addressed in the present study.

The matrices used in the present study were 1) the supernatant of an artificial human digestive mixture, i.e. chyme, and 2) water with artificial standard soil (OECD-medium). Chyme was used as a protein rich matrix, which is relevant for investigation since proteins are frequently present in pharmacological and toxicological samples. In addition, we were particularly interested in the freely dissolved concentration of several PCB congeners and lindane in chyme and in the availability of these analytes for intestinal uptake (127). OECD-medium was used since it contains organic matter, which enables comparison with other studies on matrix effects.

Scope

In the present study we propose an uptake model for hydrophobic analytes into the SPME fiber coating. This model considers a flux towards the fiber of freely dissolved analytes and of

analytes desorbing from matrix constituents. To investigate whether this latter flux can bias nonequilibrium SPME measurements, experimental data were generated. Subsequent limitations of nonequilibrium SPME are discussed for the determination of freely dissolved concentrations in complex matrices. Finally, recommendations for the use of SPME are given.

THEORY

Depletion

Significant depletion of the freely dissolved concentration can lead to disturbed equilibria and thus to erroneous measurements. The depletion is negligible when $k_1 V_f/k_2 V_l<<1$, as is described by Vaes *et al.* (*122*). The depletion depends on the amount of analyte extracted and can be approximated as a function of the equilibration time t:

$$\%\text{depletion}\,(t) = 100\% \times \frac{[X]_{f,t} \times V_f}{[X]_{l,t=0} \times V_l} = 100\% \times \left(\frac{k_1 \times V_f}{k_2 \times V_l} \right) \times \left(1 - e^{-k_2 \times t} \right) \tag{3.1}$$

where k_1 (min^{-1}) represents the uptake rate constant for compound X from the water phase into the fiber coating, and k_2 (min^{-1}) the elimination rate constant. $[X]_{l,t}$ (mg/l) and $[X]_{f,t}$ (mg/l) are the concentrations of compound X in the liquid and the fiber coating, respectively, at time t. V_l (l) and V_f (l) represent the volume of the liquid and of the fiber coating, respectively.

Conceptual uptake model matrix effects

The transport of analytes from complex matrices into the fiber coating is schematically presented in Figure 1. The rate-limiting step of the uptake process for highly hydrophobic analytes can be assumed to be diffusion through the unstirred water layer (UWL) (*128*). An UWL can be envisioned as a layer that compounds only can cross via diffusion. Furthermore, it can be expected that only the non-bound analytes diffuse into the hydrophobic fiber coating. As a result of analyte uptake by the fiber the freely dissolved concentration in the UWL is reduced. Analytes sorbed to matrix constituents in the UWL can desorb and subsequently contribute to the analyte flux towards the SPME fiber. As a consequence, equilibrium between the fiber and the sample is reached earlier than for a sample without matrix. The flux originating from desorbed analytes is not present when 1) the rate-limiting step of the transport is diffusion of the analyte within the coating, since in that case the concentration gradient in the UWL is not formed, 2) equilibrium SPME is used, since the uptake flux does not influence the steady state concentration in the fiber coating, and 3) the desorption of the analyte from matrix constituents is slow compared to diffusion through the UWL, since in that case the bound forms do not desorb and contribute to the uptake flux.
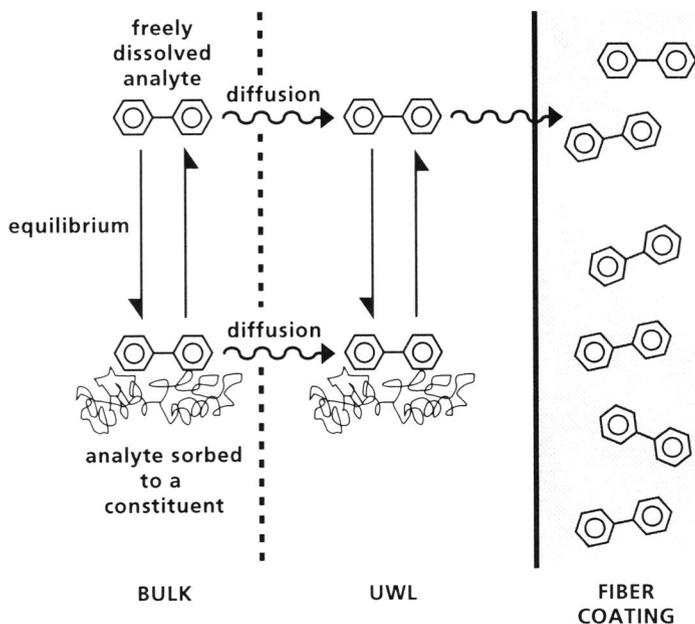
Figure 1. Conceptual representation of the uptake model for analyte fluxes towards the SPME fiber coating. Both the freely dissolved analytes and the sorbed analytes diffuse into the unstirred water layer (UWL). Only the freely dissolved analytes in the UWL partition into the fiber coating. If diffusion through the UWL is the rate-limiting step for the entire uptake process, a concentration gradient in the UWL is formed. Depending on the concentration of sorbed analytes in the UWL and on their desorption kinetics, desorbed analytes contribute to the flux towards the fiber coating.

In order to visualize the parameters that influence the flux of hydrophobic organics towards the fiber, the uptake process is described by equations. The uptake of a compound X by the fiber coating is described by a one-compartment first-order kinetic model:

$$\frac{\partial [X]_{f,t}}{\partial t} = k_1 [X]_{l,t} - k_2 [X]_{f,t} \tag{3.2}$$

If the aqueous concentration does not change in time, $[X]_{l,t} = [X]_{l,t=0}$, eq 3.2 can be integrated to:

$$[X]_{f,t} = \frac{k_1}{k_2} \times [X]_{l,t=0} \times \left(1 - e^{-k_2 \times t}\right) \tag{3.3}$$

30

The rate constant k_2 determines the transport of analytes into the fiber coating. In fugacity terms, k_2 can be related to the conductivity D (mol/Pa×s) of the UWL, via $k_2=D/(V×Z)$ *(129)*. V refers to volume (m^3) and Z to fugacity capacity (mol/m^{3}Pa) of the UWL.

Two contributions to the total flux towards the fiber can be distinguished: the flux of freely dissolved analytes and the flux originating from analytes that are desorbed from matrix constituents. These fluxes are compared for the situation that the kinetics between the freely dissolved analytes and the sorbed analytes are instantaneous, i.e. equilibrium conditions prevail in the entire UWL. Furthermore, we assume the rate-limiting step of the transport to be diffusion through the UWL. The conductivity of the UWL for the freely dissolved analytes, D_{free}, and for analytes sorbed to a constituent, D_{sorb}, can then be described by:

$$D_{free} = k_{free} \times A \times Z_{free} \qquad (3.4)$$

$$D_{sorb} = k_{sorb} \times A \times Z_{sorb} \qquad (3.5)$$

where k_{free} and k_{sorb} (m/s) represent the mass transfer coefficient in the UWL of the freely dissolved analytes and of the sorbed analytes, respectively. A (m^2) is the average UWL surface area. Z_{free} and Z_{sorb} (mol/m^{3}Pa) denote the fugacity capacity of the UWL for the freely dissolved analytes and the sorbed analytes, respectively. D_{free} and D_{sorb} contribute to the total conductivity, D_{tot}, according to the relative volume of the water, v_{free}, and of sorbing phase, v_{sorb} in the UWL, respectively.

$$D_{tot} = D_{sorb} \times v_{sorb} + D_{free} \times v_{free} \qquad (3.6)$$

Mass transfer coefficients can be described as diffusivities in the UWL (m^2/s) divided by the thickness of the UWL, l (m). The diffusivities of the freely dissolved analyte and of the sorbed analyte are represented by d_{free} and d_{sorb}, respectively. Inserting eq 3.4 and 3.5 into eq 3.6 yields:

$$D_{tot} = \frac{A}{l}\left(d_{sorb} \times Z_{sorb} \times v_{sorb} + d_{free} \times Z_{free} \times v_{free}\right) \qquad (3.7)$$

A flux towards the fiber that is additional to that caused by freely dissolved analytes is not expected as long as $D_{sorb} \ll D_{free}$, i.e. as long as $\{d_{sorb}\times(Z_{sorb}/Z_{free})\times(v_{sorb}/v_{free})\} \ll d_{free}$.

EXPERIMENTAL SECTION

Chemicals and SPME fibers

PCB congeners 2,2',5,5'-tetrachlorobiphenyl (IUPAC PCB #52), 2,3',4,4',5-pentachlorobiphenyl (IUPAC PCB #118), 2,2',4,4',5,5'-hexachlorobiphenyl (IUPAC PCB #153), 2,2',3,4,4',5,5'-heptachlorobiphenyl (IUPAC PCB #180) and lindane were the analytes investigated. All chemicals were of analytical grade. The logarithms of their octanol-water partition coefficients, log K_{ow}, are 6.1, 6.2-6.5, 6.9, 7.2 and 3.8, respectively (*26,38*).

The purchased SPME fibers (Supelco, Bellefonte, IL) were 1 cm long and coated with a 7 μm thick film of polydimethylsiloxane (PDMS). Some fibers were cut manually to 1 or 3 mm. According to the manufacturer, the volume of the coating of a 1 cm long fiber was 0.026 μl. Before use, the fibers were conditioned for 2 hours at 320 °C in the injector of a GC.

Matrices

Chyme was artificially prepared and contained 3.7 g/l protein (mainly bovine serum albumin, mucine, pancreatine and pepsin) and 0.9 g/l freeze-dried chicken bile (*127*). In the present study, a physiologically based *in vitro* digestion model was employed that was a modification from Rotard *et al.* (*104*), and was described in detail by Sips *et al.* (*110*). Chyme was spiked with analytes via an acetone solution, or by performing an artificial digestion with spiked OECD-medium. The former method was used for the air-bridge experiments.

The generator column technique was used to obtain water contaminated with the sparsely soluble analytes without crystals being present in the solution (*106,130*). In short, the analytes were dissolved in hexane and added to an inert support, i.e. chromosorb. The hexane was evaporated so that the chromosorb was coated with the analytes. The coated chromosorb was transferred into a glass tube through which the water was pumped. Water spiked with PCBs was mixed with water spiked with lindane and meanwhile the analyte concentrations were diluted approximately 10 and 2500 times, respectively. OECD-medium is standardized, artificial soil and consists of 10% peat, 20% kaolin clay and 70% sand, and was prepared according OECD-guideline no. 207 (*98*). The samples containing 1 g/l OECD-medium were prepared by adding the spiked water to uncontaminated OECD-medium. These samples were shaken overnight at 150 rpm to distribute the analytes between the OECD-medium and the water.

Analytical procedure

Glass vials with sample were closed with black Viton septa (Supelco, Bellefonte, IL) and placed on a temperature controlled autosampler (37±1 °C). The SPME fiber was vibrated in the

sample by the autosampler (Varian 8200 CX) and subsequently transferred into the injector of a GC for thermal desorption. The GC (Varian Star 3400 CX) was equipped with a 30 m long, 0.32 mm i.d. J&W Scientific DB 5MS column and a ^{63}Ni electron capture detector (ECD). The injector temperature was 315 °C. After each measurement the SPME fiber was vibrated for 1 min in acetone and subsequently cleaned thermally in the injector of the GC for several minutes. With this method, almost all compounds were measured and carry-over between runs was less than 2%. However, for successive samples containing different concentration ranges of analytes, carry-over can be of importance. Therefore, two different fibers were used for the air-bridge experiments, one for the high concentration in the liquid vial, and one for the low concentration in the headspace vial. For the air-bridge experiments the detector of the GC was set to a more sensitive mode after headspace-SPME than after liquid-SPME.

Determination of k_1 and k_2

The rate constants of the fiber-water partitioning were determined from the accumulation of the analytes in a 1 mm long fiber after varying vibration times of the SPME fiber in spiked water, i.e. an uptake curve. The initial water concentration of the analytes was measured by hexane extraction. Losses of the hydrophobic analytes from the water to the air and/or glass wall are likely to occur during the experiment due to the long vibration times and the time that was required for the previous samples (*131,132*). Therefore, extra samples with spiked water were measured by SPME in a standard manner in-between the samples for the uptake curve. The amount of analytes extracted in the standard manner decreased during the experiment, which formed the basis for the loss curve. The waiting period of each sample of the uptake curve was known. Therefore, the areas of the uptake curve were corrected for the loss of analytes at a specific waiting period via the loss curve to the situation without losses. The values of k_1 and k_2 and their standard deviations were obtained from the corrected uptake curves, which were fitted to eq 3.3 by the program GraphPad Prism (San Diego, CA).

Air-bridge experiments

The purpose of the experiments was to investigate whether desorbed analytes contribute to the flux towards the SPME fiber. Therefore, an air-bridge system was designed similar to a system used by Ai (*133*), in which the equilibrated headspace could be disconnected. In the present study two 14 ml glass vials were connected via a glass tube, which could be closed by a Teflon valve (Figure 2). To one vial 6 ml of liquid was added. The air-bridge was kept open until equilibrium between the two vials was reached. Nonequilibrium SPME was performed in the liquid vial, and equilibrium SPME in the disconnected headspace vial. These measurements are referred to as liquid-SPME and headspace-SPME, respectively.
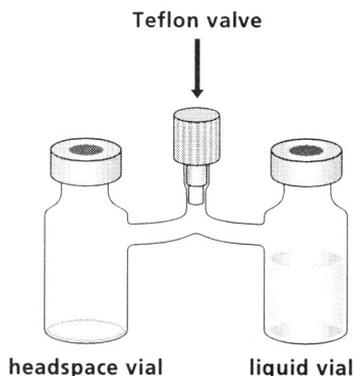
Figure 2. Schematic representation of an air-bridge system consisting of two vials connected by a glass tube. Chyme, water or water with OECD-medium (6 ml) was added to the liquid vial. The two vials were equilibrated via the glass tube. Just before measurement, the headspace vial was disconnected by the Teflon valve.

According to Henry's law, the equilibrium concentration of an analyte in the air (i.e. headspace) is a measure of the freely dissolved concentration in the aquatic solution (*38,134,135*). Before sampling, the two vials were disconnected to prevent redelivery of analytes in the liquid to the headspace. Therefore, headspace-SPME is a measure of the freely dissolved concentration in the liquid. The area ratio of liquid-SPME/headspace-SPME is matrix independent if nonequilibrium SPME in the liquid measures the freely dissolved concentration, and is higher if an additional flux due to desorbed analytes is present in complex matrices. Pure water samples without sorbing constituents are assumed to give a ratio that is a measure of the freely dissolved concentration.

Experimental set-up of air-bridge experiments

PCB #52 was the only analyte measurable by headspace-SPME and, therefore, the only analyte mentioned for air-bridge experiments. Unless stated otherwise, 0.5 min of vibration in the liquid vial with 1 cm long SPME fibers was performed for air-bridge experiments. A ratio of peak areas was compared from identically analyzed samples. These areas were in the linear range of the GC detector, and the y-intercept of a calibration curve in hexane was negligible compared to the areas observed for SPME. Therefore, external calibration was not necessary.

Equilibration times of air-bridge experiments

The time to reach equilibrium between the two connected vials was experimentally determined with spiked water as liquid. The disconnected headspace vial was measured by SPME for different equilibration periods of the air-bridge. No increase in the response of headspace-SPME was observed after 180 min. All experiments were thus performed with an air-bridge equilibration time of at least 270 min. Subsequently, a series of experiments was performed to determine the vibration time in the headspace vial that is necessary for equilibrium SPME, which was 20 min. In further experiments, headspace-SPME with 30 min of vibration was used.

Ratio liquid-SPME/headspace-SPME in air-bridge experiments

For samples containing spiked chyme, water and water with OECD-medium the area ratio of liquid-SPME/headspace-SPME was determined. The data were analyzed by a one tail-paired t-test to determine whether this ratio was significantly higher for complex matrices than for pure water.

Liquid-SPME approaching equilibrium in air-bridge experiments

For water and chyme samples the equilibrium between the fiber coating and the liquid was followed in time. Measurements with liquid-SPME of 0.5, 2, 10, 30 and 60 min were performed. The SPME fibers were shortened for longer vibration times, respectively to 1, 1, 0.3, 0.1 and 0.1 cm. The final, equilibrium distribution of the analytes between the fiber coating and the liquid is independent of the matrix effects. Therefore, the effect of desorbed analytes is expected to decrease with increasing vibration time in the liquid, i.e. the ratio liquid-SPME/headspace-SPME for a complex matrix is expected to become more similar to that of water at longer times of liquid-SPME.

Variable protein concentration in chyme

The concentration of proteins (and thus of sorbing constituents) in chyme was varied in order to investigate the performance of nonequilibrium SPME in a more realistic situation, and to separate the contribution on matrix effects of the main constituents of chyme: protein and bile. The 1 mm long SPME fiber was vibrated for 1 min in 12 ml of the different chyme solutions. Since protein was a sorbing constituent of minor importance for the hydrophobic analytes in chyme (*127*), we expected a slight decrease of the freely dissolved concentration with increasing protein content. A deviation from this curve was expected when more than the freely dissolved concentration was measured by SPME.

RESULTS

Determination of k_1 and k_2

The uptake curves are shown in Figure 3. The k_1 and k_2 range from 3.1×10^3 to 9.6×10^3 min^{-1} and from 9.7×10^{-3} to 1.2×10^{-1} min^{-1}, respectively, for the different analytes (Table 1). The logarithm of the partition coefficient between the fiber and the water, $\log K_{fw}$, ranges from 4.4 to 5.9 (Table 1). The use of a loss curve and the long vibration and waiting times may have introduced additional errors that have not been accounted for in the standard deviation. For example, the concentration of test compounds in the fiber should not decrease at the longest vibration time of 600 min. Nevertheless, our values of K_{fw} were in general accordance with Mayer *et al.*, who measured the values for K_{fw} taking great care to avoid experimental artifacts (*128*). The determined uptake and elimination rate constants can thus be considered to be precise enough to estimate the depletion.
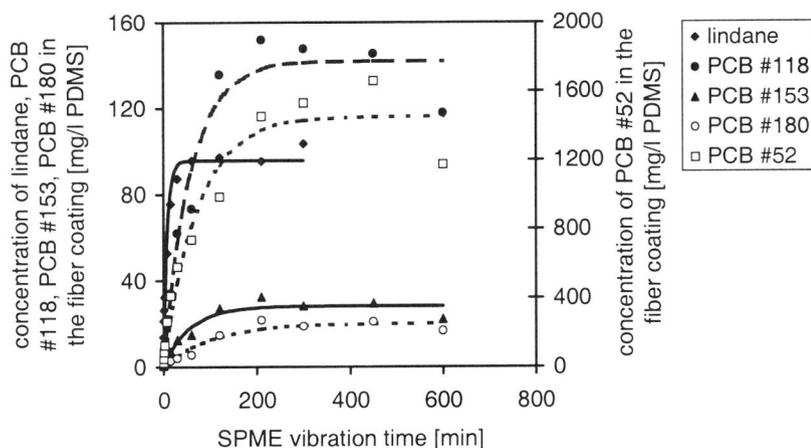

Figure 3. Uptake curves of the analytes from spiked water into a 1 mm long SPME fiber at 37 °C. The left y-axis represents the concentration of lindane, PCB #118, PCB #153 and PCB #180 in the fiber coating, while the right y-axis applies for PCB #52. The curves are corrected for losses and fitted to eq 3.3.

Table 1. The uptake (k_1) and elimination (k_2) rate constants for the analytes, their octanol-water partition coefficient (logK_{ow}), and their calculated fiber-water partition coefficient (logK_{fw}). The experiments were performed at 37 °C with a 1 mm long SPME fiber in samples of 12 ml spiked water. The standard deviations were derived from the fit to eq 3.3 of the corrected uptake curves.

Compound	LogK_{ow}	k_1 (min^{-1}) ($\pm$SD)	k_2 (min^{-1}) ($\pm$SD)	LogK_{fw} ($\pm$SD)
lindane	3.8	$(3.1\pm0.6)\times10^3$	0.13 ($\pm$0.03)	4.4 ($\pm$0.1)
PCB #52	6.1	$(6.7\pm1.2)\times10^3$	0.014 ($\pm$0.003)	5.7 ($\pm$0.1)
PCB #118	6.2-6.5	$(9.6\pm1.3)\times10^3$	0.017 ($\pm$0.003)	5.8 ($\pm$0.1)
PCB #153	6.9	$(3.4\pm0.6)\times10^3$	0.018 ($\pm$0.004)	5.3 ($\pm$0.1)
PCB #180	7.2	$(6.9\pm1.3)\times10^3$	0.0097 ($\pm$0.002)	5.9 ($\pm$0.2)

Ratio liquid-SPME/headspace-SPME in air-bridge experiments

The depletion of the freely dissolved concentration of PCB #52 in the whole sample was 1.4%, calculated according to eq 3.1. This indicates that the first precondition of negligible depletion was met. The ratio liquid-SPME/headspace-SPME was significantly different for chyme, $\alpha\leq0.001$, compared to the ratio for pure water and for water with OECD-medium (Figure 4). The ratios for water and the water with OECD-medium were not significantly different.
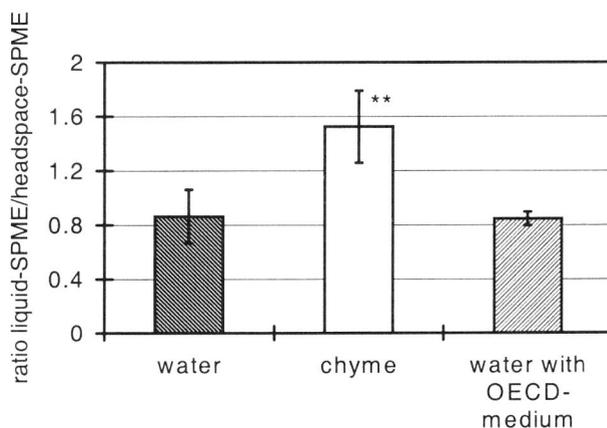
Figure 4. The ratio of peak areas of liquid-SPME/headspace-SPME for samples of water (n=7), chyme (n=7) and water with OECD-medium (n=3) for a liquid-SPME vibration time of 0.5 min. The error bars represent the standard deviation of different samples. The ratio was significantly different for chyme ($\alpha\leq0.001$) compared to the ratio for pure water and for water with OECD-medium.
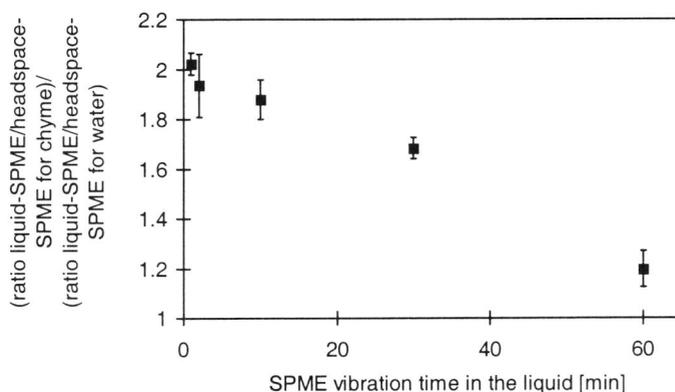
Figure 5. The ratio liquid-SPME/headspace-SPME for chyme divided by the ratio liquid-SPME/headspace-SPME for pure water at different vibration times of liquid-SPME. The error bars represent standard deviations, which were derived from 3 ratios liquid-SPME/headspace-SPME for chyme and 3 ratios for water.

Liquid-SPME approaching equilibrium in air-bridge experiments

Due to the shorter fibers the depletion of the freely dissolved concentration in the aqueous sample was relatively small (1.4%, 5.7%, 8.1%, 7.1% and 11.9% for the increasing times of liquid-SPME). An increase in the equilibration time of the SPME fiber in the liquid vial resulted in a more similar ratio liquid-SPME/headspace-SPME for chyme and water (Figure 5). The data are presented as the ratio liquid-SPME/headspace-SPME for chyme divided by the ratio liquid-SPME/headspace-SPME for water to correct for a new set of SPME fibers that showed somewhat different ratios.

Variable protein concentration in chyme

After the artificial digestion, an aliquot of the chyme was transferred into another vial and extracted by hexane, which indicated that on average 103% (±16%) of the analytes were recovered (*127*). Therefore, no significant losses of compounds occurred during the digestion. The depletion of the freely dissolved concentration in the whole sample due to the SPME extraction was negligible, i.e. <<1% for all analytes. Figure 6 shows an increase in the amount of PCB #52 extracted by nonequilibrium liquid-SPME with increasing protein concentration in chyme. The other analytes showed a similar response, suggesting that in chyme desorption of all tested analytes contributed to the uptake flux. Based on nonequilibrium SPME measurements, the percentage of "freely dissolved analytes" in chyme of default composition (i.e. 3.7 g/l protein) was 10%, 1.4%, 0.4%, 0.9% and 0.4% for lindane, PCB #52, PCB #118, PCB #153 and PCB #180, respectively. Extrapolating from Figure 4, this freely dissolved concentration is probably overestimated by a factor of 2.
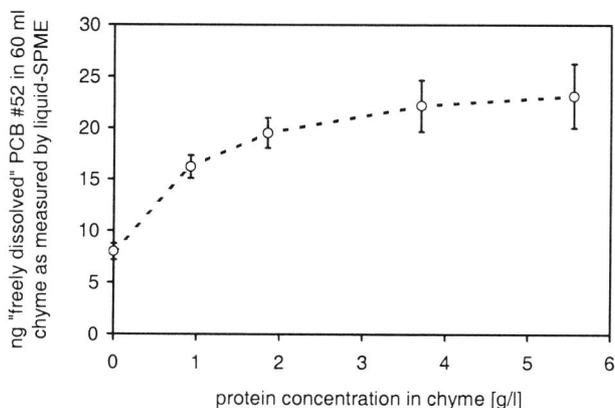
Figure 6. The amount of PCB #52 in 60 ml of chyme that was measured as freely dissolved by nonequilibrium SPME at variable protein concentration in chyme. The error bars represent the standard deviations from 4 individual samples.

DISCUSSION

The results of all experiments in the present study supported the proposed uptake model. Figure 4 shows an increased liquid-SPME/headspace-SPME ratio for chyme relative to water. Figure 5 shows that the ratio liquid-SPME/headspace-SPME for chyme becomes more similar to that ratio for water at longer liquid-SPME vibration times. In Figure 6 an increase is observed in the amount of analyte extracted by nonequilibrium liquid-SPME with increasing protein concentrations in chyme. Nevertheless, in the following section two alternative explanations are discussed. Subsequently, the uptake model is compared to uptake models for other analytical techniques and used to address the limitations of nonequilibrium SPME in complex matrices.

Surface tension

Bile has surface-active properties. These might physically affect the properties of the UWL and thereby induce an increased relative uptake flux in a chyme compared to a water solution. To distinguish between this mechanism for matrix effects and the mechanism described in the proposed model is difficult since both mechanisms can increase the uptake rate. Further research on this subject is required. However, in the present study an increase in the amount of PCB #52 extracted by nonequilibrium SPME in chyme with increasing protein content and constant bile concentration was measured. This indicates that proteins play a key role in the

explanation of the matrix effects. Therefore, the observed matrix effects cannot be explained by surface-active properties of bile as the (main) reason, while analyte desorption from proteins can.

Protein adsorption

Protein adsorption to a PDMS fiber has been mentioned by Poon *et al.* for samples containing human blood plasma (*136*) (containing approximately 70 g of protein/l), although PDMS is known for its non-sticky surface. Poon *et al.* could visually observe the proteins, had irreproducible SPME data, and a rapid deterioration of the fiber. Proteins with sorbed analytes that adsorb on the fiber surface can explain the experimental results in the present study. The summed amount of analytes ad- and absorbed (in)to the fiber would be higher for chyme than for pure water, while also an increase in the extracted amount of analyte with increasing protein content is plausible. At increasing liquid-SPME times, the relative amount of PCB #52 that would be adsorbed onto the fiber coating is expected to decrease, resulting in a more similar ratio liquid-SPME/headspace-SPME for chyme and water samples. However, this explanation is unlikely for the present situation because of a number of observations. First, rinsing of the fiber in water after liquid-SPME in chyme and before thermal desorption in the GC-injector did not influence the response (data not shown). Due to the low k_2-value this was as expected for an absorption process. When adsorbed proteins or adhering chyme with analytes were present on the fiber, a decrease in the GC-response was expected because some proteins and analytes could be washed off. Second, a rapid deterioration of the fiber due to a film of carbonized proteins was not observed. The fiber performed well for many samples and the background signal was low. Third, a Bradford assay was performed to determine the amount of protein on a 1 cm long fiber, which was vibrated for 1 min in the chyme. This amount was below the detection limit of the assay of 1 μg, which cannot explain the increased SPME response for chyme samples.

Uptake models of other analytical techniques

The uptake model described by Figure 1 is analogous to the uptake model for metals by a mercury droplet in voltammetric studies (*76,137*). Only the free metal ion can diffuse into the mercury droplet, which is a sink for the metal. Similarly, the diffusion through the UWL is the rate-limiting step for the uptake process. The uptake consists of a flux of both the freely dissolved metal ion and the labile metal complexes, i.e. complexes that are in dynamic equilibrium with the freely dissolved metal ion.

Jeannot *et al.* used solvent microextraction to determine the freely dissolved concentration of a hydrophobic organic analyte (*117*). A droplet of *n*-octanol instead of a SPME fiber was used.

Although solvent microextraction is not SPME, similar principles are valid. Also, Jeannot *et al.* considered a flux towards the solvent droplet that consisted of both freely dissolved analytes and analytes desorbed from protein. They assumed that equilibrium between both analyte forms prevailed at all times. Indeed, Jeannot *et al.* determined an enhanced relative uptake flux after addition of protein to the sample (*117*). This means that for voltammetric studies and for solvent microextraction similar transport processes were assumed and experimentally verified as are presently proposed for SPME.

Limitations of nonequilibrium SPME for determination of the freely dissolved concentration in complex matrices

Matrix effects can bias the determination of the freely dissolved concentration by nonequilibrium SPME. For the situation that 1) the kinetics between the sorbed and freely dissolved analytes are fast and 2) diffusion through the UWL is the rate-limiting step of the uptake process, the presence and the magnitude of a flux due to desorbed analytes should be evaluated on the basis of the uptake model. The diffusivity of both analyte forms through the UWL, d_{sorb} and d_{free}, affects the magnitude of the matrix effects, which can be quantified by comparing d_{free} to $d_{sorb} \times (Z_{sorb}/Z_{free}) \times (v_{sorb}/v_{free})$ (see eq 3.7). Due to the large molecular size of the matrix constituents, such as proteins, d_{sorb} is considerable smaller than d_{free}. Therefore, the flux due to desorbed analytes can only exist for samples containing high concentrations of sorbing constituent (v_{sorb}/v_{free}), and their ability to sorb the analytes should be large (Z_{sorb}/Z_{free}), which is the case for hydrophobic analytes.

Published SPME studies in perspective of the uptake model

Many studies on SPME have been published, although few have used SPME to determine the freely dissolved concentration. These studies are discussed in the perspective of the uptake model. In the experiments performed by Vaes *et al.* medium hydrophobic compounds ($0.8 < \log K_{ow} < 4.8$) and a fiber coated with polyacrylate were used (*122,123*). The rate-limiting step for the uptake process was the diffusion of the analytes within the fiber coating (*123*). Therefore, there was no concentration gradient of the freely dissolved analytes in the UWL and the freely dissolved concentration was measured. Equilibrium SPME was used by Yuan *et al.* (*124*) (in the headspace) and Pörschmann *et al.* (*118-120*). At equilibrium the processes in the UWL do not influence the amount of analyte absorbed into the fiber coating. Therefore, if the precondition of nondepletive extraction is fulfilled, the freely dissolved concentration is measured. Urrestarazu Ramos *et al.* worked with nonequilibrium SPME (with a PDMS coating) in samples containing humic acids and hydrophobic organics (*121*). They concluded that the matrix did not interfere with the determination of the freely dissolved concentration. However, they worked with relatively low concentrations of humic acids ($\approx 10\text{-}100$ mg/l). Therefore, the flux due to desorbed analytes could have been negligible. Furthermore, as has been shown in

the present study for a sample with a relatively high concentration OECD-medium of 1 g/l, the ratio liquid-SPME/headspace-SPME was similar to that of pure water. This indicates that desorption of the hydrophobic analytes from the humic acids/OECD-medium might have been slow compared to diffusion of the freely dissolved analytes through the UWL. The flux towards the fiber from desorbed analytes was then not present.

Pörschmann *et al.* (*118*) described that the addition of humic or fulvic acid to a water sample with organotin compounds decreased the uptake flux that was normalized to the equilibrium situation, i.e. the time to reach equilibrium was increased. This matrix effect can be explained in the current context, although it cannot be deduced from eq 3.7 since this is based on instantaneous kinetics between the freely dissolved and the sorbed analyte form. The uptake flux depends on the diffusion of the analyte through the UWL if the freely dissolved analyte is locally depleted in the UWL due to the extraction by the fiber, and analyte desorption from the humic or fulvic acid is slow. Slow desorption of organotin compounds from organic matter is plausible since the complexation is governed by complexation by carboxylate and phenolate groups (*138*). Subsequently, a decrease in the concentration of freely dissolved analytes in the sample due to addition of the humic or fulvic acid results in a increased local depletion of freely dissolved analytes and to a decrease in the normalized uptake flux.

Recommendations

Nonequilibrium SPME is a valuable tool for measuring the freely dissolved analyte concentration. Since the rate-limiting step for uptake of hydrophobic compounds is likely diffusion through the UWL, the possibility of an enhanced flux in complex matrices exists and should be evaluated on the basis of eq 3.7. This evaluation represents a worst case since an instantaneous equilibrium between sorbed analytes and freely dissolved analytes is assumed. It should be kept in mind that the deviation from the freely dissolved concentration in chyme in the present study was approximately a factor 2 for 0.5 min of vibration in the liquid vial. Such a deviation can be considered acceptable, depending on the type and aim of the research. Equilibrium SPME can be an alternative if depletion of the freely dissolved concentration is negligible.

On the other hand, the described phenomenon is of interest for the uptake of hydrophobic compounds by biota. Similar diffusion and kinetic processes can be expected in the UWL adjacent to a membrane. Thus, if the UWL is similar for SPME and the biotic barrier under study, nonequilibrium SPME can measure the concentration that is kinetically available for uptake. Further research into this phenomenon is required.

Availability of polychlorinated biphenyls (PCBs) and lindane for uptake by intestinal Caco-2 cells

Agnes G. Oomen, Johannes Tolls, Maaike Kruidenier, Sieto S.D. Bosgra,
Adrienne J.A.M.Sips, and John P. Groten

Abstract

Children may ingest contaminated soil via hand-to-mouth behavior. To assess this exposure route, the oral bioavailability of the contaminants should be known. Two determining steps in bioavailability of soil-borne contaminants are: 1) mobilization from soil during digestion, which is followed by 2) intestinal absorption. The first step has been investigated in previous studies that showed that a substantial fraction of PCBs and lindane is mobilized from soil during artificial digestion. Furthermore, almost all contaminants are sorbed to constituents of artificial human small intestinal fluid (i.e. chyme), while only a small fraction is freely dissolved. In the present study, the second step is examined using intestinal epithelial Caco-2 cells. The composition of the apical exposure medium was varied by addition of artificial chyme, bile or oleic acid at similar or increasing total contaminant concentrations. The uptake curves were described by rate constants. It appeared that the uptake flux was dose-dependent. Furthermore, different exposure media with similar total contaminant concentrations resulted in various uptake rates. This can be attributed to different freely dissolved concentrations and carrier effects. In addition, the large fractions of contaminants in the cells indicate that PCBs and lindane sorbed to bile, oleic acid and digestive proteins contributed to the uptake flux towards the cells. These results can be qualitatively extrapolated to the *in vivo* situation. Since the sorbed contaminants should be considered available for absorption, the step of mobilization from soil, is the most important step for oral bioavailability of the presently investigated contaminants.

INTRODUCTION

For children, ingestion of contaminated soil via hand-to-mouth behavior can be a main route of exposure to contaminants such as polychlorinated biphenyls (PCBs) and lindane. To accurately assess reference values for soil-borne contaminants, the oral bioavailability has to be taken into account. Several steps can be distinguished for bioavailability of soil-borne contaminants: 1) soil ingestion, which is on average 50-200 mg/day (*66,67,69*), 2) mobilization from soil and distribution among different physicochemical contaminant forms in digestive fluid, 3) intestinal absorption, and 4) liver metabolism. In this study, soil ingestion is considered a given fact, while liver metabolism is not relevant or has been investigated extensively for the presently used contaminants. In a previous study, the second step has been investigated using a physiologically based *in vitro* digestion model (*127*). The distribution of several PCB congeners and lindane among constituents of artificial human intestinal fluid, i.e. chyme, and digested soil has been studied (*127*). It appeared that for fasting conditions, approximately 25% of the PCBs were sorbed to bile salt micelles, 15% to digestive proteins and 60% were still sorbed to the soil. The respective values for lindane were 23%, 32% and 40%. The percentage of contaminants that was freely dissolved was <1% for the PCBs and approximately 5% for lindane (*111,127*). More hydrophobic organic contaminants (HOCs) were mobilized from soil when more bile or protein was added during the artificial digestion (*127*). Other studies showed that HOC mobilization from soil is dependent on the soil type (*103,104*), and that addition of dry whole milk increases the PCB mobilization from soil (*103*). Therefore, it can be concluded that sorbing phases may increase the contaminant mobilization from soil during the digestion.

In studies utilizing *in vitro* digestion models, the amount of contaminant that is mobilized from soil is considered to represent the maximum amount that is available for intestinal absorption. *In vivo* studies in rat indeed showed that intestinal absorption of PCBs administered via spiked soil is lower than PCBs ingested via corn oil (*9*). Yet, it is unclear to what extent mobilized HOCs are absorbed, and what the effect of constituents such as bile, proteins and fatty acids in chyme is on intestinal absorption and bioavailability of HOCs. For example, the constituents may cause carrier effects, and may decrease the freely dissolved HOC concentration, which is the fraction that is at least available for absorption.

In the present study, the third step of oral bioavailability, i.e. transport of the mobilized contaminants across the intestinal wall, is investigated using *in vitro* differentiated intestinal cells. To that end, the effect of chyme (containing bile and digestive proteins), bile, and oleic acid as a fatty acid on the uptake of several PCB congeners and lindane into intestinal cells is investigated. Research is restricted to intestinal absorption since it is the predominant uptake

pathway (*23,58*). The Caco-2 cell line was used as a model system to simulate human intestinal absorption. Caco-2 cells originate from an epithelial colon cancer and after growing to confluency on a filter, they start to differentiate into polarized, columnar cells that show many morphological and physiological characteristics of mature enterocytes of the small intestine. These cells are extensively used in drug absorption research (*63,139-141*). Experimentally, the composition of the exposure medium was varied at similar or increasing total HOC concentrations. The HOC uptake by the cells and transport over the cells was measured in time. These time curves were described by rate constants, allowing quantitative discrimination.

Aim

The aim of the present study is to investigate 1) to what extent PCBs and lindane are absorbed by *in vitro* intestinal Caco-2 cells, 2) the effect of sorbing constituents on absorption of the HOCs, which includes the issue whether HOCs that are mobilized from soil during digestion contribute to the uptake into the intestinal cells, and 3) which factors have the largest impact on oral bioavailability of the soil-borne HOCs.

MATERIALS AND METHODS

Chemicals

PCB congeners 2,2',5,5'-tetrachlorobiphenyl (IUPAC PCB #52), 2,3',4,4',5-pentachlorobiphenyl (IUPAC PCB #118), 2,2',4,4',5,5'-hexachlorobiphenyl (IUPAC PCB #153), 2,2',3,4,4',5,5'-heptachlorobiphenyl (IUPAC PCB #180) and lindane (γ-hexachlorocyclohexane, γ-HCH) were used as test compounds. The logarithms of their octanol-water partition coefficients, log K_{ow}, are 6.1, 6.2-6.5, 6.9, 7.2 and 3.8, respectively (*26,38*). The internal standards for the PCBs were 2,3,3',5,6-pentachlorobiphenyl (IUPAC PCB # 112) and 2,2',4,4',6,6'-hexachlorobiphenyl (IUPAC PCB #155), and for lindane α-hexachlorocyclohexane (α-HCH). All chemicals were of analytical grade.

OECD-medium was employed as artificial standard soil. Dry OECD-medium consisting of 10% peat, 20% kaolin clay, and 70% sand was prepared according to OECD-guideline 207 (*98*). The appropriate amounts of PCBs dissolved in hexane were added to dry, uncontaminated OECD-medium. The hexane was evaporated under continuous shaking. To prevent losses of lindane during spiking, lindane was added to the OECD-medium as an aqueous solution that was prepared using the generator column technique (*106,130*). The OECD-medium was spiked with a mixture of 7 mg PCB #52, 7 mg PCB #118, 14 mg PCB #153, 7 mg PCB #180 and 2 mg lindane per kg dry OECD-medium, which is referred to as the reference contamination level, or with a three or five fold higher level. The concentration of lindane of 2 mg/kg

represents the current Dutch ecotoxicological intervention value (*37*). PCB #153 is environmentally abundant. Therefore, its level was chosen higher than that of the other PCBs. The spiking levels of the PCBs are of environmental relevance (*107*), although relatively high for the PCBs in the perspective of the current Dutch intervention value of 1 mg PCB/kg dry soil (*37*).
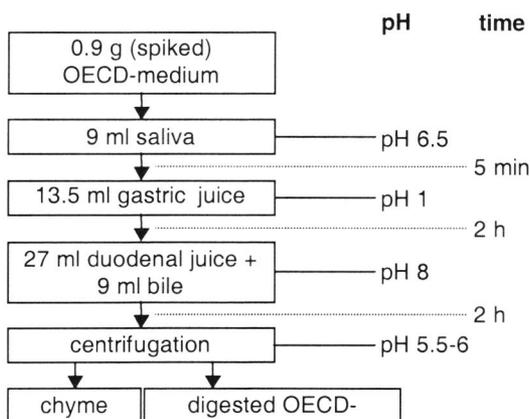

Figure 1. Schematic representation of the procedure of an artificial digestion.

Artificial digestion

The physiologically based *in vitro* digestion model designed by Rotard *et al.* (*104*) was employed in this study in a modified version as described by Sips *et al.* (*110*). The digestion process was based on physiological constituents and transit times for fasting conditions of children. The digestion model is schematically presented in Figure 1. In short, synthetic saliva, gastric juice, duodenal juice and bile were prepared. The saliva was added to 0.9 g OECD-medium and rotated at 60 rpm for 5 min at 37 °C. Subsequently, gastric juice was added, and the mixture was rotated at 60 rpm for 2 h. In the last digestion step duodenal juice and bile were added, and this mixture was rotated at 60 rpm for 2 more hours. Finally, the mixture was centrifuged for 5 min at 3000g, yielding a pellet (i.e. digested OECD-medium) and about 58.5 ml of supernatant (i.e. artificial chyme). Important constituents of the digestion were freeze-dried chicken bile, bovine serum albumin (BSA), mucine, pancreatine, pepsin and urea. After the artificial digestion, 0.9 g/l bile, 15.4 g/l OECD-medium and 3.7 g/l protein were present in the system. The ionic strength of the chyme was 0.14 M and the pH was 5.5 (±0.2). Freshly prepared chyme was used in all exposure experiments.

Cell Culture

Cells from passage 30-45 were grown on Millipore culture plate inserts of mixed cellulose esters (4.2 cm^2, 0.45 μm pore size) for 3 to 4 weeks. During this time the cells were maintained at 37 °C in a humidified atmosphere containing 95% air and 5% CO_2, in culture medium. Culture medium consist of Dulbecco's Modified Eagle's Medium (DMEM), containing 25 mM Hepes and 4.5 g/l glucose, which was amended with 10% inactivated fetal calf serum (FCS), 1% non essential amino acids (NEAA), 2 mM glutamine, and 50 mg/l gentamicine.
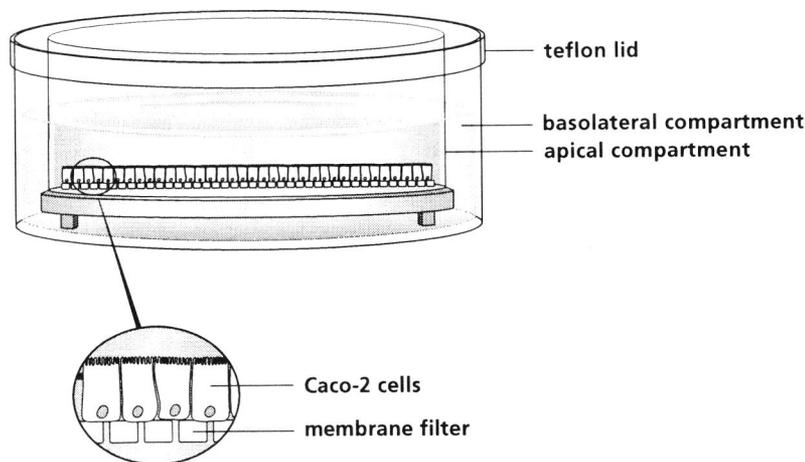
Figure 2. Schematic side-view of a well with a monolayer of Caco-2 cells.

Experiments

The exposure system is schematically presented in Figure 2. The system has an apical and a basolateral side, which represent the intestinal lumen and the blood and lymph drain, respectively. The test compounds were always presented at the apical side, and in all experiments an uncontaminated mixture of DMEM and chyme (1:1, v:v) was added to the basolateral compartment. This mixture of DMEM and chyme will be referred to as DMEM/chyme. Similar conditions as during cell culture were employed, except that the well plates were stirred at approximately 60 rpm. Furthermore, unless mentioned otherwise, DMEM amended with 1% NEAA, 2 mM glutamine and 150 mg/l gentamicine was used for exposure experiments. For all experiments, care was taken not to exceed the solubility of the HOCs based on solubility data of a study of Dulfer *et al.* on DMEM with oleic acid (*79*) and of Oomen *et al.* on chyme (*127*). Losses of test compounds via the air and cross-contamination between and within the wells were prevented by closing the well and insert with a Teflon lid.

Table 1. Overview of the experimental variations.

Apical exposure medium	Spike apical medium (μM)
DMEM/chyme	0.2-0.3 μM by acetone spike
DMEM + 0.5 mM oleic acid	0.2-0.4 μM by acetone spike
DMEM + 0.5 mM oleic acid + 0.9 g/l bile	0.2-0.4 μM by acetone spike
DMEM/chyme	1$\times$, 3$\times$ and 5$\times$ reference level [a], by artificial digestion
DMEM/chyme	5$\times$ reference level [a] by artificial digestion + 50 μM total PCB by acetone spike

[a] DMEM/chyme was prepared with chyme that was obtained from an artificial digestion with spiked OECD-medium. The reference HOC level in OECD-medium was: 7 mg PCB #52, 7 mg PCB #118, 14 mg PCB #153, 7 mg PCB #180 and 2 mg lindane per kg dry OECD-medium.

Several exposure experiments were performed with Caco-2 cells, see Table 1. First, the composition of the apical medium was varied. To the apical compartment 2 ml of 1) DMEM/chyme, 2) DMEM that contained 0.5 mM oleic acid, or 3) DMEM that contained 0.5 mM oleic acid and 0.9 g/l freeze dried chicken bile was added. Oleic acid was chosen as model fatty acid since it is a major product from dietary lipid hydrolysis. An acetone solution with the test compounds was used to spike the different media. In the second series of experiments, different apical concentrations of PCBs and lindane in DMEM/chyme were utilized. Therefore, chyme was artificially prepared with OECD-medium that was spiked with one, three or five times the reference contamination level. In that manner, three chyme solutions with increasing concentrations of mobilized HOCs were obtained. In addition, PCB congeners other than our test compounds were added to the exposure medium with chyme from an artificial digestion with OECD-medium that was spiked with five times the mentioned HOC mixture (total PCB concentration ±1.5 μM). In this manner, a DMEM/chyme solution with a total PCB concentration of 50 μM was obtained.

Sampling procedure

The cells were incubated with PCBs and lindane for various periods of time up to 24 h. A 250 μl aliquot of the apical medium was taken to determine lactate dehydrogenase (LDH) leakage of the cells. Subsequently, several samples of each well were taken for HOC determination. The complete basolateral medium and the rest of the apical medium were sampled and transferred to separate glass tubes that contained 2 ml hexane and internal standards. The apical and basolateral compartments were rinsed twice with 2 ml phosphate buffered saline (PBS) and the basolateral compartment also with 2 ml hexane. The washes were added to the corresponding samples. The apical volume can decrease and the basolateral volume can increase, due to active transport across the cells. Therefore, a correction was performed for the amount of test compound in the LDH sample based on volume determination

via weighing of the samples for HOC determination. The cells were disrupted by 2 ml ethanol and resuspended. This solution was subsequently transferred into a glass sample tube. The remaining filter was rinsed once with 2 ml PBS and once with 2 ml hexane. The washes were added to the cell sample. Thus, all compartments (apical, basolateral and cell) were sampled from each well. In addition, three wells were used for each combination of exposure time and medium.

Sample treatment

2 ml 18 M H_2SO_4 were added to each sample in order to degrade organic interferences. After extensive stirring, about 10 ml water were added, and each sample was restirred. Subsequently, the water phase was frozen by storage at –25 °C, and the liquid hexane phase was collected. Then, about 2 ml new hexane was added to the aqueous sample. The sample was melted, stirred again and stored at –25 °C. This procedure was performed thrice. The combined hexane extracts were evaporated under a gentle nitrogen stream to approximately 100 to 500 µl, prior to analysis by GC-ECD.

Data handling

The time course of the HOC amounts in the different compartments was fitted to a first-order two compartment model (the apical and cell compartment) with the Scientist program of ChemSW™ (Fairfield, Ca). Hence, the curves could be compared quantitatively. An exponential loss term from the apical medium was included in order to account for losses of test compounds during the experiment.

$$\frac{dC_{med}}{dt} = k_{cm} \times C_{cell} - k_{mc} \times C_{med} - k_{ml} \times C_{med} \tag{4.1}$$

$$\frac{dC_{cell}}{dt} = k_{mc} \times C_{med} - k_{cm} \times C_{cell} \tag{4.2}$$

Eq 4.1 represents the change in concentration of a HOC in the exposure medium, C_{med}, in time, t. Eq 4.2 represents the change in concentration of a HOC in the cell compartment, C_{cell}, in time, t. Several rate constants are involved: a constant that represents transport from the apical medium to the cell compartment (k_{mc}), from the cell to the apical medium compartment (k_{cm}), and losses from the apical medium (k_{ml}). A cell volume of 10.6 µl per well was estimated, based on a cell height of 25 µm (*140*) and the filter surface. The standard deviations of the rate constants were estimated by the fit program. Two rate constants are considered to be significantly different ($\alpha \leq 0.05$) if the average values plus or minus two times the standard deviation of both constants do not overlap. The maximum uptake flux, $J_{u,max}$, can be calculated by extrapolation of the uptake flux to zero time, based on eq 4.2. A_{filter} represents the surface

area of the filter, and $C_{med.t=0}$ the contaminant concentration in the apical compartment at zero time:

$$J_{u,\,max} = \frac{\left(k_{mc} \times C_{med,t=0}\right)}{A_{filter}} \tag{4.3}$$

Quality control

The experimental validity was investigated in several manners. The mass balance of the test compounds was calculated by summing up the amounts of each compound measured in the apical, basolateral and cell compartment. These summed amounts were compared to amounts of the corresponding test compounds in the exposure media that were added to cells at the beginning of the experiment.

Furthermore, blanks were always included. Samples of uncontaminated media, chyme, PBS and hexane, and of cells exposed to uncontaminated DMEM/chyme were taken. Also the HOC content of some filters was determined, which had been employed during exposure experiments and had been sampled.

In addition, several system control experiments were performed. First, transfer of the test compounds in time over a filter without Caco-2 cells was determined. Second, sorption of the HOCs to the insert wall was investigated.

The integrity of the cell monolayer of each well was checked by determination of the transepithelial electric resistance (TEER) at room temperature with a Mitchell-ERS Epithelial Voltohmmeter (Millipore Co., Bedford, MA). Cell viability and toxicity after exposure to DMEM/chyme was assessed by means of neutral red uptake by the cells, and by means of determination of the LDH leakage (BM/Hitachi 911, using pyruvate as substrate) from the cells into the apical medium, which is a measure of cell disruption. The LDH leakage was sampled in all wells after exposure and therefore also assessed toxicity due to the other exposure media and contaminants.

Finally, the effect of DMEM/chyme on transport of the reference compounds ^{3}H-mannitol, fluorescein isothiocyanate dextran FD4 (Mw 4000), and fluorescein across Caco-2 monolayers was studied.

RESULTS AND DISCUSSION

Artificial Digestion

During the artificial digestion 54% of lindane and between 30 and 47% of the PCBs were mobilized from spiked OECD-medium. This percentage is similar to results of previous experiments (*127*).

Quality Control

Recovery. 95% (± 18%) were recovered by summation of the amounts of contaminants in the apical, basolateral and cell compartments after 0.5 h of exposure, compared to the amounts of contaminants that were measured in the exposure media. In some cases a gradual decrease in the recovered HOC amount in the system was observed during the 24 h of exposure. However, this decrease was in general only a minor fraction: in most cases more than 70% of each HOC was present after 24 h of exposure compared to 0.5 h of exposure. This indicates that no major losses of test compounds occurred during exposure. We consider the mass balance to be satisfying, especially in light of the extreme hydrophobicity of the contaminants, which results in a high tendency of the HOCs to evaporate and to sorb to surfaces.

Blanks. All blank samples, the filters, and the uncontaminated solutions and compartments of unspiked wells, did not show traces of test compounds. Therefore, the measured test compounds in the different compartments originated from exposure media only, and the sampling procedure was appropriate to remove all HOCs from the filter. In addition, the absence of test compounds in the blank well compartments after 24 h of exposure indicates that no cross-contamination between wells took place.

Filter. Transport of the HOCs over the insert filter without a cell layer appeared to be low: <2% of PCB #118, PCB #153 and PCB #180, and <10% of lindane and PCB #52 were measured in the basolateral compartment after 24 h of exposure. This is in line with a similarly low basolateral HOC concentration after 24 h of exposure with a Caco-2 cell layer (see Figure 3 and 4). Therefore, the filter itself is a major barrier for the HOCs.

The mechanism of HOC transport across the cells is not fully known. Extremely hydrophobic compounds such as PCBs are assumed to go along with the cellular pathway for lipid assimilation. Lipids are transported through the cells via very low density lipoproteins (VLDL) (*78,79*), and subsequently enter the lymph flow (*23,78,80*). Although the presently used cell line expresses some lipid transport, the extent is probably not fully comparable to the *in vivo* situation (*142*). These considerations suggest that the present experimental set-up allows us to study the first step for intestinal absorption, transport of HOCs from the apical medium into the cells.

Sorption to insert walls. Approximately 10-15% and 3% of the total amount in the apical compartment of respectively the PCBs and lindane were sorbed to insert walls. These are minor fractions that will not largely influence the time curves. Therefore, sorption to the insert wall is not considered further, although it might be partly represented by the undefined loss term in eq 4.1.

Cell viability and integrity. The TEER was approximately 500 Ω/cm^2. This shows that the enterocyte cells were mature and that no holes were present in the cell monolayers (*140*).

Neutral red uptake by cells after pre-exposure for 24 h to DMEM/chyme was the same as the uptake by cells after pre-exposure for 24 h to culture medium. This indicates that chyme did not decrease the active uptake of neutral red, which is a measure for cell viability. The LDH values increased with exposure time. However, this was also the case for wells that were exposed to culture medium only, indicating that the cell viability was not compromised by the different media or HOCs. In general, less than 5% of the total amount of cells were disrupted after 24 h of exposure, which we consider to be acceptable.

Reference compounds. The reference compounds showed a clear increase in the amount that was transported across the Caco-2 cells to the basolateral compartment when the cells were exposed to DMEM/chyme compared to culture medium only. The increase in the apparent permeability of mannitol and FD4 approximated a factor 5 to 7 after 2 h of exposure to both media. The apparent permeability of mannitol was increased by a factor 15 after 24 h of pre-exposure to DMEM/chyme and subsequent exposure to mannitol for 1 h, compared to exposure to culture medium only. In a similar experiment the apparent permeability for fluoresceïne was increased by a factor 40. The reference compounds are known to be transported paracellularly, i.e. through the tight junctions and intracellular spaces. The increase in the transport of reference compounds indicates that chyme most probably affected the cell-cell junctions, without clear signs of cellular toxicity. Also *in vivo* it is known that bile salts alter the intrinsic permeability of the intestinal membrane, leading to increased permeation via paracellular or transcellular routes (*23*). Therefore, we regard this state of the monolayer as realistic and workable.

In the two series of experiments 1) the composition and 2) the contaminant concentration of the apical medium were varied. Consequently, both the freely dissolved and the total HOC concentration in the apical compartment were manipulated.

Composition exposure medium

For the first series of experiments, the distribution of PCB #153 among the apical, basolateral and cell compartments as a function of exposure time is presented in Figure 3. Other test compounds showed similar patterns. In the remainder of this paper PCB #153 will be presented graphically as representative of all test compounds. As can be seen in Figure 3, at all time points hardly any contaminants were present in the basolateral compartment. Hence, the first-order two compartment model can be applied to fit the uptake of HOCs from the apical medium into the Caco-2 cells. Furthermore, the amount of contaminant in the cells increased rapidly to reach a steady state within a few hours. Steady state can be assumed when the lines for the apical, cell and total amounts run parallel. Meanwhile, the amount of contaminant in the apical compartment decreased within the same time frame. The amount of contaminants in the cell compartment at steady state is the largest contaminant fraction present in the system. This is illustrated by the ratio k_{mc}/k_{cm}, which represents the HOC concentration ratio over the cell and apical compartment at steady state. This ratio is approximately 10^3, see Table 2 and 3. Therefore, at steady state, the concentration of a HOC is about a factor 10^3 higher in the Caco-2 cells than in the apical medium. Previous studies showed that the freely dissolved concentration of the PCBs and lindane in chyme is small, respectively <1% and ±5% (*111,127*). Thus, the freely dissolved HOC fraction is much smaller than the total fraction that accumulated into the cells, which was always more than 50%. This indicates that more than the freely dissolved compounds contributed to the uptake into the cells.
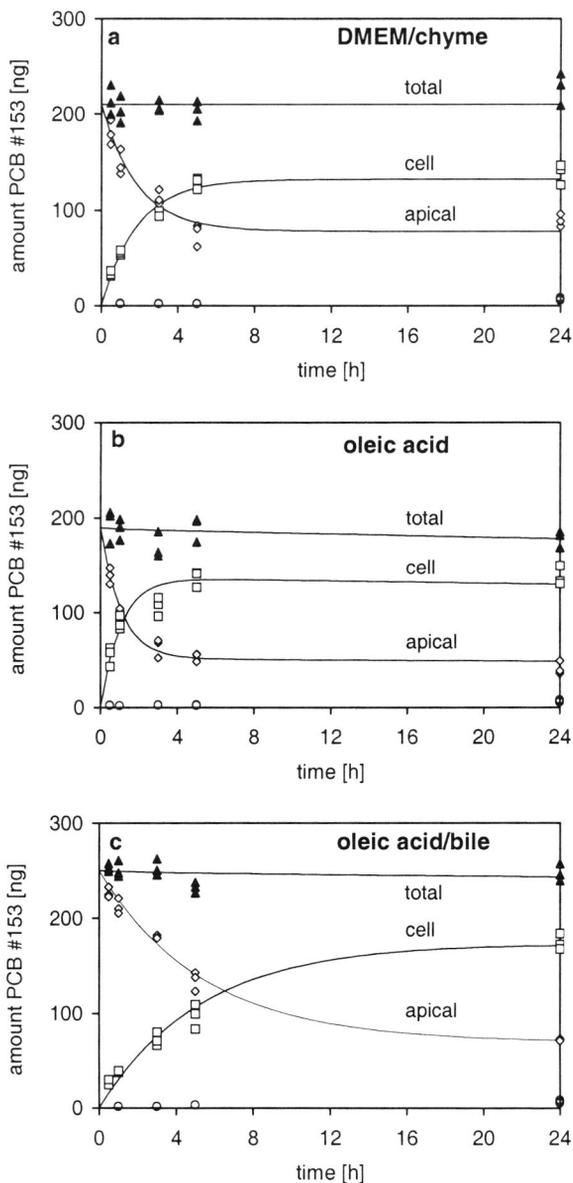
Figure 3. Time curves for PCB #153 for different composition of the apical medium. a) A mixture of DMEM and chyme (1:1, v:v), i.e. DMEM/chyme, b) DMEM with 0.5 mM oleic acid, and c) DMEM with 0.5 mM oleic acid + 0.9 g/l bile. The symbols represent the measured amounts of PCB #153 in the apical (open diamonds), cell (open squares), and basolateral (open circles) compartments, and the sum of these amounts (solid triangles). The lines represent the fitted curves.

Table 2. Rate constants ± standard deviation (±SD) of HOC transport into Caco-2 cells for different apical exposure media. Rate constants are considered to be significantly different if the average value (± 2×SD) of both constants do not overlap, which represents $\alpha \leq 0.05$.

Compound	Apical medium	$(k_{mc} \pm SD) \times 10^{-4}$ (h^{-1})[a]	$(k_{cm} \pm SD) \times 10^{-7}$ (h^{-1})[b]	$(k_{ml} \pm SD) \times 10^{-5}$ (h^{-1})[c]
Lindane	DMEM/chyme	15 ± 1	10 ± 3	
	DMEM + oleic acid	12 ± 1	7 ± 3	
	DMEM + oleic acid + bile	12 ± 1	9 ± 3	
PCB #52	DMEM/chyme	9 ± 1	10 ± 4	
	DMEM + oleic acid	38 ± 4	56 ± 10	
	DMEM + oleic acid + bile	5 ± 1	15 ± 5	
PCB #118	DMEM/chyme	8 ± 1	21 ± 3	6 ± 1
	DMEM + oleic acid	19 ± 1	32 ± 4	18 ± 2
	DMEM + oleic acid + bile	3 ± 0.2	8 ± 2	6 ± 1
PCB #153	DMEM/chyme	7 ± 1	22 ± 3	
	DMEM + oleic acid	14 ± 1	28 ± 4	2 ± 1
	DMEM + oleic acid + bile	3 ± 0.1	6 ± 1	0.5 ± 0.3
PCB #180	DMEM/chyme	6 ± 1	19 ± 7	7 ± 2
	DMEM + oleic acid	7 ± 1	9 ± 4	15 ± 3
	DMEM + oleic acid + bile	2 ± 0.2	6 ± 1	2 ± 0.4

Rate constants representing [a] HOC transport from the apical medium to the Caco-2 cells, [b] from the cells to the apical medium, and [c] losses from the apical medium.

Steady state distributions for different apical media were rather comparable. Apparently, the capacity of the cells for HOCs mainly determines the steady state situation. Uptake into Caco-2 cells occurred fastest for DMEM with oleic acid, than for DMEM/chyme, and slowest for DMEM with fatty acids and bile. This is illustrated by statistically different k_{mc} and k_{cm} values, which are presented in Table 2. The k_{mc} for PCB #153 varied between 3×10^{-4} and 14×10^{-4} h^{-1}, and k_{cm} between 6×10^{-7} and 28×10^{-7} h^{-1}. The difference in the values of the rate constants can be attributed to several counteracting processes that the sorbing constituents exert on the intestinal absorption of HOCs. These processes are presently addressed, assuming that only the freely dissolved HOCs can traverse the membrane.

Possible effects exerted by sorbing constituents. First, constituents such as micelles and proteins can sorb HOCs, and in this manner, decrease the freely dissolved concentration. If the sorbed contaminates do not dissociate, the contaminant fraction that is available for intestinal absorption is reduced. This can result in a lower absorption.

Second, bile salt micelles have been mentioned to act as carriers for fatty acids and HOCs, which are able to traverse the unstirred water layer (UWL) along the intestinal wall (23,79). Thereby, the apparent thickness of the UWL is reduced, which may result in an uptake flux that

is higher than based on the concentration of freely dissolved contaminants. It has been shown that PCBs sorbed to chyme constituents can participate in the uptake flux towards a passive sampling phase, a Solid Phase MicroExtraction (SPME) fiber (*111*). Probably, the rate-limiting step of HOC uptake for both the intestinal membrane and the SPME fiber is diffusion of the HOC through the UWL along the sampling phase. HOCs may dissociate from the micelles and/or proteins in the UWL and subsequently be absorbed. The release can occur due to 1) restoration of the decrease in freely dissolved HOC concentration next to the sampling phase. If the freely dissolved HOCs at the membrane surface are rapidly absorbed, the freely dissolved concentration decreases locally. Subsequently, if association and dissociation kinetics between sorbed HOCs and freely dissolved HOCs are dynamic, sorbed HOCs can dissociate in order to restore this equilibrium. 2) Release of HOCs in the UWL can also occur due to a physiologically based degradation of micelles/proteins. The low pH microclimate near the intestinal wall might induce micelles to disintegrate (*79*) and release sorbed HOCs (*143*). The digestion of proteins to di- and tri-peptides may induce a release of HOCs. The magnitude of the contribution of sorbed HOCs to the uptake flux compared to the situation that all HOCs were freely dissolved depends on two opposing processes. Carriers with sorbed HOCs have a lower diffusivity than the freely dissolved HOCs. This can reduce the transport of HOCs sorbed to bile salts, fatty acids and proteins towards the intestinal wall. On the other hand, these constituents may contain a relatively high load of HOCs. Hence, enough sorbed contaminants may be present in the UWL to maintain a high concentration gradient of the freely dissolved contaminant between the UWL and intestinal cells.

Increasing exposure concentration

Time curves for the second series of experiments with increasing apical exposure concentrations are presented in Figure 4. Since the distribution of the test compounds in chyme is based on partitioning (*127*), the concentration of freely dissolved contaminants and sorbed contaminants can be assumed to increase proportionally with increasing concentration of HOC. The total amount of PCB #153 in the different compartments increases, but the distribution among the compartments in time remains similar. This is also apparent from the rate constants k_{mc} and k_{cm} in Table 3, which are not significantly different. The k_{mc} for PCB #153 varied between 4×10^{-4} and 7×10^{-4} h^{-1}, and the k_{cm} values between 2×10^{-7} and 13×10^{-7} h^{-1}. In addition, the corresponding maximum uptake fluxes were calculated according to eq 4.3, and are presented in Table 4. The maximum uptake fluxes increased with increasing exposure concentration and varied for PCB #153 between 2.4×10^{-3} and 13.2×10^{-3} pmol/cm$^2 \times$s. This indicates that at higher concentrations in the apical medium more HOCs accumulate into the cells, whereas steady state is reached within the same time period: dose-dependent behavior.
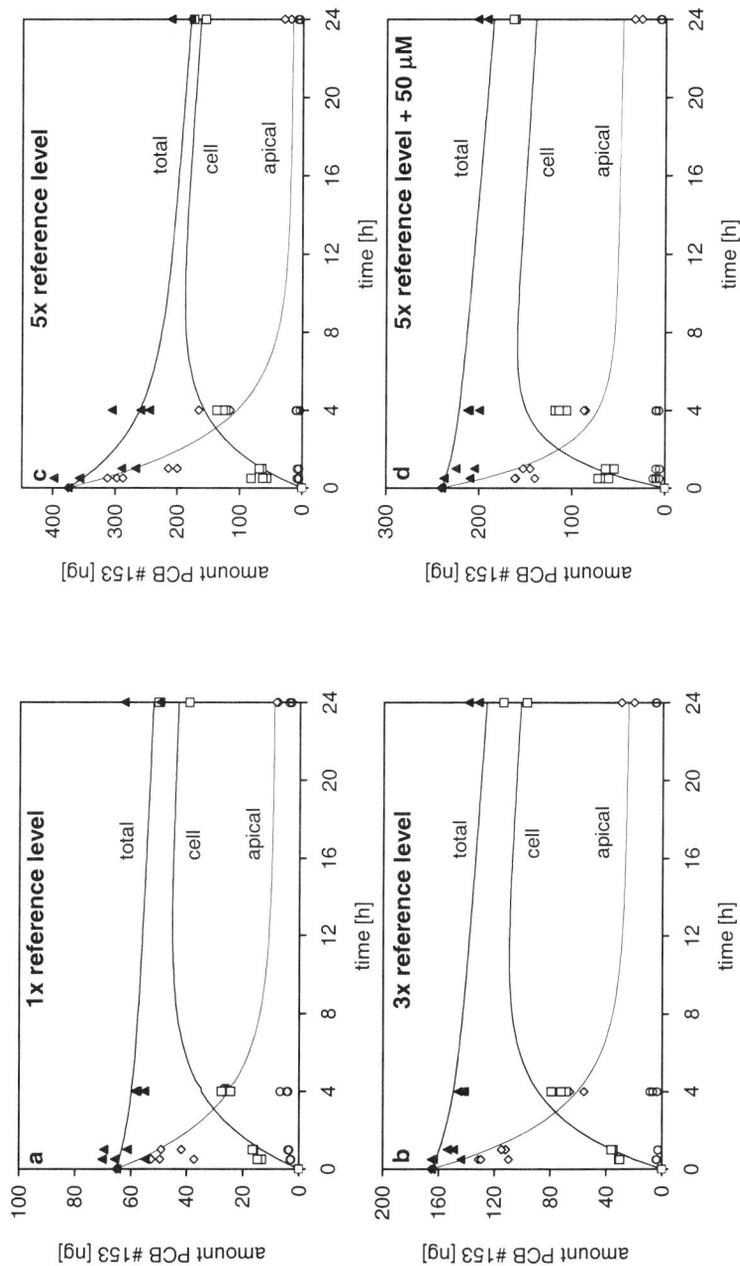
Figure 4. Time curves for PCB #153 for increasing apical exposure concentrations in DMEM/chyme. To that end, chyme was employed that was contaminated via an artificial digestion with spiked OECD-medium. The OECD-medium was spiked with a) 1×, b) 3×, c) and d) 5× the reference mixture: 7 mg PCB #52, 7 mg PCB #118, 14 mg PCB #153, 7 mg PCB #180 and 2 mg lindane per kg dry OECD-medium. For situation d) 50 µM of other PCB congeners were added via an acetone spike. See Figure 3 for explanation of the symbols. For t=1 and t=4 h two replicate wells were used.

Table 3. Rate constants (±SD) for increasing apical HOC concentrations in DMEM/chyme. For explanation reference levels see Table 1. For explanation statistics and rate constants see Table 2.

Compound	Apical exposure concentration	$(k_{mc} \pm SD)$ $\times 10^{-4}$ (h^{-1})	$(k_{cm} \pm SD)$ $\times 10^{-7}$ (h^{-1})	$(k_{ml} \pm SD)$ $\times 10^{-5}$ (h^{-1})
Lindane	1× reference level	11 ± 2	31 ± 8	10 ± 2
	3× reference level	14 ± 1	18 ± 4	14 ± 3
	5× reference level	13 ± 1	11 ± 4	35 ± 7
	5× reference level + 50 µM	19 ± 2	25 ± 6	12 ± 3
PCB #52	1× reference level	7 ± 1	3 ± 4	
	3× reference level	10 ± 2	13 ± 5	
	5× reference level	7 ± 1	5 ± 3	
	5× reference level + 50 µM	9 ± 1	8 ± 2	7 ± 3
PCB #118	1× reference level	15 ± 3	29 ± 11	4 ± 3
	3× reference level	8 ± 1	11 ± 5	
	5× reference level	6 ± 2	5 ± 2	6 ± 2
	5× reference level + 50 µM	10 ± 2	17 ± 7	5 ± 3
PCB #153	1× reference level	4 ± 1	2 ± 2	14 ± 4
	3× reference level	5 ± 1	7 ± 2	7 ± 1
	5× reference level	4 ± 1	4 ± 2	21 ± 3
	5× reference level + 50 µM	7 ± 1	13 ± 4	4 ± 2
PCB #180	1× reference level	8 ± 2	15 ± 7	
	3× reference level	6 ± 1	8 ± 3	
	5× reference level	5 ± 1	9 ± 3	10 ± 2
	5× reference level + 50 µM	9 ± 1	14 ± 4	

Table 4. Maximum uptake fluxes $J_{u,max}$ (±SD) for increasing apical HOC concentrations. For explanation reference level see Table 1, for explanation statistics see Table 2.

	$(J_{u,max} \pm SD) \times 10^{-3}$, for 1× reference level $(pmol/(cm^2 \times s))$	$(J_{u,max} \pm SD) \times 10^{-3}$, for 3× reference level $(pmol/(cm^2 \times s))$	$(J_{u,max} \pm SD) \times 10^{-3}$, for 5× reference level $(pmol/(cm^2 \times s))$	$(J_{u,max} \pm SD) \times 10^{-3}$, for 5× reference level + 50 µM other PCBs $(pmol/(cm^2 \times s))$
Lindane	1.3 ± 0.2	4.7 ± 0.5	5.8 ± 0.7	7.8 ± 0.8
PCB #52	2.5 ± 0.5	9.1 ± 1.5	12.0 ± 2.1	11.0 ± 1.3
PCB #118	3.0 ± 0.6	7.7 ± 1.4	8.7 ± 0.9	13.5 ± 2.6
PCB #153	2.4 ± 0.4	6.5 ± 0.7	11.3 ± 1.6	13.2 ± 1.8
PCB #180	2.3 ± 0.5	4.0 ± 0.5	6.8 ± 0.9	8.2 ± 1.1

Dulfer *et al.* (*79*) measured a similar pattern for PCB uptake by Caco-2 cells at higher PCB concentrations. They loaded their medium with PCBs to their solubility, and obtained a higher PCB concentration due to a higher solubility in the exposure medium caused by addition of oleic acid to a DMEM solution with sodium taurocholate, a bile salt. However, Dulfer *et al.* measured a PCB flux into the basolateral compartment, which is not found in the present study. The same test system was employed in both studies, except that Dulfer *et al.* used polycarbonate insert filters, higher PCB concentrations (35-100 times higher total PCB concentrations), and did not use Teflon lids. In order to investigate whether higher PCB concentrations caused an increased flux to the basolateral compartment, possibly due to an increased permeability of the cells, we exposed the cells to 50 μM extra PCBs. However, no significant differences were observed, see Table 3 and compare Figure 4c and 4d.

Implications

Most HOCs accumulated into the Caco-2 cells. Therefore, high absorption efficiencies can also be expected *in vivo*, probably even higher than *in vitro* since the contaminant concentration in intestinal cells will be lower due to HOC transport from the cells into the body. This is in accordance with rat *in vivo* studies that showed almost complete absorption of PCBs after ingestion in a corn oil matrix (*9,100*). However, with the present knowledge, a quantitative extrapolation to the *in vivo* situation cannot be performed.

Furthermore, these high absorption efficiencies indicate that besides the freely dissolved HOCs, also HOCs sorbed to bile, proteins and oleic acid contributed to the uptake flux towards the Caco-2 cells. It appeared that these constituents affected the intestinal uptake rate. Such processes will most probably also affect the *in vivo* intestinal absorption since environmentally relevant contaminant concentrations and physiologically constituent concentrations are employed. Nevertheless, HOCs that are mobilized from soil should be regarded available for intestinal absorption. Hence, mobilization of HOCs from soil during digestion is considered the most important step that determines the oral bioavailability of the presently used contaminants.

Acknowledgement

Chapter 5

Lead speciation in artificial human digestive fluid

Agnes G. Oomen, Adrienne J.A.M. Sips, Johannes Tolls, Marc A.G.T. van den Hoop

Abstract

For children, soil ingestion via hand-to-mouth behavior can be a main route of exposure to contaminants such as lead. The ingested lead can be mobilized from the soil and form new species during the digestion process. Speciation is known to affect the availability of metals for uptake by biological membranes. In the present study, *in vitro* digestions were performed with (spiked) standard soil. Lead speciation was investigated in the artificial human intestinal fluid, i.e. chyme, in order to gain insight into the lead species and lead fractions that may be available for intestinal absorption. To that end, both a lead Ion Selective Electrode (Pb-ISE) and a voltammetric technique (Differential Pulse Anodic Stripping Voltammetry, DPASV) were used. The results indicate that in chyme only a negligible lead fraction is present as free Pb^{2+}, while lead phosphate and lead bile complexes are important fractions. The lead phosphate complexes appear to be voltammetrically labile, i.e. in dynamic equilibrium with Pb^{2+}. Labile complexes can dissociate and the produced metal ion can subsequently be absorbed. Lead bile complexes may contribute to absorption in a similar manner, or this organometal complex may be able to traverse the intestinal membrane. Therefore, substantially more than only the free metal ion should be considered available for absorption.

INTRODUCTION

Children daily ingest on average 50-200 mg of soil via hand-to-mouth behavior (*66,67,69*). Therefore, for compounds such as lead, soil ingestion can be a main route of exposure in comparison to exposure via air, skin or food. In order to estimate the associated health risk, lead absorption from the gastro-intestinal tract after soil ingestion should be known. Ingested material undergoes a series of digestion processes that affects its absorption. It is generally assumed that the lead that is mobilized from the soil in the small intestine represents the lead fraction that is at maximum available for intestinal absorption. The mobilization of lead from the soil already starts in the mouth. This mobilization process continues more extensively at entering the low pH climate of the stomach, with a pH between 1 and 5. In the subsequent intestinal climate, pH between 5 and 7.5, new Pb complexes may be formed.

Absolute lead absorption from dietary sources typically range from 7 to 15% for adults and from 40 to 53% for children (*144*). It is well known that intestinal absorption in *in vivo* experiments is affected by the form in which lead is added, i.e. lead administered as different salts, in a soil matrix or lead in food (*11-13,16,17,145*). For example, a twelve fold relative difference in absorption in rat was found for seven different lead salts that were added to the diet at approximately equal concentrations (*16*). *In vivo* lead absorption from a soil matrix appears to be highly variable, ranging from 1 to >80% relative to the lead absorption of well soluble lead salts in an aqueous solution. Currently, several factors are discussed with regard to the chemical appearance of lead and intestinal absorption.

The uptake of metals by biological membranes is highly dependent on the physico-chemical form of the metal, i.e. its speciation (*146*). At least the free metal ions can bind to the (intestinal) membrane and/or traverse the membrane. Lead complexes are in most cases not able to overcome the membrane as a whole. Known exceptions are hydrophobic organometal complexes and absorption of lead complexes via processes such as endocytosis. However, assuming that only the free metal ions can be absorbed, a contribution from complexed forms to the metal absorption should be taken into account as well. The kinetics of association and dissociation processes of metal complexes play a key role (*147*). For example, labile species are in dynamic equilibrium with the free metal ion. Such species can dissociate and the thus produced free metal ion can subsequently be absorbed (*147*). In this case, the flux towards the membrane consists of both the free metal ion and labile lead species, while only lead in the form of free Pb^{2+} traverses the membrane. In contrast, the equilibrium is static for inert species, so that these species cannot dissociate and thus cannot be absorbed. Since absorption of ingested lead mainly takes place in the small intestine (*82*), information on the lead speciation such as the physico-chemical lead forms in the small intestinal fluid and their kinetic behavior

can be a powerful approach to understand the availability of lead for intestinal absorption. Such information is presently hardly available, but can be useful for risk assessment purposes.

In the present study, several aspects of lead speciation in artificial human small intestinal fluid, i.e. chyme, are investigated in order to gain insight into the lead species and lead fractions that may be available for intestinal absorption. Human physiologically based *in vitro* digestions were performed with (spiked) standard soil so as to obtain reproducible samples, while also the digestion can be modified as required. Speciation experiments were performed with both a lead Ion Selective Electrode (Pb-ISE) and a voltammetric technique, Differential Pulse Anodic Stripping Voltammetry (DPASV). Emphasis was put on 1) comparison between a chyme and a phosphate solution, 2) the effect of bile on several speciation features and 3) lead speciation patterns in chyme from artificial digestions that were performed with soil spiked with different lead salts.

MATERIAL AND METHODS

All chemicals were of analytical grade and only acid-rinsed materials were employed. OECD-medium was used as standardized artificial soil. The OECD-medium contained 10% peat, 20% kaolin clay, and 70% sand and was prepared according to OECD-guideline 207 (*98*). The dry sand fraction was extensively mixed with a ground and solid lead salt ($PbSO_4$, $Pb(CH_3COO)_2$, $Pb(NO_3)_2$ or $PbCl_2$). Subsequently, the peat and clay fractions were added. After further mixing, 50 mass% of water was added. OECD-medium was spiked at 1, 3 or 5 times the current Dutch intervention value of 530 mg Pb/kg dry matter soil (*37*), i.e. 530, 1590 and 2650 mg/kg dry matter soil. The OECD-medium was stored at 5 °C. Spiking was performed about two years before the artificial digestions and speciation measurements.

Physiologically based *in vitro* digestion
An *in vitro* digestion model designed by Rotard *et al.* (*104*) was employed in the present study in a modified version described by Sips *et al.* (*110*). The digestion process was based on transit times for fasting conditions and physiological constituents of children, and is schematically presented in Figure 1. In short, the digestive juice, saliva, gastric juice, duodenal juice and bile, were prepared synthetically. The saliva was added to 0.9 g OECD-medium and rotated at 60 rpm for 5 min at 37 °C. Subsequently, the gastric juice was added, and the mixture was rotated at 60 rpm for 2 h. In the last digestion step duodenal juice and bile were added, and this mixture was rotated at 60 rpm for 2 more hours. Finally, the mixture was centrifuged for 5 min at 3000*g*, yielding a pellet (i.e. the digested OECD-medium) and about 58.5 ml of supernatant (i.e. the artificial chyme). The chyme contained about 0.9 g/l freeze-dried chicken

bile, 2.6 mM phosphate and had an ionic strength of 0.14 M. Phosphate is present in saliva, gastric juice and duodenal juice (*148,149*). The concentration of dissolved organic carbon was 115±5 mM C (measured by an automatic photometric procedure using a Skalar PhotoMeter 6010/6000), both in the absence and presence of bile or OECD-medium during the *in vitro* digestion. The pH of chyme was about 5.7 directly after digestion, and increased to approximately 6.5 upon overnight storage in the freezer. The pH further increased to approximately 7.5 during storage for several months. These pH values all fall within the physiological pH range that is present in the human small intestine (*23*). For experiments with chyme, which took longer than a few hours, sodium azide (NaN$_3$) was added to prevent bacterial growth.
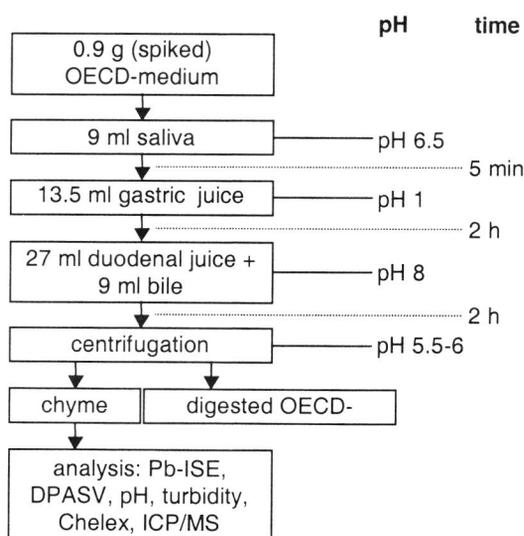
Figure 1. Schematic representation of the procedure of an *in vitro* digestion and the subsequent analysis.

Pb-ISE

The activity of the free Pb^{2+} ion in chyme was determined using a Pb-ISE (Radiometer, ISE25PB9) in combination with a reference electrode with a double salt bridge (Radiometer, REF251). The potential difference between the electrodes in the chyme solution was recorded with a Radiometer PHM95 pH/ion meter. All potentiometric measurements were performed at 25.0±0.5 °C using a water thermostated vessel. Calibration of the potentiometric equipment was performed using a 0.14 M KNO$_3$ solution containing different concentrations of Pb(NO$_3$)$_2$.

In addition, potentiometric titration experiments were performed. To that end, small aliquots of a lead nitrate solution (0,001, 0,01 or 1 M) were added to chyme and the potentiometric

response was read after each addition. Such experiments were performed with 1) freshly prepared chyme and chyme that had been stored at -20 °C, 2) a ten times diluted chyme and an undiluted chyme solution, 3) chyme solutions from digestions in which OECD-medium was used that was spiked with different lead salts (PbSO$_4$, Pb(CH$_3$COO)$_2$, Pb(NO$_3$)$_2$ or PbCl$_2$), 4) chyme solutions from digestions in which the spiking level of the OECD-medium was varied, 5) chyme solution from a digestion with and without bile, and 6) a phosphate solution with a pH, ionic strength and phosphate concentration similar to chyme. Unless mentioned otherwise, chyme was employed from a digestion with uncontaminated OECD-medium and that was subsequently stored at -20 °C. Dilutions of chyme were performed with a 0.14 M KNO$_3$ solution in order to minimize changes in ionic strength.

Turbidity and pH measurements

For several samples, the turbidity (HACH 2100 N) and the pH (Metrohm 744) of the solution were measured after each addition of lead nitrate, in parallel with the potentiometric titration experiment.

DPASV

DPASV measures voltammetrically labile lead, which consists of the free lead ions plus the lead complexes that dissociate within the time-scale of the experiment. Voltammograms were obtained using a Metrohm 663VA stand controlled by a PSTAT 10 potentiostat (AutoLab). Working, reference and counter electrodes were HMDE, Ag/AgCl,KCl$_{sat}$ and glassy carbon, respectively. The deposition potential and time were -0.8 V and 300 s, respectively. A modulation amplitude of 0.05 V was used. Under these conditions, the detection limit for lead was found to be 10 nM.

The voltammetrically labile lead concentration was determined in chyme that was obtained from a digestion in which OECD-medium spiked with Pb(NO$_3$)$_2$, PbCl$_2$ or PbSO$_4$ was employed. Furthermore, chyme with and without bile was prepared and analyzed for OECD-medium spiked with Pb(NO$_3$)$_2$. These chyme solutions were also analyzed with respect to the lead that could be extracted by Chelex, which complexes lead strongly. A column filled with Chelex ion exchanger (100-200 mesh, p.a., Biorad) was used. The Chelex was transferred into the Ca-form after eluting it with consecutively: 2 M HNO$_3$, MilliQ, 1 M NaOH, MilliQ, 2 M Ca(NO$_3$)$_2$ and finally MilliQ. The exchanged lead ions were eluted from the column with 2 M HNO$_3$. The pH of the Chelex extracts was increased to about 2.5 by NaOH, after which the lead concentration was determined by DPASV. The total lead concentrations in the chyme solutions were determined by Inductively Coupled Plasma/Mass Spectrometry (ICP/MS) (Perkin Elmer, Elan 6000).

In addition, the following experiments were performed:

1) The voltammetric complexing capacity of chyme for lead was determined from additions of a lead nitrate solution (10 μM) to a ten times diluted chyme solution, and subsequent analyses by DPASV.

2) The lability of lead complexes in a chyme and in a phosphate solution (with a pH and ionic strength similar to that of chyme) was investigated from the DPASV-signal at varied stirring rates (*137,150*). The sample solutions were 0.14 M KNO_3 spiked with 40 μM $Pb(NO_3)_2$ and with different additions of the phosphate or chyme solution.

3) The average stability constant, K, of lead complexes in chyme was estimated from the decrease in DPASV-signal due to additions of chyme to a 0.14 M KNO_3/40 μM $Pb(NO_3)_2$ solution, buffered by acetate to pH 5.7, according to the procedure described by Van den Hoop *et al.* (*151,152*).

For these experiments chyme from an artificial digestion with uncontaminated OECD-medium was used. Experiments 1) and 3) were performed for chyme that was prepared with and without bile.

RESULTS AND DISCUSSION

Pb-ISE

Pb^{2+} activity measurements in all chyme solutions were below the detection limit of 10^{-5} M. In Figure 2a, several potentiometric titration curves are presented. Included is the calibration curve for $Pb(NO_3)_2$, which covers an activity range from 10^{-6} M up to approximately 10^{-1} M. The calibration curve shows typical Nernstian behavior with a slope of circa 29 mV per log unit of lead activity, starting at approximately 10^{-5} M up to 10^{-1} M. For an undiluted chyme solution it was found that addition of lead up to a concentration of circa 10^{-3} M did not result in a change of the measured potential, indicating that the added lead is complexed by chyme components. Further addition of lead, first induced a large unexpected change in potential (more than 100 mV), whereas at higher lead activities the behavior became again Nernstian, with a slope similar to the one of the calibration curve. Hence, in this region the added lead is certainly free in solution. Therefore, the potentiometric complexing capacity for undiluted chyme is estimated at 10^{-3} M Pb. A ten times diluted chyme solution showed a comparable pattern though one log unit earlier, as was expected, see Figure 2a.
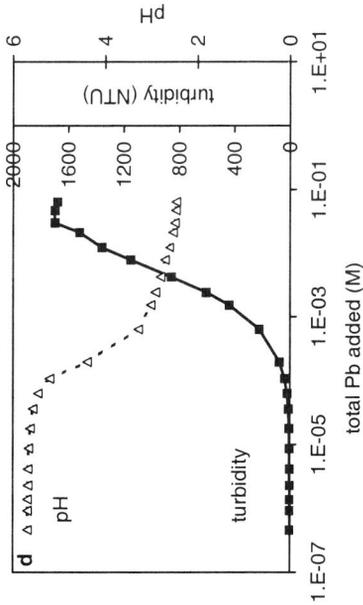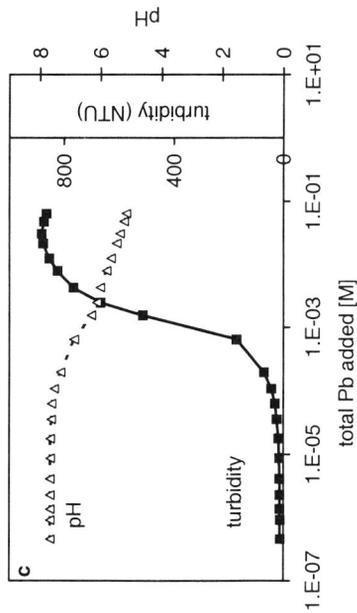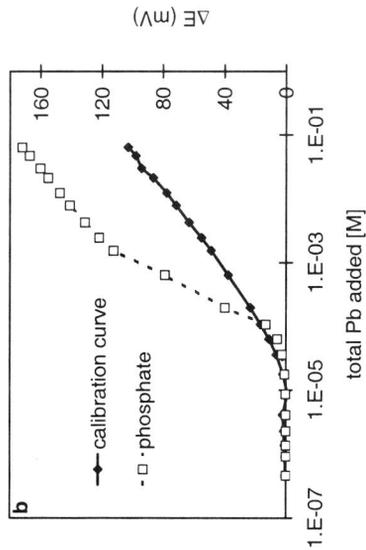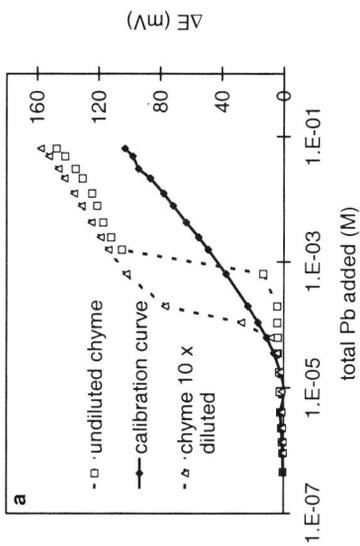
Figure 2. a) A typical ISE calibration curve (solid symbols) and a typical potentiometric titration curve for an undiluted and a ten times diluted chyme solution (open symbols). b) The same ISE calibration curve (solid symbols) and a titration curve for a phosphate solution of the same ionic strength (0.14 M) and phosphate concentration (2.6 mM) as chyme (open symbols). The lower panel shows the effect of the titration on the pH (open triangles) and turbidity (solid squares) for the undiluted chyme, c), and for the phosphate solution, d). The x-axes represent the total lead in the sample due to lead nitrate additions.

Although in some way speculative, we ascribe the large increase in potential to matrix effects, which are clearly observed from pH and turbidity measurements (see Figure 2c). Around the particular lead concentration of 10^{-3} M, the pH of the chyme solution decreases and the turbidity increases. Whereas the potentiometric titration procedure is sensitive enough to distinguish interactions of lead with chyme at different chyme concentrations, differences in lead behavior within approximately a factor 5 are difficult to detect, as the large increase in potential hampers accurate determination of the complexing capacity. We found that no difference could be distinguished between the potentiometric titration curves for 1) fresh chyme and chyme stored at -20 °C, 2) chyme solutions obtained from artificial digestions performed with OECD-medium that was spiked with the different lead salts, 3) chyme solutions from artificial digestions in which the spiking level of the OECD-medium was varied and 4) chyme solutions with and without bile.

Lead phosphate complexes

The chyme became turbid at lead levels of approximately 10^{-3} M, indicating the formation of insoluble complexes. The phosphate concentration in chyme (2.6×10^{-3} M) is within the same range as the potentiometric complexing capacity (10^{-3} M) of chyme for lead, suggesting that lead phosphate complexes comprise an important fraction of the complexing capacity. In addition, considering the anion composition of chyme, formation of lead phosphate complexes is plausible. Lead and phosphate are known to form thermodynamically favorable and insoluble salts. This is illustrated by studies in which phosphate amendments have been used to reduce the solubility and mobility of lead in contaminated soil (*153*). Furthermore, Zhang *et al.* (*154,155*) determined rapid (within 60 min) and complete transformation of soil lead to the lead phosphate complex chloropyromorphite ($Pb_5(PO_4)_3Cl$ (s)) in experiments mimicking gastric and intestinal pH values and in the presence of the phosphate mineral hydroxyapatite. In order to verify the formation of lead phosphate complexes for the present system, potentiometric titrations comparable to the chyme experiments were performed with a phosphate solution. The chyme and the phosphate solution indeed displayed similar behavior, as can be seen by comparison of Figures 2a and 2b. First, both solutions showed an increase in potential, ΔV, at the potentiometric complexing capacity that was sharper than expected. Second, at elevated levels of added lead both showed ΔV values that were higher than the corresponding ΔV values of the calibration curve. Third, for both the phosphate and chyme solution a decrease in pH was observed upon titration (compare Figures 2c and 2d). This pH effect can be explained by deprotonation of $H_2PO_4^-$ and HPO_4^{2-}, which is necessary for formation of lead phosphate complexes. Finally, both solutions displayed increasing turbidity upon titration (compare Figures 2c and 2d). This can be explained by formation of a suspension of insoluble lead phosphate complexes. It appeared that the point at which a potential increase was observed occurred at a lower total lead concentration for the phosphate than for the chyme solution. The

point at which the titration curve became Nernstian, i.e. slope ±29 mV/log unit Pb, was almost similar for both solutions. As it is unclear which reference point to take for comparison, it remains inconclusive whether the titration curve of the phosphate solution is similar to the curve of chyme or of ten times diluted chyme. The possible lower complexing capacity of the phosphate solution than of the undiluted chyme solution might be due to the presence of additional complexing agents in chyme. Nevertheless, the similarities in observations for the chyme and phosphate solutions indicate that an important fraction of Pb in chyme seems to be present as lead phosphate complexes.

DPASV

Voltammetry was used as it is a more sensitive technique than Pb-ISE. In addition, DPASV provides complementary information because voltammetrically labile lead can be measured, which consists of the free lead ions plus the lead complexes that dissociate within the experimental time-scale. However, in this study the absolute labile lead concentration cannot be determined. The DPASV signal depends on diffusion of both the Pb^{2+} ions and the labile lead complexes to the mercury droplet. Since the diffusion coefficient of the labile complexes is unknown, but always smaller than that of the Pb^{2+} ion, the DPASV response represents a fraction of the actual labile lead concentration. Therefore, these data can only be used relative to each other. Table 1 presents the measured voltammetrically labile lead concentrations for different chyme solutions that were obtained from digestions with OECD-medium that was spiked with $Pb(NO_3)_2$, $PbCl_2$ or $PbSO_4$. The voltammetrically labile lead concentration appears to be independent of the initially added lead salt.

Table 1. Concentrations and standard deviations ($\pm$ SD) of the determined voltammetrically labile lead (volt. labile), of the Chelex extractable and of total lead in chyme originating from artificial digestions with OECD-medium that was spiked with different lead salts. Digestions were performed in the presence or absence of bile. The number of replicate measurements is represented by n.

Chyme from digestion with OECD-medium spiked with	Bile	Determined volt. labile lead (μM)	Chelex extractable lead (μM)	Total lead (μM)
$Pb(NO_3)_2$	Yes	0.042 ± 0.010 (n=5)	1.93 ± 0.20 (n=4)	6.0 ± 0.3 (n=2)
$Pb(NO_3)_2$	No	0.086 ± 0.015 (n=4)	1.04 ± 0.16 (n=4)	2.8 ± 0.7 (n=2)
$PbCl_2$	Yes	0.048 ± 0.018 (n=5)	1.79 ± 0.38 (n=4)	5.8 ± 1.0 (n=2)
$PbSO_4$	Yes	0.030 ± 0.004 (n=2)	2.47 ± 0.70 (n=4)	5.6 ± 0.6 (n=2)

Furthermore, Table 1 also presents the total and the Chelex extractable lead concentrations for the different chyme solutions. The total lead concentration represents the lead that was mobilized from the OECD-medium into chyme during artificial digestion. The Chelex

extractable lead represents at least the Pb^{2+} ions, the labile Pb complexes and a fraction of lead complexes that exerts slower dissociation kinetics (*156*). Hence, the Chelex extractable lead (30-40% of the total lead) gives an indication of the lability of lead in chyme, and thereby possibly on the availability of lead for intestinal absorption. Yet, the amount of lead that is absorbed not only depends on the lability of lead, but also on the exposure time and characteristics of the biological phase, the intestinal cells, such as the rate and extent of lead uptake. As expected, the Chelex extractable lead concentrations (about 2 μM) were larger than the fractions of voltammetrically labile lead concentrations (about 0.04 μM), but smaller than the total lead concentrations (about 6 μM). Both the Chelex extractable lead and the total lead concentrations appear to be independent of the initially added lead salt.

The concentrations of Chelex extractable lead, total lead and the fraction of the voltammetrically labile lead have also been measured for a chyme solution that was obtained from a digestion without bile. Table 1 shows that the mobilization of lead from OECD-medium spiked with $Pb(NO_3)_2$ was halved for chyme without bile (11%) compared to chyme with bile (23%). Two explanations are possible: 1) bile salts exert surfactant-like properties and thus might enhance the rate of lead mobilization from OECD-medium due to a decrease in surface tension of the chyme solution, i.e. wetting, or 2) bile increases the capacity of the chyme to complex lead so that more lead can be mobilized.
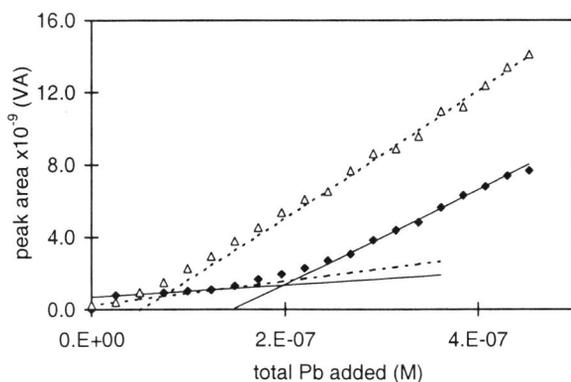
Figure 3. Voltammetric titration curve of a ten times diluted chyme solution that was prepared in a digestion with uncontaminated OECD-medium and with (solid diamonds) and without (open triangles) bile. The voltammetric complexing capacities of these chyme solutions for lead are respectively estimated from the intersecting solid and broken lines. The x-axis represents the total lead in the sample due to the lead nitrate additions, and the y-axis represents the DPASV response.

Figure 3 shows the voltammetric titration curve of chyme solutions from a digestion with or without bile. The voltammetric complexing capacities of these chyme solutions can be quantified via the increase in DPASV signal, and were 2 μM and 0.3 μM, respectively. This difference shows that bile was indeed able to complex lead. Therefore, the lower total lead concentration in chyme without bile was (at least partly) due to a lower in the capacity of chyme to complex lead. The complexing capacity represent the number of binding sites, which is required knowledge to estimate the stability constant K of the following equilibrium:

$$Pb^{2+} + chyme \rightleftharpoons Pb\text{-}chyme \qquad (5.1)$$

The corresponding stability constant K is:

$$K = \frac{[Pb - Chyme]}{[Pb^{2+}] \times [Chyme]} \qquad (5.2)$$
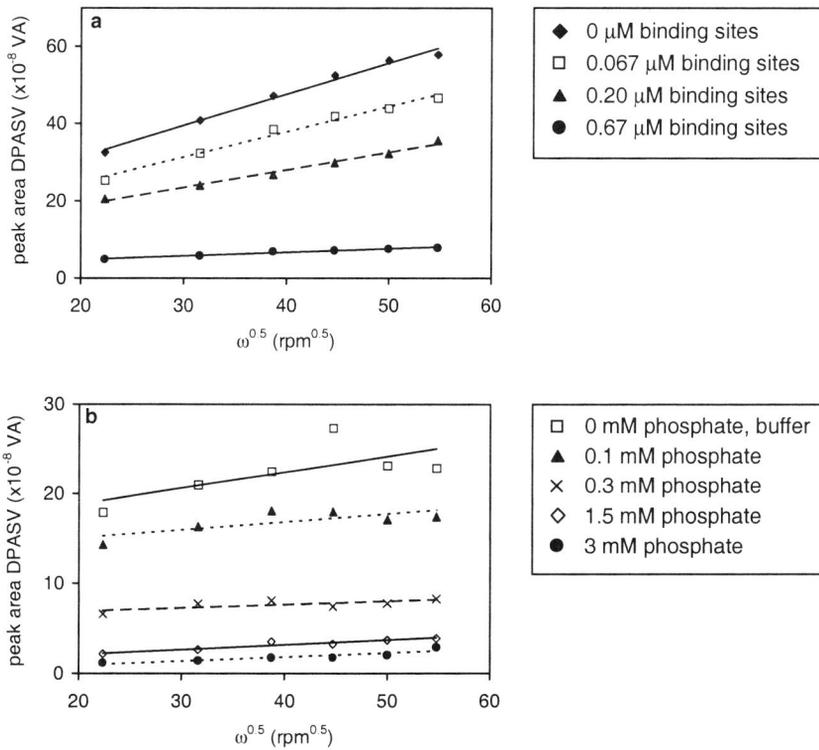
**Figure 4.** The square root of the stirring rate, $\omega^{0.5}$, against the DPASV response in a 0.14 M KNO$_3$/40 μM Pb(NO$_3$)$_2$ solution with different additions of a chyme a) and a phosphate b) solution. The samples with phosphate additions were buffered by acetate to pH 5.7.

Furthermore, an estimate of K can only be made for a system that is voltammetrically labile (*157*). Therefore, experiments were performed in which the stirring rate was varied. A linear relationship between the square root of the stirring rate against the DPASV response was observed for both chyme and phosphate additions, see Figure 4. The samples with phosphate additions were buffered by acetate to pH 5.7. Clearly, lead and acetate forms complexes resulting in steeper sloops and higher DPASV values in the absence (4a) than in the presence of acetate buffer (4b).

The linear relationships in Figure 4 indicate (*137,150*) that the chyme and the phosphate system can be considered as voltammetrically labile for lead. As a consequence, K can be estimated from the decrease in DPASV signal for a 40 μM $Pb(NO_3)_2$ solution after additions of chyme, according to Van den Hoop *et al.* (*151,152*). This decrease in DPASV signal is shown in Figure 5 for a chyme solution with and without bile. The estimated average K for chyme with bile was $10^{6.5}$, and for chyme without bile $10^{7.1}$, assuming complexation capacities of 2 and 0.3 μM, respectively. The chyme solutions for determination of the voltammetric complexation capacities were not buffered, so that the pH was about 7. A higher complexation capacity of the chyme solutions can be expected for pH 7 than for pH 5.7. As calculation for the estimation of K requires the number of binding sites, which is represented by the complexing capacity, the estimated K values for pH 5.7 represent an underestimation.
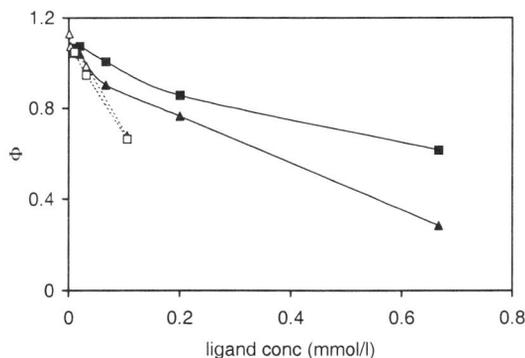
Figure 5. Additions of chyme with (solid symbols) or without (open symbols) bile to a 0.14 M KNO_3/40 μM $Pb(NO_3)_2$ solution against Φ, which represents the DPASV peak area after a certain chyme addition divided by the peak area of the 0.14 M KNO_3/40 μM $Pb(NO_3)_2$ solution.

Different lead salts

The different lead salts and lead concentration levels in the OECD-medium did not clearly show distinct behavior for both the ISE and the DPASV experiments, although differences in

lead absorption between different lead salts in *in vivo* experiments have been observed by others *(13,16,17)*. Comparable to the *in vivo* experiments both well soluble (Pb(CH₃COO)₂, Pb(NO₃)₂ and PbCl₂) and sparingly soluble lead salts (PbSO₄) were investigated. The lack of difference in speciation features is plausible for the ISE experiments since the total lead concentration at the potentiometric complexing capacity (10^{-3} M) originating from additions was much larger than the contribution to the lead concentration from the digestion of OECD-medium (at maximum 3 to 6 μM for OECD-medium spiked at the intervention value of 530 mg Pb/kg dry soil). Therefore, possible differences could not be distinguished. However, since DPASV is a more sensitive technique than ISE, we had expected to see some differences in voltammetrically labile lead concentrations for the DPASV experiments with different lead salts. Nevertheless, the differences were not significant. This can be explained by a similar lead speciation within the differently spiked portions of OECD-medium. The lead from the different lead salts could have formed new and similar species at the moment it became in contact with the OECD-medium or during the 2 years before use. For example, zinc has been shown to be (partly) redistributed over fractions that could be physically separated within 1 to 30 days after spiking *(158)*. In addition, the lack of differences can be explained by different pH values in the stomach compartment. It has been shown that lead dissolution from soil is highly pH dependent *(159)*. Therefore, it is possible that the maximum amount of lead dissolves from the soil at the present low pH of the stomach compartment of the *in vitro* digestion system (pH≈1), so that the speciation differences in the subsequent intestinal compartment might be small. In contrast, less lead is mobilized from soil at the pH in the stomach directly after food ingestion (up to pH 4 to 5), which can be more lead salt dependent, resulting in different speciation patterns in the intestinal compartment.

In vitro digestion models

Up to date, many studies have been performed on lead mobilization in the gastric and intestinal environment using *in vitro* digestion models. These studies provide information on the matrix dependent amount of lead that can be mobilized from matrices such as soil. The mobilized lead is considered to represent the maximum amount of lead that can be absorbed after ingestion of that matrix. Therefore, such experiments might be useful to estimate the site-specific exposure to contaminants from soil *(144)*. In the present study additional information on lead speciation in chyme is obtained, which provides a more detailed understanding of complexation processes in the intestine and of the lead fraction that may be available for absorption. The experiments were performed with chyme that was obtained from an *in vitro* digestion model. Therefore, extrapolation to the *in vivo* situation should be performed cautiously. Yet, we think that *in vitro* and *in vivo* lead speciation in chyme is based on the same principles and complexation processes, which makes such information valuable.

Availability for intestinal absorption

Lead absorption independent of lead speciation via processes such as pinocytosis is considered negligible (*63*). Therefore, lead speciation can be assumed to influence the availability of lead for intestinal absorption. Lead bile complexes appeared to represent important complexes in chyme, and these organometal complexes might be able to traverse the intestinal membrane by passive diffusion based on hydrophobic interaction.

Furthermore, recently, Van Leeuwen (*147*) theoretically described the cases in which labile species contribute to bio-uptake, i.e. transport across a biological membrane. Accordingly, several absorption scenarios can be described if we assume that only free Pb^{2+} ions can bind to the intestinal membrane and/or traverse the membrane. First, if the rate-limiting step of the absorption process is transport across the membrane, the Pb^{2+} concentration is a measure of the intestinal absorption. Second, if transport across the membrane is fast, Pb^{2+} ions are absorbed and the Pb^{2+} concentration next to the membrane decreases. Then, the labile lead complexes can dissociate and these thus produced Pb^{2+} ions can be absorbed as well. Therefore, not the free metal ion concentration is a measure of the absorbable lead, but the labile Pb^{2+} concentration. Third, depending on the time scale of the uptake process, more slowly dissociating lead complexes can dissociate and the subsequent Pb^{2+} ions can be absorbed. These considerations stress the importance of speciation studies for the understanding of metal uptake by membranes.

In the present study, all experiments indicate that important fractions of the lead in chyme are lead phosphate complexes and lead bile complexes. These experiments include different analytical techniques, which measured different aspects of lead speciation. Although chyme is a difficult and unconventional matrix, the results show a consistent picture. The presence of lead phosphate complexes in chyme is evident from the ISE experiments that showed similar behavior for chyme and phosphate solutions, while also the expected decrease in pH and increase in turbidity with increasing lead additions were observed. Additionally, the DPASV experiments showed that both the chyme and phosphate solution contain voltammetrically labile lead complexes. The presence of lead bile complexes is evident from the decreased lead mobilization from soil during artificial digestion without bile, and from the difference in voltammetric complexing capacity and stability constants for chyme with and without bile. Furthermore, the estimated stability constants show that the percentage of lead that is present as free Pb^{2+} is small. This is in agreement with the inability of the Pb-ISE to measure the Pb^{2+} activity in chyme directly, and the high total lead concentration (10^{-3} M) that was necessary to reach the potentiometric complexing capacity of chyme in the titration experiments.

Also several other studies mention the (possible) formation of lead phosphate complexes such as chloropyromorphite (*154,155,160*) and of lead bile complexes (*161*). Since lead

phosphate complexes are thermodynamically stable and appear as insoluble salts, it was assumed that lead phosphate complexes are not available for intestinal absorption. However, the present study showed that lead phosphate complexes can be voltammetrically labile, and should therefore be considered candidates for dissociation and subsequent intestinal absorption. Formation of slightly soluble and labile lead bile complexes was shown by Feroci *et al.* (*161*) for four different bile salts, while lead bile complexes might also be able to diffuse through the intestinal membrane. All this indicates that substantially more than the free Pb^{2+} fraction should be considered as available for absorption.

In the present study some main features of lead speciation in chyme were investigated. This allows a better understanding of lead species and lead fractions that might be available for intestinal absorption. However, the speciation data should be related to intestinal absorption data, while also more detailed speciation information might be useful for risk assessment purposes.

Acknowledgement

Chapter 6

Intestinal lead uptake and transport in relation to speciation: an *in vitro* study

Agnes G. Oomen, Johannes Tolls, Adrienne J.A.M. Sips, and John P. Groten

Abstract

Children might be exposed substantially to contaminants such as lead via soil ingestion. In risk assessment of soil contaminants there is a need for information on oral bioavailability of soil-borne lead. Oral bioavailability can be seen as the result of four steps 1) soil ingestion, 2) mobilization from soil during digestion, i.e. bioaccessibility, 3) absorption from the intestinal lumen, and 4) first-pass effect. Lead bioaccessibility and speciation in artificial human small intestinal fluid, i.e. chyme, have been investigated in previous studies. In the present study, intestinal lead absorption was investigated using the Caco-2 cell line. Cell monolayers were exposed to (diluted) artificial chyme. In 24 h, approximately 27% of the lead accumulated into the cells and 3% were transported across the cell monolayer, without signs of approaching equilibrium. Lead accumulation into the cells showed a linear relationship with the total amount of lead in the system. Bile levels did not affect the fraction of lead that accumulated in the Caco-2 cells. Extrapolation of the lead flux across the cell monolayer to *in vivo* absorption indicates that absorption of bioaccessible lead is incomplete. Furthermore, the results indicate that, as the free Pb^{2+} concentration in chyme was negligible, also lead species other than the free metal ion must have contributed to the lead flux towards the cells. On the basis of lead speciation in chyme, this can be attributed to dissociation of labile lead species such as lead phosphate and lead bile complexes, and subsequent transport of the released free metal ions across the intestinal membrane. The incomplete absorption of bioaccessible lead indicates that less than the bioaccessible fraction of soil-borne lead becomes bioavailable.

INTRODUCTION

Children ingest soil, either accidentally via hand-to-mouth behavior or deliberately. In this manner, a child ingests on average between 50 and 200 mg soil/day, although amounts of as much as 60 g/day have also been observed (*66,67,69*). Hence, soil ingestion can be a main route of exposure to soil-borne contaminants to children. An ubiquitous soil-borne pollutant that may cause health hazards is the heavy metal lead (*1,56*). In current Dutch risk assessment of contaminated soils, oral bioavailability of soil-borne lead is set equal to oral bioavailability of food-borne lead (*1*). However, several studies using test animals demonstrated that absorption and toxicity for lead ingested with soil is lower than for lead ingested with food or aqueous solution (*11-14,17*). In order to gain insight into the health risk associated to lead exposure via soil ingestion, the critical steps determining oral bioavailability of soil-borne contaminants should be investigated.

Oral bioavailability of a soil-borne contaminant is defined as the contaminant fraction that reaches the systemic circulation. Four steps can be distinguished before a contaminant becomes bioavailable: 1) soil ingestion, 2) mobilization of the contaminant from soil during digestion, i.e. bioaccessibility, 3) absorption of the mobilized contaminants, and 4) first-pass effect. Information on oral bioavailability of soil-borne lead is required to assess the health risk associated to soil ingestion. The first step can be considered as a given daily amount of soil that is ingested. The last step, first-pass effect consists of biotransformation and excretion of the contaminant in the intestine or liver. Heavy metals are not biotransformed, but may undergo some biliary excretion (*18,96*). Nevertheless, the first-pass effect is of minor importance for heavy metals such as lead. Hence, knowledge on the second and third steps, bioaccessibility and absorption, can provide insight into oral bioavailability of soil-borne lead.

In a previous study, bioaccessibility of soil-borne lead has been investigated using a physiologically based *in vitro* digestion model (*162*). Digestions mimicking fasting conditions were performed with artificial standard soil, i.e. OECD-medium, spiked with 530 mg Pb/kg dry weight (*162*). It was shown that, for conditions representing the luminal content of the small intestine, about 23% of the lead were bioaccessible. Furthermore, lead speciation in artificial human intestinal fluid, i.e. chyme, was investigated. Speciation is the distribution of a compound among different physicochemical forms. Important lead forms in chyme were lead phosphate and lead bile complexes, while the free Pb^{2+} fraction was negligible (*162*). These findings are in agreement with several other studies that discuss the (possible) formation of lead phosphate (*154,155,160*) and lead bile (*96,161*) complexes. It was also shown that the lead phosphate complexes are labile within a voltammetric time scale (*162*), indicating that the equilibrium with Pb^{2+} is dynamic: dissociation of lead phosphate complexes occurs within

tenths of seconds. In addition, the results suggest that lead bile complexes are voltammetrically labile (*162*), which is in agreement with studies of Feroci *et al.* (*161*) that showed that lead bile complexes are slightly soluble and voltammetrically labile.

In the present study, intestinal absorption of bioaccessible lead is investigated. For that purpose, *in vitro* Caco-2 cells were employed as a model to simulate human intestinal absorption. This cell line is extensively used in drug absorption research (*63,139-141*) and, more recently, to assess absorption of environmental contaminants (*79,163,164*). The flux of compounds that is transported across a Caco-2 monolayer shows good correlation with human *in vivo* absorption (*165*). Caco-2 cells originate from a colon cancer and after growing to confluency on a filter, they differentiate into polarized cells that show many morphological and physiological characteristics of mature enterocytes of the small intestine. Experimentally, the time dependence of lead accumulation into and transport across Caco-2 monolayers, concentration dependency and chyme of different bile content were investigated. The data are interpreted in terms of lead speciation in chyme as determined in previous studies (*162*).

Aim

The aim of the present study was to investigate 1) to what extent bioaccessible lead is absorbed, 2) to relate lead speciation in chyme to intestinal lead absorption, and 3) to gain insight into the processes determining oral bioavailability of soil-borne lead.

MATERIALS AND METHODS

All chemicals were of analytical grade. OECD-medium was used as standardized artificial soil. The OECD-medium contained 10% peat, 20% kaolin clay, and 70% sand and was prepared according to OECD-guideline 207 (*98*). The dry sand fraction was extensively mixed with a ground and solid lead nitrate. Subsequently, the peat and clay fractions were added. After further stirring, 50 mass% of water were added. OECD-medium was spiked at 1, 3 or 5 times the current Dutch intervention value of 530 mg Pb/kg dry weight (*37*), and stored at 5 °C. Spiking was performed approximately three years before the artificial digestions.

Artificial Digestion

The physiologically based *in vitro* digestion model designed by Rotard *et al.* (*104*) was employed in this study in a modified version as described by Sips *et al.* (*110*). The digestion process was based on physiological constituents and transit times for fasting conditions of children. The digestion model is schematically presented in Figure 1. In short, synthetic saliva, gastric juice, duodenal juice and bile were prepared. The saliva was added to 0.9 g OECD-

medium and rotated at 60 rpm for 5 min at 37 °C. Subsequently, the gastric juice was added, and the mixture was rotated at 60 rpm for 2 h. In the last digestion step duodenal juice and bile were added, and this mixture was rotated at 60 rpm for 2 more hours. Finally, the mixture was centrifuged for 5 min at 3000g, yielding a pellet (i.e. the digested OECD-medium) and about 58.5 ml of supernatant (i.e. the artificial chyme). Important chyme components were freeze-dried chicken bile (0.9 g/l) and phosphate (2.6 mM). The ionic strength of chyme was 0.14 M. The pH of chyme increased from 5.7 ($\pm$0.2) directly after digestion, to approximately 6.5 upon storage for several days in the freezer.
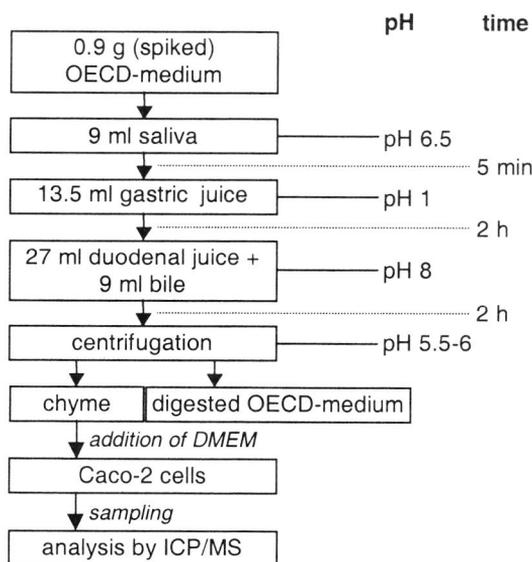
Figure 1. Schematic representation of the procedure of an artificial digestion, exposure of Caco-2 cells to a mixture of DMEM and chyme (1:1, v:v), i.e. DMEM/chyme, and analysis.

Cell Culture

Monolayers of Caco-2 cells from passage 30-45 were grown on Millipore culture plate inserts of mixed cellulose esters (4.2 cm^2, 0.45 μm pore size) for 3 to 4 weeks. During this time the cells were maintained at 37 °C in a humidified atmosphere containing 95% air and 5% CO_2 in culture medium. Culture medium consists of Dulbecco's Modified Eagle's Medium (DMEM), containing 25 mM Hepes and 4.5 g/l glucose, which was amended with 10% inactivated fetal calf serum (FCS), 1% non essential amino acids (NEAA) and 2 mM glutamine, and 50 mg/l gentamicine.

Exposure

Caco-2 cells could not be exposed to pure chyme because it affects the cell viability. Therefore, one part of chyme was diluted with one part of DMEM, amended with 1% NEAA, 2 mM glutamine and 150 mg/l gentamicine. This mixture will be referred to as DMEM/chyme. The conditions used were similar to those employed during cell culture, except for stirring the well plates at approximately 60 rpm. The exposure system is schematically presented in Figure 2. The system has an apical and a basolateral side, which represent the intestinal lumen and the blood and lymph drain, respectively. Lead was always presented at the apical side in 2 ml DMEM/chyme. To the basolateral compartment 2 ml uncontaminated DMEM/chyme was added for all experiments. The pH of DMEM/chyme was buffered by DMEM and was between 7 and 7.5. Unless mentioned otherwise, chyme of standard bile concentration (0.9 g/l) was employed to prepare DMEM/chyme (0.45 g/l bile). Furthermore, the chyme was obtained from artificial digestion with OECD-medium spiked with 2650 mg Pb/kg dry OECD-medium, i.e. 5 times intervention value of 530 mg/kg, and had been stored in the freezer for several days.
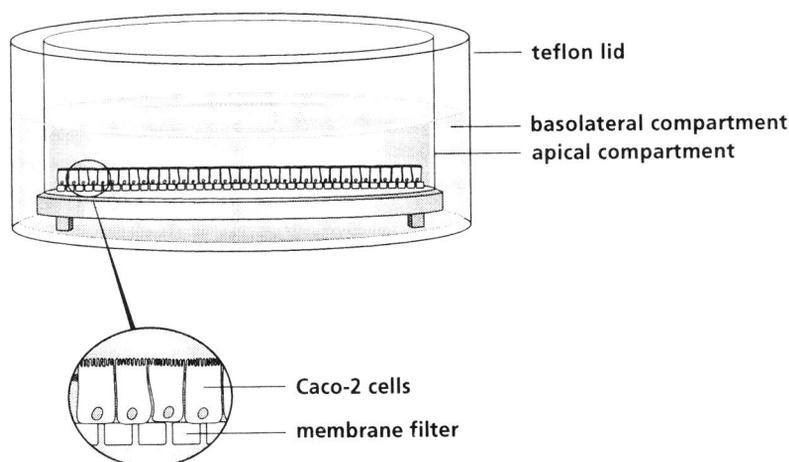
Figure 2. Schematic side-view of a well with Caco-2 cells.

Several series of exposure experiments were performed with the intestinal cell cultures (Table 1). First, the time course of lead uptake by and transport across Caco-2 monolayers was determined. Samples were taken after 1, 3, 5 and 24 h of exposure. Three time curves were obtained, which allowed for comparison between two spiking methods and between fresh and stored chyme. To that end, two exposure media were prepared with freshly made chyme, either contaminated via digestion with spiked OECD-medium or via addition of a lead nitrate solution. Furthermore, another exposure medium was prepared with chyme that had been stored

in the freezer for several days and subsequently was spiked with a lead nitrate solution. In the second series of experiments, the concentration dependency of lead uptake by Caco-2 cells was investigated. To that end, DMEM/chyme was prepared with chyme from *in vitro* digestion with OECD-medium of different spiking levels. OECD-medium spiked with 1×, 3× and 5× the current Dutch intervention value of 530 mg Pb/kg dry was used. In the last series of experiments, the contribution of lead bile complexes to the lead flux towards the cells was examined. For that purpose, DMEM/chyme was prepared with chyme of different bile concentrations: 0×, 0.25×, 0.5×, 0.75×, 1× and 1.5× the default concentration of bile in chyme (0.9 g/l) was employed. For the latter two series of experiments only samples after 24 h of exposure were taken. Three wells were used for each combination of time and medium.

Table 1. Overview of the experiments with Caco-2 cells. The exposure media consist of one part of chyme diluted with one part of DMEM.

Experiment	Chyme employed for exposure media	Exposure time
Time curve	• Freshly prepared chyme spiked with lead nitrate • Freshly prepared chyme contaminated via digestion with spiked OECD-medium • Stored chyme spiked with lead nitrate	1, 3, 5 and 24 h
Concentration dependency	Stored chyme contaminated via digestion with OECD-medium spiked with 1×, 3×, 5× intervention value lead (530 mg/kg dry matter soil).	24 h
Bile	Stored chyme with 0×, 0.25×, 0.5×, 0.75×, 1× and 1.5× the default level of bile (0.9 g/l).	24 h

Sampling procedure and treatment

After exposure, 1.2 ml of the apical and basolateral compartment of each well were transferred into a tube that contained 0.8 ml 1 M HNO_3 and 7.0 ml water. A correction was made for the volume of DMEM/chyme in the remaining apical and basolateral compartment, since the apical volume can decrease and the basolateral volume can increase, due to active transport of water across the cells. These remaining volumes were transferred into a vial and determined by weighing. Subsequently, the cells were rinsed twice with 2 ml phosphate buffered saline (PBS), and the rinses were discarded carefully so that all non-cellular lead was removed. Then, 0.8 ml 1 M HNO_3 was added to disrupt the cells, the cells were scraped off and transferred into an empty tube. Two rinse steps with 2 ml PBS were performed and the washes were added to the corresponding sample. Finally, 4.2 ml water were added to the tubes

containing cell samples. The samples were frozen at -20 °C until analysis by means of Inductively Coupled Plasma/Mass Spectrometry (ICP/MS) (Perkin Elmer, Elan 6000).

Cell viability and monolayer integrity

The integrity of the Caco-2 monolayers was checked by determination of the transepithelial electric resistance (TEER) at room temperature with a Mitchell-ERS Epithelial Voltohmmeter (Millipore Co., Bedford, MA). Cell viability was assessed by lactate dehydrogenase (LDH) leakage (BM/Hitachi 911, using pyruvate as substrate) and neutral red uptake. LDH samples were taken from each well after exposure. Neutral red uptake was measured after pre-exposure for 24 h to DMEM/chyme with low (5 µM) and high (50 µM) lead content and compared to neutral red uptake after pre-exposure to uncontaminated culture medium. Furthermore, the permeability of the monolayer for the reference compound ^{3}H-mannitol was studied after 24 hours of exposure to DMEM/chyme and culture medium.

Permeability coefficient

The permeability coefficient, P_{coeff} (cm/s), of lead and ^{3}H-mannitol is calculated according:

$$P_{coeff} = \frac{P}{A \times C_0} \tag{6.1}$$

P, the permeability flux (mol/s), represents the rate at which a compound is transferred across the Caco-2 monolayer into the basolateral compartment. C_0 is the initial apical concentration of the test compound (mol/ml), and A the surface area of the filter where the Caco-2 cells grow on (cm^2).

RESULTS

Cell integrity and viability

The TEER of the cultured cell monolayers was approximately 500 Ω/cm^2, indicating that the enterocyte cells were mature and that no holes were present in the cell layers after 3 to 4 weeks of culture (*140*).

The active uptake of neutral red by Caco-2 cells after pre-exposure for 24 h to DMEM/chyme for both Pb levels was the same as uptake by the cells after pre-exposure for 24 h to culture medium. In addition, the LDH values increased with exposure time to about 5% or less of the maximum LDH level. The LDH values did not differ for wells exposed to DMEM/chyme or culture medium. Hence, both neutral red and LDH results indicate that

neither DMEM/chyme nor lead compromised the cell viability under the present test conditions.

The P_{coeff} for ^{3}H-mannitol was 0.9×10^{-7} cm/s after exposure to culture medium only, and was increased by a factor 16 after 24 h of pre-exposure to DMEM/chyme. The increase in mannitol transport across the cell layer, without concomitant increase in LDH release, indicates that chyme most likely affected the cell-cell junctions, without clear signs of cellular toxicity. Since alterations of the permeability of the intestinal wall are also triggered by bile salts *in vivo* ((*166,167*) and references in (*23*)), we regard the observed increase in transport rate of the reference compounds as a normal physiological response. Therefore, the cell integrity and viability data indicate that the present experimental set-up functions in analogy to the physiological reality.

Time curve

As can be seen in Figure 3, the amount of lead in the apical compartment decreased by approximately one-fourth in 24 h. Within the same time interval, a corresponding increase was observed in the amount of lead in the cells. An increase of the cellular lead accumulation was observed after each time point. This indicates that the cells were not saturated with lead within 24 h of exposure. Although not always significant (considered significant if $\alpha \le 0.05$), the cellular accumulation tended to go faster between 5 and 24 hours than between 0 and 5 hours. This slightly increasing rate might have been caused by increased membrane permeability due to the chyme in the exposure medium. However, the effect of chyme on the cellular lead accumulation probably is small, since the cellular lead accumulation in time does not largely deviate from linearity.

A small fraction of lead was transported into the basolateral compartment. No large differences in the lead distribution among the compartments were observed between spiking of DMEM/chyme with a lead nitrate solution or employing contaminated chyme that was obtained from an artificial digestion with spiked OECD-medium (Figure 3a versus 3b). Furthermore, no differences were observed between the time curves of DMEM/chyme with fresh or stored chyme (Figure 3b versus 3c). This indicates that stored chyme could be employed for further experiments.
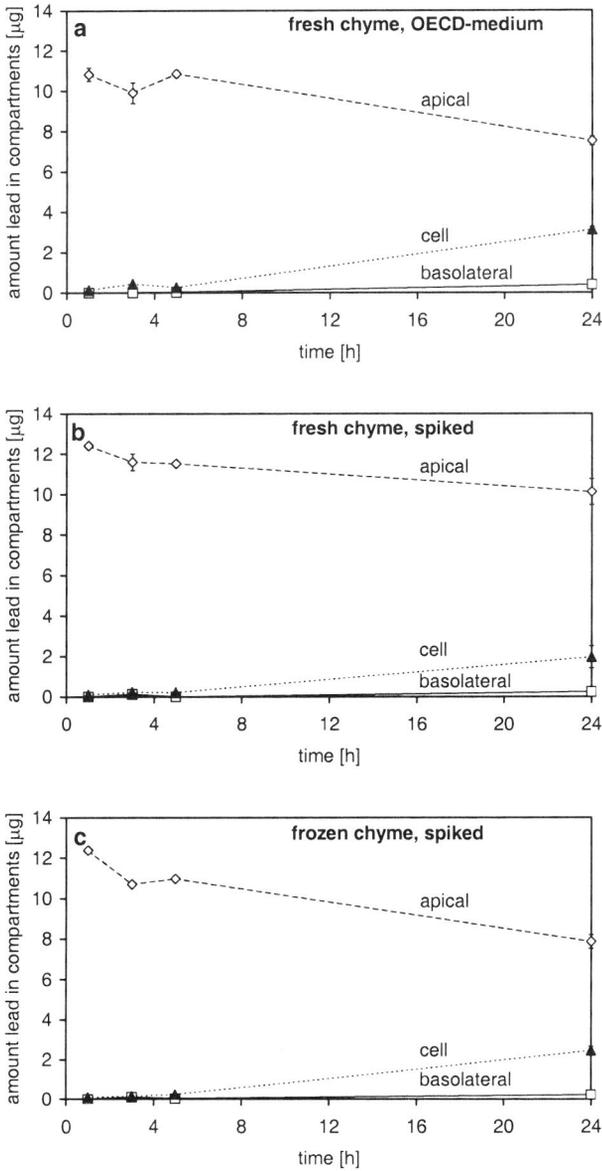
Figure 3. Time curves of lead uptake by and transport through Caco-2 monolayers after exposure to DMEM/chyme. To that end, chyme was employed that was, a) freshly prepared and contaminated with lead via an artificial digestion with spiked OECD-medium at 5× intervention value, b) freshly prepared and spiked with a lead nitrate solution, and c) stored (few days in freezer) and spiked as in b).

Concentration dependency

Figure 4 presents the lead distribution among the different compartments after 24 h of exposure to DMEM/chyme with increasing lead concentration. The amount of lead in the apical and cell compartments after 24 h showed a linear relationship with the total amount of lead in the well. The r^2 values were 0.999 and 0.997, respectively. Relationships with the amount of lead in the basolateral compartment could not be determined, since the amount of lead in the basolateral compartment was hardly measurable.
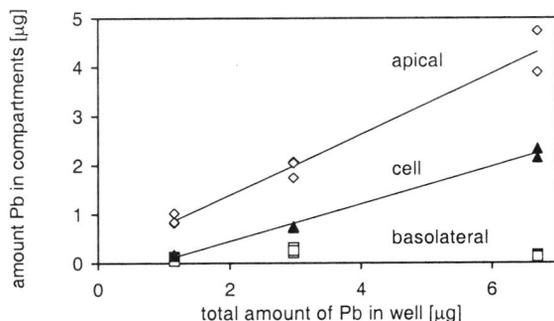
Figure 4. Distribution of lead among the apical, basolateral and cell compartment after 24 h of exposure of Caco-2 cells to DMEM/chyme with different lead concentrations. To that end, chyme was employed that was prepared by artificial digestion with OECD-medium spiked with 1×, 3× or 5× the current Dutch intervention value of 530 mg Pb/kg dry.
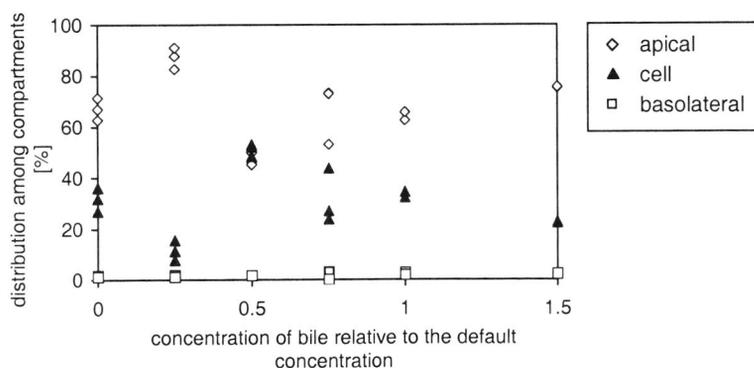
Figure 5. Relative distribution of lead among the apical, basolateral and cell compartment after 24 h of exposure to DMEM/chyme with increasing bile content. The x-axis expresses the bile concentration relative to the bile concentration in DMEM/chyme after a default situation (0.45 g/l).

Bile

Figure 5 shows the relative distribution of lead among the different compartments after exposure for 24 h to DMEM/chyme with varying bile concentrations. No increasing or decreasing trend with increasing bile concentration could be observed for all compartments within the experimental variation.

Lead transport and cellular accumulation

Considering all experiments, after 24 h of exposure on average 70% (SD ±11%) of the lead was still present in the apical compartment, 27% (SD ±11%) in the cells and 3% (SD ±3%) in the basolateral compartment. From these values, the P_{coeff} for lead can be calculated according to eq 6.1, and is $1.7×10^{-7}$ cm/s.

DISCUSSION

Experimental conditions

In the present study, an effort is made to expose Caco-2 cells to lead of a speciation similar to the *in vivo* situation. To that end, chyme obtained from an *in vitro* digestion model was employed. In order to prevent toxicity of the Caco-2 cells, the chyme was diluted with DMEM (v:v, 1:1). DMEM contains high salt concentrations that may form complexes with lead and thereby affect the lead speciation, for example phosphate, chloride and carbonate can be present in the mM range. Nevertheless, we expect that the main features of lead speciation in DMEM/chyme and in chyme are similar, since these salt concentrations are similar or even higher in chyme (*110*). Hence, it can be assumed that in both solutions the free Pb^{2+} fraction is negligible, and that important lead species are lead phosphate and lead bile complexes.

Chyme is a complex solution that may bring about some experimental difficulties. It contains many lead complexing agents such as phosphate, bile, carbonate and chloride. Especially lead phosphate complexes are extremely insoluble, and its formation is thermodynamically favored (*153,154,168-170*). Since the phosphate concentration in chyme is 2.6 mM, the solubility product of lead phosphate is most probably exceeded, as it also would be in most cell culturing media. This means that speciation studies with sparingly soluble metals are difficult to perform under conditions in which cells have to be kept viable. The presence of complexing agents in DMEM/chyme indicates that a suspension may be formed. Lead may precipitate if large particles are formed, possibly affecting the experimental results. For example, precipitation of macroscopic lead particles in DMEM/chyme or in chyme may explain the difference in the total amount of lead per well for 5× the intervention value for the first and second series of experiments (±12 µg in Figure 3 versus ±7 µg in Figure 4). Nevertheless, the presence of insoluble complexes is not an artifact, as lead phosphate

complexes are expected to exist *in vivo* too. Hence, to our opinion, the presently used experimental set-up is a valid and physiological simulation of intestinal cells exposed to chyme containing lead.

Lead speciation and cellular uptake

The mechanism of lead absorption is supposed to involve both the transcellular and paracellular pathway (*18,82,83*). In the present section we consider which lead species have contributed to the transcellular route. Therefore, we focus on the results of lead determined in the cell compartment, as this lead must have traversed or has been complexed to the luminal membrane. Previous studies showed that the free Pb^{2+} fraction in artificial chyme is negligibly small (*162*), and it can be assumed that free Pb^{2+} is negligible in DMEM/chyme as well. At least free metal ions are able to bind to the intestinal membrane and/or traverse the membranes (*74,76,77*). Yet, the *in vitro* experiments with intestinal cells show that a considerable fraction, about 27% after 24 h, of the lead presented at the apical site was determined in the cell compartment, see Figures 3, 4 and 5. Thus, a larger lead fraction than the free Pb^{2+} fraction had accumulated into the intestinal cells. This implies that lead species other than Pb^{2+} must have contributed to the flux towards the Caco-2 cells.

Furthermore, the fraction of lead that accumulated into the Caco-2 cells appeared to be independent of the bile level in DMEM/chyme (see Figure 5). Nevertheless, the experimental variation of bile was expected to have a profound effect on the lead speciation in DMEM/chyme. Previous studies showed a clear effect of the absence of bile on the complexing capacity and stability constant of lead for chyme (*162*). The range of bile concentrations for the Caco-2 experiments (0 to 0.68 g/l) was similar to the range that was employed for the lead speciation experiments (0 to 0.9 g/l). Therefore, the variation of bile in DMEM/chyme can be assumed to affect the speciation of lead. Yet, the mechanism of lead uptake should be able to explain bile-level independent lead accumulation in the cells.

The observed lead accumulation in the intestinal cells can be explained in several ways. Presently, the different possibilities are considered.

Pinocytosis. A contribution via pinocytosis of small volumes DMEM/chyme containing lead may have occurred. Although this cannot be fully excluded, pinocytosis is not a probable route for drug absorption in the intestine (*63*). Therefore, it is unlikely that about 27% of the lead was transferred from the apical medium into the Caco-2 cells in 24 h via this mechanism.

Hydrophobic lead complexes. In parallel to the free Pb^{2+} ions, hydrophobic organometal complexes may diffuse across the intestinal membrane and contribute to the lead flux towards the intestinal cells. Lead species such as lead phosphate complexes are large (compared to Pb^{2+}) and hydrophilic and are therefore considered not able to traverse the membrane by passive diffusion. However, lead bile complexes may be able to diffuse across the luminal membrane.

In that case, it can be expected that the contribution of lead bile complexes to the lead flux into the intestinal cells is much larger than the contribution of Pb^{2+}, as the free Pb^{2+} fraction is negligible. Therefore, based on this mechanism, an increasing lead accumulation into the cells is expected for increasing bile levels. However, although Figure 5 shows a lot of scatter, an increasing trend with increasing bile levels is not observed. This implies that a contribution to the lead accumulation into the intestinal cells caused by diffusion of lead bile complexes across the membrane does not play an important role.

Labile lead complexes. If transfer of Pb^{2+} across the membrane is fast compared to transport through the diffusion layer along the intestinal wall, the free metal ion concentration next to the membrane decreases due to lead uptake. Then, some complexes can dissociate within the experimental time scale and the free lead ions thus produced can be absorbed as well (*147*). Under these conditions, not only the free metal ions contribute to the metal flux across the biological membrane, but also these rapidly dissociating, i.e. labile, metal species (*147*), although only lead in the form of Pb^{2+} is transported across the luminal membrane.

The experimental results indicate that uptake took (mainly) place via dissociation of labile lead complexes that then can contribute to the lead flux towards Caco-2 cells. Lead species that may contribute are lead phosphate and lead bile complexes, as they are important lead forms in chyme and voltammetrically labile. Voltammetric lability indicates that these species can dissociate within the time scale of the voltammetric experiment, i.e. within tenths of a sec, and contribute to the lead flux towards a mercury surface used by this technique (*162*).

The experimental conditions for the transport studies with Caco-2 cells were different than for the voltammetric studies. The equilibria between Pb^{2+} and complexed lead species were disturbed in the entire exposure medium, as the Caco-2 cells were able to accumulate about 27% of the lead in 24 hours. Consequently, dissociation of lead complexes was not related to the time for lead to diffuse across the diffusion layer along the intestinal cells. This indicates that, compared to the voltammetric situation, even more slowly dissociating lead complexes may have been able to dissociate and contribute to the lead accumulation into the cells.

An explanation based on transport of Pb^{2+} across the intestinal membrane, which is buffered by labile complexes, can account for the bile-level independent lead accumulation in the cells, although lead bile complexes constitute an important lead fraction in chyme (*162*). The fraction of lead bile complexes can be assumed to increase for increasing bile concentrations in DMEM/chyme. Consequently, the free Pb^{2+} and lead phosphate fractions decrease. If lead bile complexes do not contribute to the uptake flux, a decrease in the lead fraction that accumulates into the Caco-2 cells is expected with increasing bile concentration. In contrast, if the lead bile complexes do contribute to the uptake flux, a less steep decrease, no decrease or an increase might be observed. Although Figure 5 displays a lot of scatter, the fraction of lead that

accumulated into the cells does not show a clear decreasing trend with the bile concentration. Hence, the experimental results suggest that lead bile complexes indeed contribute to the flux towards the intestinal cells.

Furthermore, a pool of labile lead complexes that dissociate in order to restore the equilibrium with Pb^{2+} can explain the concentration independent accumulation into the cells. The free Pb^{2+} concentration can be considered as the driving force for lead transfer towards the intestinal cells. For higher total lead concentrations in DMEM/chyme, also higher Pb^{2+} concentrations are expected. The free Pb^{2+} concentration is not expected to change largely in time, since the labile lead complexes buffer the Pb^{2+} concentration. Hence, if the free Pb^{2+} concentration represents a constant fraction of the total bioaccessible lead concentration, the lead accumulation in the cells would display a linear relationship, as is measured.

As lead phosphate complexes are voltammetrically labile, they should be considered available for intestinal absorption. However, if macroscopic lead phosphate particles are formed, dissociation is expected to be slower than for microscopic lead phosphate complexes, making them less available for absorption. Therefore, if redissolution becomes slower, formation of macroscopic particles may decrease the lead flux towards intestinal cells.

These experimental results are in agreement with *in situ* studies by Cikrt and Tichý (*96*), and everted gut sac studies by Hilburn *et al.* (*171*), that showed that no decrease was observed for lead transport across the intestinal epithelium comparing the presence and the absence of bile. Toxicity caused by bile salts did probably not occur. The *in situ* study was performed at or below physiological bile levels as the experiments were performed with bile duct cannulated and bile duct non-cannulated rats (*96*). For the everted gut sac experiments low bile concentrations and short exposure times (compared to *in vivo*) were employed (*171*).

In vitro versus *in vivo*

For extrapolation from the present *in vitro* observations to *in vivo* absorption, the lead flux across the Caco-2 monolayer is employed. This gives a better indication of *in vivo* absorption than the cellular lead accumulation as it includes both the para- and transcellular permeation route. Artursson and Karlsson demonstrated that a good correlation was obtained between oral absorption in humans and P_{coeff} values determined in the Caco-2 model for a broad chemical range of compounds (*165*). The correlation shows that compounds with a $P_{coeff} < 1 \times 10^{-7}$ are poorly absorbed, $> 10 \times 10^{-7}$ cm/s are well absorbed, and in between are absorbed incompletely.

In the present study, the permeability of lead (1.7×10^{-7} cm/s) was 2-fold higher than the permeability of mannitol after exposure to culture medium (0.9×10^{-7} cm/s), and 8-fold lower than the permeability of mannitol after exposure to DMEM/chyme for 24 h (14×10^{-7} cm/s). These permeabilities are comparable to the P_{coeff} for ^3H-mannitol (1.8×10^{-7} cm/s) found by

Artursson and Karlsson (*165*). Hence, extrapolation to the *in vivo* situation suggests that lead is incompletely absorbed. This is in agreement with *in vivo* studies, which typically show that lead absorption ranges from 35 to 70% for fasting adults and from 2 to 25% for soluble lead salts, while children absorb more lead than adults do (*2,19,20,56,82,89,144,145*).

Oral bioavailability of soil-borne lead

The incomplete bioaccessibility of lead determined by several physiologically based *in vitro* digestion models (for example (*160,162,172,173*)), demonstrates that mobilization from soil is an important process that decreases the bioavailability of soil-borne lead. As all food-borne lead is assumed to become bioaccessible, and risk assessment is based on lead bioavailability from food, bioaccessibility can cause a difference in the oral bioavailability of soil- and food-borne lead. In addition, the present study provides more insight into the absorption step of oral bioavailability of soil-borne lead. The results indicate that more than the free metal ion fraction is absorbed. Lead species that are likely to contribute to the lead flux towards intestinal cells are voltammetrically labile species such as lead phosphate and lead bile complexes. Due to the larger experimental time scale also more slowly dissociating lead complexes may contribute to the intestinal absorption. Nevertheless, both the *in vitro* experiments and the extrapolation to *in vivo* absorption indicate that not all bioaccessible lead is absorbed. Therefore, also the absorption process decreases the lead fraction that becomes bioavailable. It is likely that the mechanism of lead absorption, and the relation between lead absorption and lead speciation in chyme, is similar for bioaccessible lead originating from soil or from food. This suggests that bioaccessible lead from both matrices is incompletely absorbed. However, further research into this issue is recommended.

Acknowledgement

Chapter 7

Summary and general discussion

Ingestion of contaminated soil can be an important route of exposure to soil-borne contaminants, especially for children (*1*). To estimate the health risk associated to this exposure route, and to assess intervention values for contaminants in soils, one needs to know the oral bioavailability of the soil-borne contaminant. The objective of this thesis was to gain insight into the determinants of oral bioavailability of soil-borne PCBs, lindane and lead. Oral bioavailability of soil-borne contaminants is defined as the contaminant fraction that reaches the systemic circulation. Before a soil-borne contaminant becomes bioavailable it has to go through four steps, see flow chart: 1) soil ingestion, 2) mobilization from soil into chyme during digestion, i.e. bioaccessibility, 3) intestinal absorption of the bioaccessible contaminant, and 4) first-pass effect.

ingestion	bioaccessibility	absorption	first-pass effect
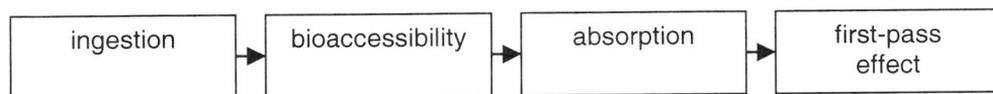
In the present chapter, the experimental results of the individual chapters are summarized and discussed from a more general point of view. First, the main results are presented for the PCBs and lindane and interpreted in the perspective of mass transfer processes. With use of this interpretation, the impact of bioaccessibility and intestinal absorption on oral bioavailability of

the soil-borne HOCs is discussed. Subsequently, the results are summarized for lead and the same topics are discussed. Differences and similarities between the HOCs and lead, and insights relevant for exposure assessment are considered. Finally, the main conclusions of this thesis are presented.

PCBs AND LINDANE

Summary PCBs and lindane

The bioaccessibility and distribution among sorbing constituents of several PCB congeners and lindane following *in vitro* digestion is described in **Chapter 2**. After artificial digestion representing fasting conditions, about 60% of the PCBs were sorbed to OECD-medium, 25% to bile salt micelles, and 15% to digestive proteins. The respective values for lindane were 40%, 23%, and 32%. Thus, about 40% of the PCBs, and 60% of lindane were bioaccessible. The mobilization of the HOCs from OECD-medium increased when more bile or protein was added during digestion. In contrast, the mobilization decreased when a constant amount of HOCs was added to the digestion system with increasing amounts of OECD-medium.

SPME was applied to a chyme solution in **Chapter 3**. The results demonstrate that PCB #52 sorbed to proteins contributed to the uptake flux towards a passive sampling phase, a SPME fiber. This contribution of sorbed species was probably caused by a dynamic equilibrium between sorbed compounds and freely dissolved compounds. If the freely dissolved concentration in a water layer surrounding the fiber is decreased due to HOC uptake by the SPME fiber, sorbed HOCs may dissociate in order to restore the equilibrium with the freely dissolved compound. These thus produced freely dissolved HOCs can diffuse into the SPME fiber. Therefore, the net flux towards the SPME fiber consisted of both the freely dissolved and sorbed contaminants, while only freely dissolved HOCs diffused into the SPME fiber coating. Such behavior is also expected for the other organic test compounds. Furthermore, assuming that only freely dissolved contaminants contributed to the flux towards the SPME fiber, the freely dissolved fraction in chyme of lindane, PCB #52, PCB #118, PCB #153 and PCB #180 was respectively 10%, 1.4% 0.4%, 0.9%, and 0.4%. As also sorbed forms contributed to the HOC accumulation into the SPME fiber, these data should be considered an upper limit.

In **Chapter 4** *in vitro* intestinal Caco-2 cells were employed to mimic intestinal absorption. The cells were exposed to HOCs in solutions with varying concentrations of chyme, bile, and oleic acid. Steady state was observed within several hours. During this exposure time a large fraction, i.e. >50%, of the HOCs accumulated into the cells, although **Chapter 2** and **3** indicate that only a small fraction of the HOCs in the exposure medium was freely dissolved. Hence,

PCBs and lindane sorbed to bile salt micelles, proteins and oleic acid must have contributed to the accumulation into the cells. Similar to the HOC flux towards the SPME fiber, such a contribution can be attributed to replenishing the depletion of freely dissolved HOCs by dissociation of sorbed HOCs, and subsequent diffusion across the intestinal membrane.

General Discussion PCBs and lindane – A mass transfer perspective

Concept. The exposure time and the capacity of the receiving phase to accommodate contaminants, largely determine the amount of contaminant that can be transferred from one phase into another. In the context of bioaccessibility and absorption, two mass transfer processes are involved: 1) transfer from contaminants in soil into chyme, and 2) transfer from contaminants in chyme into and across intestinal cells. The effect of time and capacity to accommodate HOCs is illustrated by two extreme hypothetical examples. First, after infinite transit times with infinite volumes of the digestive juices, i.e. infinite sink, all contaminants would be bioaccessible. Second, after infinite intestinal exposure time with an infinite number of intestinal cells all contaminants would be absorbed. For such conditions also extremely slowly dissociating HOCs would have been able to dissociate from soil and become bioaccessible or dissociate from sorbing chyme constituents and become absorbed. Presently, the results of the different chapters are discussed and compared in light of the experimental and physiological time scale, and the capacity of the receiving phase to accommodate the HOCs.

Bioaccessibility. Chapter 2 describes that the HOC bioaccessibility was linearly related to the total amount of HOC in OECD-medium at the start of the artificial digestion. In addition, a partitioning based model was able to fit the data. Therefore, it can be assumed that the distribution of HOCs among sorbing constituents after artificial digestion was based on partitioning, and that equilibrium was reached for this distribution. This indicates that longer transit times for the different compartments of the digestion model would not affect the HOC distribution. On the other hand, the increased bioaccessibility for increasing bile and protein levels during digestion demonstrates that the capacity of chyme to accommodate the HOCs determines the bioaccessibility. The increased bioaccessibility found for increased levels of sorbing constituents is in agreement with studies performed by Hack and Selenka (*103*), that demonstrated an increased bioaccessibility (5-40% versus 40-85%) caused by addition of milk powder during *in vitro* digestion of soil-borne HOCs.

SPME versus Caco-2 cells. Both the SPME fiber and the Caco-2 cells withdrew HOCs from a chyme solution. However, the time scale of the SPME experiments was shorter than the time scale of exposure of Caco-2 cells to HOCs: minutes versus hours. Furthermore, for longer SPME exposure times (up to 1 h) smaller fiber coating volumes were employed, thereby decreasing the capacity to accommodate HOCs. The shorter exposure times and smaller SPME

coating volumes were employed in order to determine the freely dissolved concentration, which requires that the freely dissolved HOC concentration in the entire sampling volume is not affected by the presence of the SPME fiber (*122,123*). However, the freely dissolved concentration could not be measured directly due to local depletion in the water layer surrounding the fiber, causing sorbed HOCs in this water layer to dissociate and contribute to the HOC flux towards the fiber. Both dissociation of sorbed HOCs and diffusion of freely dissolved HOCs from the bulk across the depleted water layer tend to restore the equilibrium between freely dissolved and sorbed compounds. Therefore, the time in which sorbed complexes could dissociate in order to contribute to the HOC flux towards the SPME fiber was related to the time in which freely dissolved HOCs could traverse this water layer. Hence, only rapidly desorbing HOCs were able to contribute to the flux towards the SPME fiber.

In contrast, the long exposure time and the large HOC capacity of Caco-2 cells resulted in a decrease of over 50% of the HOC concentration in the exposure medium (***Chapter 4***). This indicates that the Caco-2 cells were able to deplete the freely dissolved concentration in the entire exposure medium. Exhaustion of the freely dissolved contaminants in the bulk of the exposure medium for Caco-2 cells was compensated for by dissociation of sorbed HOCs. Due to the time scale, also relatively slowly dissociating HOC complexes may have contributed. Therefore, more sorbed HOCs have been able to desorb and contribute to the accumulation into the intestinal cells compared to the accumulation into the SPME fiber.

Although of different extent, a contribution of sorbed forms to the HOC accumulation into both the SPME fiber and the intestinal cells was observed. Precondition for similar uptake and accumulation behavior of compounds for the SPME fiber and cells is that only the freely dissolved compound can diffuse into the SPME coating or traverse the membrane, and that the compounds are not taken up by the intestinal cells via active mechanisms. These preconditions are most likely met by the HOCs as hydrophobic repulsion from the water (*38*) drives these compounds into the SPME fiber and intestinal cells, and these compounds easily diffuse through a membrane.

The similar behavior indicates that the SPME fiber may be used to investigate the dissociation and association behavior of sorbed HOC forms. The SPME fiber allows for controlled perturbation of the equilibria in unstirred water layers (UWL) surrounding the fiber or in the bulk. Both the exposure time and the capacity to accommodate HOCs can be varied, the latter by employing different fiber material and coating thickness. As the association and dissociation behavior of sorbed HOCs may provide insight into the availability of a compound to be taken up by a sorbing phase such as a biological membrane, further research into this phenomenon is recommended.

In vitro versus in vivo. Environmentally relevant contaminant concentrations and physiologically relevant constituent concentrations were employed in our *in vitro* experiments. Hence, the *in vitro* and *in vivo* processes determining HOC transport and accumulation into the intestinal cells are likely to be similar. Nevertheless, the experimental and physiological time scales and the capacity to accommodate the HOCs of *in vitro* and *in vivo* intestinal cells should be considered for quantitative extrapolation, and to gain insight into the factors determining intestinal absorption.

The capacity of the intestinal cells to accommodate HOCs can be assumed to be similar *in vitro* and *in vivo*, as the Caco-2 cells show many morphological and physiological characteristics of mature enterocytes of the small intestine *(63,140,141,165,174-176)*. Although the Caco-2 cell line expresses some lipid transport, the extent is probably smaller than for the *in vivo* situation *(142)*. As the HOCs most likely follow the pathway for lipid absorption, assimilation and transport, the *in vivo* HOC transport across the basolateral membrane is considered to occur to a larger extent than *in vitro*. Furthermore, the *in vitro* experiments demonstrated that the filter on which the cells grow is a major barrier for HOC transport to the basolateral compartment **(*Chapter 4*)**. These differences indicate that the *in vivo* concentration gradient between the apical and basolateral side is likely to be maintained, while *in vitro* equilibrium between the cells and the apical compartment was apparently reached. This may cause that less HOCs are transported towards intestinal cells *in vitro* compared to *in vivo*.

The small intestinal transit time *in vivo* is between 2 and 5 hours *(57,59-62)*. Direct comparison to the *in vitro* exposure time is not possible. For instance, the thickness of the UWL can have a profound effect on the flux towards intestinal cells, with higher absorption efficiencies for thinner UWLs *(79,177,178)*. The UWL is expected to be thinner *in vivo* than *in vitro* *(140,178)*. Nevertheless, within hours most HOCs had accumulated into the *in vitro* intestinal cells. As both the concentration gradient and the UWL tend to underestimate the *in vitro* HOC transport towards the intestinal cells, it can be expected that within the *in vivo* intestinal transit time (almost) all bioaccessible HOCs are absorbed. Hence, it can be assumed that mobilization of HOC from soil in the gastro-intestinal tract mainly determines the amount of contaminant that is absorbed. Therefore, the difference between oral bioavailability of soil-borne contaminants and oral bioavailability of contaminants ingested with food is most probably mainly caused by differences in bioaccessibility.

Chapter 2 demonstrated that an increased bioaccessibility could be obtained by an increased bile or protein concentration during digestion. Since distribution of the HOCs among sorbing constituents appeared to be partitioning based (***Chapter 2***), it can be assumed that the bioaccessible HOC fraction can also be increased by the presence of other sorbing constituents.

As mobilization from soil is a main process determining oral bioavailability of soil-borne HOCs, the presence of sorbing constituents during digestion may increase the bioaccessibility and thus the bioavailability. Hence, the physiological worst case situation for oral bioavailability of soil-borne HOCs will most likely be for fed conditions when high levels of constituents, both originating from the digestive juices and food particles, are present.

LEAD

Summary lead

Chapter 5 describes the mobilization and speciation of lead during *in vitro* digestion of OECD-medium. Approximately 23% of the lead were mobilized from spiked OECD-medium during artificial digestion. In the absence of bile during digestion only 11% of the lead became bioaccessible. Furthermore, two techniques were employed to investigate lead speciation in chyme. The lead Ion Selective Electrode (ISE) allows for determination of the activity of the free metal ion, Pb^{2+}. DPASV is a voltammetric technique with which voltammetrically labile lead can be measured. DPASV displays many similarities with SPME. It senses the flux of free Pb^{2+} and rapidly dissociating, i.e. labile, lead complexes towards a sink, a mercury droplet. Lead species other than Pb^{2+} that dissociate and contribute to the lead flux towards the mercury droplet within the experimental time scale are referred to as voltammetrically labile.

The speciation experiments indicated that in chyme only a negligible fraction of lead was present as free Pb^{2+}, while lead phosphate and lead bile complexes represent important fractions. The lead phosphate complexes were voltammetrically labile. Furthermore, Feroci *et al.* (*161*) showed that lead and different bile salts form soluble, voltammetrically labile lead bile complexes.

The next step of oral bioavailability, i.e. intestinal absorption, was mimicked by employing Caco-2 cells. *Chapter 6* describes the lead accumulation into and transport through the intestinal cells after exposure to a chyme solution. Approximately 27% of the lead accumulated into the cells and 3% were transported through the cells within 24 hours of exposure. No signs of reaching equilibrium were observed. The transport rate of a compound across the Caco-2 monolayer can be extrapolated quantitatively to human *in vivo* absorption (*165*). The lead flux across the cell monolayer indicates that lead is incompletely absorbed *in vivo*. Since the free Pb^{2+} concentration in the exposure medium is negligible (*Chapter 5*), lead species other than the free metal ions must have contributed to the lead accumulation into and transport across (both *in vitro* and *in vivo*) the intestinal cell monolayer. A contribution to the lead flux via pinocytosis or via diffusion of lead bile complexes across the luminal membrane appeared to be improbable (*Chapter 6*). Therefore, the high lead flux towards intestinal cells can probably be

attributed to dissociation of labile complexes and subsequent transport of the produced Pb^{2+} ions across the apical membrane. Likely candidates for contribution to the lead flux towards the intestinal cells are labile complexes such as lead phosphate and lead bile.

General discussion lead – A mass transfer perspective

Below, the experimental results for lead are interpreted based on the same concept of mass transfer as for the HOCs.

Bioaccessibility. Chapter 5 demonstrates that only part of the lead became bioaccessible during *in vitro* digestion. The bioaccessibility of lead for different transit times of the digestive compartments was not investigated. Therefore, from the present experimental results, it remains inconclusive whether lead distribution among chyme and OECD-medium after the *in vitro* digestion had reached equilibrium. However, Ruby *et al.* studied the time dependence of lead bioaccessibility and showed that equilibrium between the soil and the gastric juice is reached after hundreds of hours (*160*). This suggests that lead bioaccessibility may be limited by the transit times. Furthermore, the absence of bile caused a decrease in lead bioaccessibility (***Chapter 5***), indicating that bile increased the lead mobilization from soil via enhanced wetting, or that bile increased the capacity of chyme to accommodate lead. The latter explanation is likely to hold, as lead bile complexes appeared to be important lead forms in chyme (***Chapter 5***).

Voltammetry versus Caco-2 cells. The time scale of the voltammetric speciation experiments was much shorter than the time scale of exposure of Caco-2 cells: several minutes versus hours. Furthermore, the mercury droplet employed by the voltammetric DPASV technique negligibly depleted the lead concentration in the sample. DPASV only depleted the free metal ion concentration in a small water layer surrounding the mercury droplet. Both diffusion of the free metal ion across the water layer and dissociation of labile complexes aim at restoration of this depletion. Consequently, the time in which complexes could dissociate and contribute to the flux towards the mercury droplet was related to the time scale of diffusion of the free metal ion across the depleted water layer.

During the exposure time, the lead concentration in the apical exposure medium of the Caco-2 cells decreased to about 70% of the concentration at the beginning of the experiment. This indicates that the Caco-2 cells were able to deplete the lead concentration in the entire exposure solution. Lead complexes probably dissociated in order to restore the depletion of the free metal ion concentration in the bulk solution. As the time scale in which lead complexes could dissociate was not related to the time scale of diffusion across a water layer, also more slowly dissociating complexes may have contributed to the lead accumulation into the cells than the complexes that contributed to the metal accumulation into the mercury droplet.

In vitro versus in vivo. In line with the HOC discussion, extrapolation from the *in vitro* results to *in vivo* is based on expectations of similar processes determining lead bioaccessibility and transport across the intestinal membrane.

Chapter 5 demonstrates that not all lead was mobilized from soil during digestion. Therefore, this step can be assumed to decrease the lead fraction that becomes bioavailable relative to the ingested lead. Hence, variations in bioaccessibility may affect bioavailability. The bioaccessibility is, among others, affected by the physiological status of the gastro-intestinal tract. The gastric pH is expected to play a main role, and can be as low as 1 for fasting conditions, and as high as 6 for fed conditions. Several *in vitro* digestion studies demonstrated that a higher lead fraction becomes bioaccessible at low gastric pH than at high gastric pH (*160,179*). This probably is an important aspect of the difference between lead absorption in *in vivo* studies, which was about 30 to 60% under fasting conditions compared to about 4 to 10% for lead administered in food (*20,145*). Therefore, the worst case situation for bioaccessibility and oral bioavailability of soil-borne contaminants can be assumed to be for fasting conditions. Furthermore, *Chapter 6* shows that *in vitro* 27% of the bioaccessible lead had accumulated into the intestinal cells and 3% was transported through the cells in 24 h of exposure. This indicates that a smaller fraction than the bioaccessible lead fraction can be absorbed and subsequently can reach the systemic circulation, i.e. become bioavailable. Therefore, the absorption process too is a major determinant for oral bioavailability of soil-borne lead.

HOCs VERSUS LEAD

Speciation and mass transfer

The distribution of a compound among different physicochemical forms is defined as speciation. Speciation is a common term in research on metals. However, this term can also be applied for organic compounds. For example, HOCs sorbed to bile salt micelles, digestive proteins and soil can be viewed at as different physicochemical forms. Therefore, the distribution of PCBs and lindane among these sorbing constituents can be considered as speciation. Speciation is known to affect the availability of compounds for uptake via biological membranes (*5,74,76,77,137,146,147,156,180,181*).

Of the different physicochemical species, at least the freely dissolved contaminants can be transferred across a membrane (*74-77*). In the present thesis, contribution to contaminant accumulation in and transport across intestinal cells via pinocytose was considered negligible. Furthermore, transcellular transport of hydrophobic lead forms was improbable (*Chapter 6*).

We were able to explain the observed results based on transport of freely dissolved contaminants across the membrane only.

The mechanism employed to explain that more contaminants contribute to the flux towards a phase than the freely dissolved concentration is based on rapid equilibria between the freely dissolved contaminant and the sorbed contaminant. This mechanism for mass transfer was applicable for organic and inorganic compounds for chemical phases (SPME fiber and mercury droplet in voltammetry). Hence, it is likely that such a contribution also occurred for a biological phase, i.e. Caco-2 cells.

This mechanism implies that mass transfer towards a sorbing phase, i.e. SPME fiber, mercury droplet or Caco-2 cells, is driven by the concentration gradient of the freely dissolved contaminant. The pool of physicochemical species that are able to desorb determines the amount of contaminant that can be transferred into the sampling phase. The extent to which sorbed species can dissociate and contribute to the mass transfer towards the sorbing phase depends on the time scale of exposure and the capacity of the receiving phase to accommodate the contaminants. Therefore, the freely dissolved contaminant concentration as well as the lability of the different physicochemical forms of the contaminant are important determinants for uptake by a sampling phase.

Both the soil-borne HOCs and lead were partially bioaccessible. However, the extent of absorption of the bioaccessible fraction was different. A major HOC fraction was taken up by the Caco-2 cells, indicating that intestinal absorption probably is (almost) complete. Lead uptake into Caco-2 cells and the expected intestinal absorption were lower. Consequently, the results indicate that both mobilization from soil and intestinal absorption are processes that reduce the amount of the ingested soil-borne lead that becomes bioavailable, while for the ingested soil-borne HOCs only mobilization from soil does. These differences probably also represent the main differences between oral bioavailability of soil-borne PCBs and lead, as the first-pass effect can be assumed to be small (*Chapter 1*). Lindane may undergo liver metabolism (*41-43*), resulting in a further decrease of the ingested amount that becomes bioavailable.

Batch versus continuous

Studies employing an *in vitro* digestion model assume that contaminants that are still sorbed to soil, for conditions representing the small intestine, are not available for absorption (*103,144,173,179,182*). This assumption is supported by several *in vivo* studies that showed that absorption of contaminants is lower after ingestion with soil than with food, aqueous solution or with an olive oil carrier (*6,7,9-14,183*). However, in principle, as a consequence of

contaminant absorption, the equilibrium between the contaminants sorbed to soil and in chyme may be disturbed *in vivo*. Then, these contaminants sorbed to soil may dissociate and contribute to the mass transfer towards the intestinal cells. It should be noted that the time in which these processes can take place is limited by the transit time of the small intestine. The artificial digestion model is a batch model and does therefore not account for possible dissociation from soil caused by continuous contaminant absorption. Hence, the bioaccessible fraction as determined by the artificial digestion model might be an underestimation of the fraction that is available for intestinal absorption.

Such a contribution of contaminants sorbed to soil is not expected for lead as dissociation from soil probably is slow compared to the time scale of digestion (*160*). However, for HOCs this contribution may take place, since: 1) the distribution of HOCs among chyme and OECD-medium after digestion represented equilibrium (***Chapter 2***), indicating that dissociation of HOCs sorbed to soil may occur within the time scale of digestion, and 2) the bioaccessible HOCs are assumed to be almost completely absorbed (***Chapter 4*** and (*7,8,101,184*)), so that the freely dissolved and bioaccessible HOC concentration in the bulk of the chyme solution can be decreased, inducing sorbed species to dissociate.

In the present thesis, the assumption that contaminants that are still sorbed to soil in the small intestine cannot be absorbed, is not verified. Nevertheless, such information would provide more insight into the validity of the bioaccessible fraction as determined by an *in vitro* digestion model. To further investigate this issue, the contaminant accumulation in and transport through *in vitro* intestinal cells after exposure to a chyme solution with and without soil could offer an appropriate approach. If the contaminants sorbed to soil do not dissociate and contribute to the flux towards the cells, no difference should be observed between the presence and absence of soil. An experimental problem might be that the chyme should be diluted in order to keep the cells viable, and that the soil particles may settle on the surface of the cells, possibly inducing unpredictable results.

SPME in chyme with and without soil offers another approach that would give information on the dissociation behavior of HOCs sorbed to soil. The SPME fiber should be able to deplete the contaminant concentration in the entire exposure solution. Therefore, fibers with thick coatings and small exposure solutions are recommended. A similar HOC accumulation into the fiber in time should be observed if the contaminants sorbed to soil do not dissociate and contribute to the flux towards the fiber.

Also the extent of mobilization of contaminants from digested soil by uncontaminated chyme in time would be clarifying, as this also gives an indication of the readiness of the contaminants to dissociate when the equilibrium between the chyme and the soil is disturbed. Hence, such experiments are recommended, although the readiness of contaminants to

dissociate should always be evaluated in light of physiological conditions such as transit times and absorbability of the contaminant.

Soil

In the present thesis, artificial standard soil, i.e. OECD-medium, has been employed. The OECD-medium was contaminated via spiking under controlled conditions. This approach reduced the variation in oral bioavailability caused by the type of ingestion matrix. Nevertheless, it can be expected that oral bioavailability of soil-borne contaminants is influenced by the type of soil, and whether the soil is historically contaminated or spiked in the laboratory *(24,25,103,144,172,179)*. As this can be an important issue for risk assessment, further research in these topics is recommended.

Implications for exposure assessment

In current Dutch risk assessment of soil-borne contaminants, the assumption is made that oral bioavailability of a soil-borne contaminant is equal to oral bioavailability of the corresponding food-borne contaminant *(1)*. The research described in the present thesis provides insight into processes determining oral bioavailability of some soil-borne contaminants. These insights may be applied to strategies in order to establish more accurate exposure assessment and soil intervention values.

The results demonstrate that only part of the soil-borne PCBs and lindane are bioaccessible. HOCs ingested with food are assumed to be completely bioaccessible. Hence, oral bioavailability for the soil-borne HOCs is expected to be lower than for the HOCs ingested in food. Given the results of *Chapter 2*, it can be expected that bioaccessibility for other HOCs is based on partitioning. In addition, absorption of other HOCs is likely to be based on passive diffusion across the intestinal membrane. Consequently, it can be assumed that bioaccessibility has also a large impact on oral bioavailability of other HOCs. This implies that mobilization from soil during digestion is an important process that should be studied to investigate oral bioavailability of other soil-borne HOCs than employed in the present thesis.

In addition, bioaccessibility and thus oral bioavailability of soil-borne HOCs can change with the physiological status. Therefore, bioaccessibility studies should be performed at conditions representing the worst case. In case of PCBs and lindane, and most likely for other HOCs, the worst case situation is probably the fed situation with high concentrations of sorbing constituents.

For lead, the experiments indicate that both mobilization from soil and absorption are processes that decrease the fraction that reaches the systemic circulation and becomes bioavailable relative to the ingested dose. The partial bioaccessibility is assumed to cause differences between oral bioavailability of soil-borne lead and of lead ingested with food or liquid. In risk assessment it is assumed that 40 to 50% of lead ingested with food is absorbed (*1*). This figure is extrapolated to oral bioavailability of soil-borne contaminants, assuming that 40 to 50% of the bioaccessible contaminant can be absorbed. The present results indicate that indeed not all lead that is mobilized from soil is absorbed, suggesting that the use of a factor to account for the absorption step is justified. However, from the present research it remains inconclusive whether this factor is the same for bioaccessible lead from soil and from food. Further research into this issue is recommended.

Extrapolation of the results for lead bioaccessibility and absorption to other metals is not straightforward since each metal forms different physicochemical species in chyme that behave differently. However, the presently employed approach to investigate bioaccessibility, speciation and absorption may be applied to obtain a similar detailed picture for other metals.

There is evidence that the physiological status affects the bioaccessibility and thus the oral bioavailability of soil-borne lead. Therefore, as a worst case approach for bioaccessibility of soil-borne lead a digestion model simulating fasting conditions, i.e. low gastric pH, should be employed.

The results indicate that the physiological conditions representing the worst case situation for bioaccessibility are contaminant dependent. Therefore, for future assessments for which the worst case is not known beforehand, we recommend assessing the bioaccessibility of soil-borne contaminants for both the fasted and the fed state.

It is recommended to consider whether the bioaccessible fraction of a soil-borne contaminant that is determined by a batch artificial digestion system is a good representative for the fraction that is at maximum available for intestinal absorption. Additional experiments may be useful to investigate possible desorption from soil induced by disturbed equilibria in chyme due to intestinal absorption of the contaminant.

Conclusions

Following ingestion of soil-borne PCBs, lindane and lead, the freely dissolved fraction of these contaminants in chyme can be assumed to be small. Expected important fractions for the HOCs are PCBs and lindane sorbed to bile salt micelles, digestive proteins and soil, whereas lead phosphate, lead bile and lead soil complexes are important fractions for lead. The distribution of the presently used HOCs among sorbing constituents in chyme was based on partitioning.

The *in vitro* experiments indicate that not all ingested and soil-borne PCBs, lindane and lead are mobilized from soil during digestion, i.e. become bioaccessible, and therefore do not reach the systemic circulation and become bioavailable. Furthermore, not all bioaccessible lead is expected to be absorbed, causing a further reduction of the lead fraction that becomes bioavailable relative to the ingested amount.

Physicochemical conditions in the gastro-intestinal tract are expected to affect the bioaccessibility and thereby the oral bioavailability of the soil-borne contaminants. The physiological worst case situation for the PCBs and lindane is most likely the fed state, since that results in high concentrations of sorbing constituents in the gastro-intestinal tract. The worst case situation for lead is most likely the fasted state so that the gastric pH is low, inducing a high mobilization from soil.

The PCBs, lindane and lead have in common that more than the freely dissolved fraction is transported across the intestinal membrane. The freely dissolved concentration can be considered the driving force for the contaminant flux towards the intestinal cells, while the labile contaminants represent the pool of contaminants that may dissociate and contribute to the flux.

Chemical sampling techniques such as SPME and DPASV technique offer possibilities to investigate mass transfer of contaminants in a complex medium towards biological phases like Caco-2 cells.

References

1) Lijzen JPA, Baars AJ, Crommentuijn T, Otte PF, van de Plassche E, Rikken MGJ, Rompelberg CJM, Sips AJAM, Swartjes FA. Herziening interventiewaarde lood. Evaluatie van de afleiding van de interventiewaarde grond/sediment en grondwater. Report no 711701013. National Institute of Public Health and the Environment, 1999.

2) Mushak P. Uses and limits of empirical data in measuring and modeling human lead exposure. *Environ Health Perspect* **106**: 1467-1484 (1998).

3) Davis A, Bloom NS, Que Hee SS. The environmental geochemistry and bioaccessibility of mercury in soils and sediments: a review. *Risk Anal* **17**: 557-569 (1997).

4) Paustenbach DJ, Shu HP, Murray FJ. A critical examination of assumptions used in risk assessments of dioxin contaminated soil. *Regul Toxicol Pharmacol* **6**: 284-307 (1986).

5) Paustenbach DJ, Bruce GM, Chrostowski P. Current views on the oral bioavailability of inorganic mercury in soil: implications for health risk assessments. *Risk Anal* **17**: 533-544 (1997).

6) Sheppard SC, Evenden WG, Schwartz WJ. Heavy metals in the environment. Ingested soil: bioavailability of sorbed lead, cadmium, cesium, iodine, and mercury. *J Environ Qual* **24**: 498-505 (1995).

7) Bonaccorsi A, Domenico di A, Fanelli R, Merli F, Motta R, Vanzati R, Zapponi GA. The influence of soil particle adsorption on 2,3,7,8-tetrachlorodibenzo-p-dioxin biological uptake in the rabbit. *Arch Toxicol* **Suppl.7**: 431-434 (1984).

8) Umbreit TH, Hesse EJ, Gallo MA. Bioavailability of dioxin in soil from a 2,4,5-T manufacturing site. *Science* **232**: 497-499 (1986).

9) Fries GF, Marrow GS, Somich CJ. Oral bioavailability of aged polychlorinated biphenyl residues contained in soil. *Bull Environ Contam Toxicol* **43**: 683-690 (1989).

10) Shu H, Paustenbach D, Murray FJ, Marple L, Brunck B, Dei Rossi D, Teitelbaum P. Bioavailability of soil-bound TCDD: oral bioavailability in the rat. *Fundam Appl Toxicol* **10**: 648-654 (1988).

11) Freeman GB, Johnson JD, Liao SC, Feder PI, Davis AO, Ruby MV, Schoof RA, Chaney RL, Bergstrom PD. Absolute bioavailability of lead acetate and mining waste lead in rats. *Toxicology* **91**: 151-163 (1994).

12) Freeman GB, Johnson JD, Killinger JM, Liao SC, Feder PI, Davis AO, Ruby MV, Chaney RL, Lovre SC, Bergstrom PD. Relative bioavailability of lead from mining waste soil in rats. *Fundam Appl Toxicol* **19**: 388-398 (1992).

13) Freeman GB, Dill JA, Johnson JD, Kurtz PJ, Parham F, Matthews HB. Comparative absorption of lead from contaminated soil and lead salts by weanling Fisher 344 rats. *Fundam Appl Toxicol* **33**: 109-119 (1996).

14) Casteel SW, Cowart RP, Weis CP, Henningsen GM, Hoffman E, Brattin WJ, Guzman RE, Starost MF, Payne JT, Stockham SL, Becker SV, Drexler JW, Turk JR. Bioavailability of lead to juvenile swine dosed with soil from the smuggler mountain NPL site of Aspen, Colorado. *Fundam Appl Toxicol* **36**: 177-187 (1997).

15) Descotes J, Evreux JC. Comparative effects of various lead salts on delayed hypersensitivity in mice. *J Appl Toxicol* **4**: 265-266 (1984).

16) Barltrop D, Meek F. Absorption of different lead compounds. *Postgrad Med J* **51**: 805-809 (1975).

17) Dieter MP, Matthews HB, Jeffcoat RA, Moseman RF. Comparison of lead bioavailability in F344 rats fed lead acetate, lead oxide, lead sulfide, or lead ore concentrate from Skagway, Alaska. *J Toxicol Environ Health* **39**: 79-93 (1993).

18) Diamond GL, Goodrum PE, Felter SP, Ruoff WL. Gastrointestinal absorption of metals. *Drug Chem Toxicol* **20**: 345-368 (1997).

19) Heard MJ, Chamberlain AC. Effect of minerals and food on uptake of lead from the gastrointestinal tract in humans. *Hum Toxicol* **1**: 411-415 (1982).

20)	James HM, Hilburn ME, Blair JA. Effects of meals and meal times on uptake of lead from the gastrointestinal tract in humans. _Hum Toxicol_ **4**: 401-407 (1985).

21)	Maddaloni M, Lolacono N, Manton W, Blum C, Drexler J, Graziano J. Bioavailability of soilborne lead in adults, by stable isotope dilution. _Environ Health Perspect_ **106**: 1589-1594 (1998).

22)	Hörter D, Dressman JB. Influence of physicochemical properties on dissolution of drugs in the gastrointestinal tract. _Advan Drug Delivery Rev_ **25**: 3-14 (1997).

23)	Charman WN, Porter CJH, Mithani S, Dressman JB. Physicochemical and physiological mechanisms for the effects of food on drug absorption: the role of lipids and pH. _J Pharm Sci_ **86**: 269-282 (1997).

24)	Davies NA, Edwards PA, Lawrence MAM, Taylor MG, Simkiss K. Influence of particle surfaces on the bioavailability of different species of 2,4-dichlorophenol and pentachlorophenol. _Environ Sci Technol_ **33**: 2465-2468 (1999).

25)	Clapp TC, Umbreit TH, Meeker RJ, Kosson DS, Gray D, Gallo MA. Bioavailability of lead and chromium from encapsulated pigment materials. _Bull Environ Contam Toxicol_ **46**: 271-275 (1991).

26)	Mackay D, Ying Shiu W, Ching Ma K. Illustrated handbook of physical-chemical properties and environmental fate for organic chemicals; Vol I: Monoaromatic hydrocarbons, chlorobenzenes, and PCBs. Lewis Publishers: Chelsea, MI, 1992.

27)	Jensen S. Report of a new chemical hazard. _New Sci_ **32**: 612-615 (1966).

28)	Jensen S, Johnels AG, Olssen M, Otterlind G. DDT and PCB in marine animals from Swedish waters. _Nature_ **224**: 247-250 (1969).

29)	Koeman JH, ten Noever-De Brauw MC, de Vos RH. Chlorinated biphenyls in fish, mussels and birds from the river Rhine and the Netherlands coastal area. _Nature_ **221**: 1126-1128 (1969).

30)	Skaare JU, Markussen NH, Norheim G, Haugen S, Holt G. Levels of polychlorinated biphenyls, organochlorine pesticides, mercury, cadmium, copper, selenium, arsenic, and zinc in the harbour seal, Phoca vitulina, in Norwegian waters. _Environ Pollut_ **66**: 309-324 (1990).

31)	Thomas DJ, Tracey B, Marshall H, Norstrom RJ. Arctic terrestrial ecosystem contamination. _Sci Total Environ_ **122**: 135-164 (1992).

32)	Alawi MA, Heidmann WA. Analysis of polychlorinated biphenyls (PCB) in environmental samples from the Jordan Valley. _Toxicol Environ Chem_ **33**: 93-99 (1991).

33)	van Zoest R, van Eck GTM. Historical input and behaviour of hexachlorobenzene, polychlorinated biphenyls and polycyclic aromatic hydrocarbons in two dated sediment cores from the Scheldt estuary, SW Netherlands. _Mar Chem_ **44**: 95-103 (1993).

34)	Bossi R, Larsen B, Premazzi G. Polychlorinated biphenyl congeners and other chlorinated hydrocarbons in bottom sediment cores of Lake Garda (Italy). _Sci Total Environ_ **121**: 77-93 (1992).

35)	Safe S. Polychlorinated bihenyls (PCBs), dibenzo-p-dioxins (PCDDs), dibenzofurans (PCDFs), and related compounds: environmental and mechanistic considerations which support the development of toxic equivalency factors (TEFs). _CRC Crit Rev Toxicol_ **21**: 51-88 (1990).

36)	Cogliano VJ. Assessing the cancer risk from environmental PCBs. _Environ Health Perspect_ **106**: 317-323 (1998).

37)	Swartjes FA. Risk-based assessment of soil and groundwater quality in the Netherlands: standards and remediation urgency. _Risk Anal_ **19**: 1235-1249 (1999).

38)	Schwarzenbach RP, Gschwend PM, Imboden DM. Environmental organic chemistry. John Wiley & Sons Inc.: New York, 1993.

39)	Padmakar DG, Karanth NG, Karanth NGK. Biodegradation of hexachlorocyclohexane isomers in soil and food environment. _Crit Rev Microbiol_ **20**: 57-78 (1994).

40)	Lal R, Saxena DM. Accumulation, metabolism, and effects of organochlorine insecticides on microorganisms. _Microbiol Rev_ **46**: 95-127 (1982).

41)	Yvelin C, Yvelin JM, Lievremont M. Uptake and transformation of lindane by the liver during short exposure times. _Bull Environ Contam Toxicol_ **32**: 140-147 (1984).

42)	Beurskens JEM, Stams AJM, Zehnder AJB, Bachmann A. Relative biochemical reactivity of three hexachlorocyclohexane isomers. _Ecotoxicol Environ Safety_ **21**: 128-136 (1991).

43)	Gopalaswamy UV, Aiyar AS. Biotransformation of lindane in the rat. _Bull Environ Contam Toxicol_ **32**: 148-156 (1984).

44) Joy RM, Albertson TE. Factors responsible for increased excitability of dentate gyrus granule cells during exposure to lindane. *Neurotoxicology* **8**: 517-528 (1987).

45) Dési I. Neurotoxicological effects of small quantities of lindane. *Int Arch Arbeitsmed* **33**: 153-162 (1974).

46) Tusell JM, Sunol C, Gelpi E, Rodriguez-Farre E. Relationship between lindane concentration in blood and brain and convulsant response in rats after oral or intraperitoneal administration. *Arch Toxicol* **60**: 432-437 (1987).

47) Hall RCW, Hall RCW. Long-term psychological and neurological complications of lindane poisoning. *Psychosomatics* **40**: 513-517 (1999).

48) Fischer TF. Lindane toxicity in a 24-year-old woman. *Ann Emerg Med* **24**: 972-974 (1994).

49) Videla LA, Barros SBM, Junqueira VBC. Lindane-induced liver oxydative stress. *Free Rad Biol Med* **9**: 169-179 (1990).

50) Criswell KA, Loch-Caruso R, Stuenkel EL. Lindane inhibition of gap junctional communication in myometrial myocytes is partially dependent on phasphomositide-generated second messengers. *Appl Pharmacol* **130**: 280-293 (1995).

51) van Velsen FL, Danse LHJC, van Leeuwen FXR, Dormans JAMA, van Logten MJ. The subchronic oral toxicity of the b-isomer of hexachlorocyclohexane in rats. *Fundam Appl Toxicol* **6**: 697-712 (1986).

52) Silvestroni L, Palleschi S. Effects of organochlorine xenobiotics on human spermatozoa. *Chemosphere* **39**: 1249-1252 (1999).

53) Nieuwkoop JAW. Bodemverontreiningen op voormalige bedrijfsterreinen. De erfenis van anderhalve eeuw industriële ontwikkeling in Noord-Brabant. PhD thesis; Eindhoven Technical University: Eindhoven, 1993.

54) Weiss D, Shotyk W, Appleby PG, Kramers JD, Cheburkin AK. Atmospheric Pb deposition since the industrial revolution recorded by five Swiss peat profiles: enrichment factors, fluxes, isotopic composition, and sources. *Environ Sci Technol* **33**: 1340-1352 (1999).

55) Thomas VM, Socolow RH, Fanelli JJ, Spiro TG. Effects of reducing lead in gasoline: an analysis of the international experience. *Environ Sci Technol* **33**: 3942-3948 (1999).

56) Skerfving S, Gerhardsson L, Schütz A, Strömberg U. Lead - biological monitoring of exposure and effects. *J Trace Elem Exp Med* **11**: 289-301 (1998).

57) Kararli TT. Comparison of the gastrointestinal anatomy, physiology, and biochemistry of human and commonly used laboratory animals. *Biopharm Drug Dispos* **16**: 351-380 (1995).

58) Friedman HI, Nylund B. Intestinal fat digestion, absorption, and transport. A review. *Am J Clin Nutr* **33**: 1108-1139 (1980).

59) Christensen FN, Davis SS, Hardy JG, Taylor MJ, Whalley DR, Wilson CG. The use of gamma scintigraphy to follow the gastrointestinal transit of pharmaceutical formulations. *J Pharm Pharmacol* **37**: 91-95 (1985).

60) Coupe AJ, Davis SS, Wilding IR. Variation in gastrointestinal transit of pharmaceutical dosage forms in healthy subjects. *Pharm Res* **8**: 360-364 (1991).

61) Devereux JE, Newton JM, Short MB. The influence of density on the gastrointestinal transit of pellets. *J Pharm Pharmacol* **42**: 500-501 (1990).

62) Adkin DA, Davis SS, Sparrow RA, Huckle PD, Philipps AJ, Wilding IR. The effects of pharmaceutical excipients on small intestinal transit. *Br J Clin Pharmacol* **39**: 381-387 (1995).

63) Hillgren KM, Kato A, Borchardt RT. In vitro systems for studying intestinal drug absorption. *Med Res Rev* **15**: 83-109 (1995).

64) Sheppard SC, Evenden WG. Systematic identification of analytical indicators to measure soil load on plants for safety assessment purposes. *Intern J Environ Anal Chem* **59**: 239-252 (1995).

65) Schmidt CW. A closer look at chemical exposure in children; new research initiatives should help regulators more accurately assess risks and set exposure tolerances. *Environ Sci Technol* **33**: 72A-75A (1999).

66) van Wijnen JH, Clausing P, Brunekreef B. Estimated soil ingestion by children. *Environ Res* **51**: 147-162 (1990).

67) Calabrese EJ, Stanek EJ, James RC, Roberts SM. Soil ingestion. A concern for acute toxicity in children. *J Environ Health* **61**: 18-23 (1999).

68) Calabrese EJ, Barnes R, Stanek III EJ, Pastides H, Gilbert CE, Veneman P, Wang X, Lasztity A, Kostecki PT. How much soil do young children ingest: an epidemiologic study. *Regul Toxicol Pharmacol* **10**: 123-137 (1989).

69) Davis S, Waller P. Quantitative estimates of soil ingestion in normal children between the ages of 2 and 7 years: population-based estimates using aluminium, silicon, and titanium as soil tracer elements. *Arch Environ Health* **45**: 112-122 (1990).

70) Simon SL. Soil ingestion by humans: a review of history, data, and etiology with application to risk assessment of radioactively contaminated soil. *Health Phys* **74**: 647-672 (1998).

71) Calabrese EJ, Stanek EJ, James RC, Roberts SM. Soil ingestion: a concern for acute toxicity in children. *Environ Health Perspect* **105**: 1354-1358 (1997).

72) Castela-Papin N, Cai S, Vatier J, Keller F, Souleau CH, Farinotti R. Drug interaction with diosmectite: a study using the artificial stomach-duodenum model. *Int J Pharm* **182**: 111-119 (1999).

73) Serajuddin ATM, Sheen P-C, Mufson D, Bernstein DF, Augustine MA. Physicochemical basis of increased bioavailability of a poorly water-soluble drug following oral administration as organic solutions. *J Pharm Sci* **77**: 325-329 (1988).

74) Freedman ML, Cunningham PM, Schindler JE, Zimmerman MJ. Effect of lead speciation on toxicity. *Bull Environ Contam Toxicol* **25**: 389-393 (1980).

75) Seydel JK, Schaper K-J. Quantitative structure-pharmacokinetic relationships and drug design. *Pharm Ther* **15**: 131-182 (1982).

76) Florence TM. Electrochemical approaches to trace element speciation in waters. A review. *Analyst* **111**: 489-505 (1986).

77) Florence TM, Morrison GM, Stauber JL. Determination of trace element speciation and the role of speciation in aquatic toxicity. *Sci Total Environ* **125**: 1-13 (1992).

78) Busbee DL, Yoo J-SH, Norman JO, Joe CO. Polychlorinated biphenyl uptake and transport by lymph and plasma components. *Proc Soc Exp Biol Med* **179**: 116-122 (1985).

79) Dulfer WJ, Groten JP, Govers HAJ. Effect of fatty acids and the aqueous diffusion barrier on the uptake and transport of polychlorinated biphenyls in Caco-2 cells. *J Lipid Res* **37**: 950-961 (1996).

80) Turner JC, Shanks V. Absorption of some organochlorine compounds by the rat small intestine-in vivo. *Bull Environ Contam Toxicol* **24**: 652-655 (1980).

81) van Barneveld AA, van den Hamer CJA. Influence of Ca and Mg on the uptake and deposition of Pb and Cd in mice. *Toxicol Appl Pharmacol* **79**: 1-10 (1985).

82) Mushak P. Gastro-intestinal absorption of lead in children and adults: overview of biological and biophysico-chemical aspects. *Chem Speciation Bioavailability* **3**: 87-104 (1991).

83) Fullmer CS. Intestinal interactions of lead and calcium. *Neurotoxicology* **13**: 799-808 (1992).

84) Clarkson TW. Molecular and ionic mimicry of toxic metals. *Annu Rev Pharmacol Toxicol* **32**: 545-571 (1993).

85) Foulkes EC, McMullen DM. Kinetics of transepithelial movement of heavy metals in rat jejunum. *Am J Physiol G* **253**: 134-138 (1987).

86) Foulkes EC. On the mechanism of transfer of heavy metals across cell membranes. *Toxicology* **52**: 263-272 (1988).

87) Foulkes EC. Further findings on the mechanism of cadmium uptake by intestinal mucosal cells (step 1 of Cd absorption). *Toxicology* **70**: 261-270 (1991).

88) Foulkes EC, Bergman D. Inorganic mercury absorption in mature and immature rat jejunum: transcellular and intercellular pathways in vivo and in everted sacs. *Toxicol Appl Pharmacol* **120**: 89-95 (1993).

89) Ziegler EE, Edwards BB, Jensen RL, Mahaffey KR, Fomon SJ. Absorption and retention of lead by infants. *Pediat Res* **12**: 29-34 (1978).

90) Bronner F, Pansu D. Nutritional aspects of calcium absorption. *J Nutr* **129**: 9-12 (1999).

91) Gan L-S, L., Thakker DR. Applications of the Caco-2 model in the design and development of orally active drugs: elucidation of biochemical and physical barriers posed by the intestinal epithelium. *Advan Drug Delivery Rev* **23**: 77-98 (1997).

92) Ito K, Kusuhara H, Sugiyama Y. Effects of intestinal CYP3A4 and P-glycoprotein on oral drug absorption - theoretical approach. *Pharm Res* **16**: 225-231 (1999).

93) Watkins PB. The barrier function of Cyp3A4 and P-glycoprotein in the small bowel. *Advan Drug Delivery Rev* **27**: 161-170 (1997).

94) Wilkinson GR. Cytochrome P4503A (CYP3A) metabolism: prediction of in vivo activity in humans. *J Pharmacok Biopharm* **24**: 475-490 (1996).

95) Casarett and Doull's Toxicology. The basic science of poisons. Eds. Klaassen Cd, Amdur MO, Doull JD. Third Edition. Macmillan Publishing Company: New York, 1986.

96) Cikrt M, Tichý M. Role of bile in intestinal absorption of 203Pb in rats. *Experientia* **31**: 1320-1321 (1975).

97) Pocock DM-E, Vost A. DDT absorption and chylomicron transport in rat. *Lipids* **9**: 374-381 (1974).

98) OECD. Guideline for testing of chemicals no. 207. Earthworm, acute toxicity test, 1984.

99) Janssen PJCM, Apeldoorn van ME, Engelen van JGM, Schielen PCJI, Wouters MFA. Maximum permissible risk levels for human intake of soil contaminants: fourth series of compounds. Report no 711701004. National Institute of Public Health and the Environment, 1998.

100) Tanabe S, Nakagawa Y, Tatsukawa R. Absorption efficiency and biological half-life of individual chlorobiphenyls in rats treated with Kanechlor products. *Agr Biol Chem* **45**: 717-726 (1981).

101) Koganti A, Spina DA, Rozett K, Ma B-L, Weyand EH. Studies on the applicability of biomarkers in estimating the systemic bioavailability of polynuclear aromatic hydrocarbons from manufactured gas plant tar-contaminated soils. *Environ Sci Technol* **32**: 3104-3112 (1998).

102) Embleton JK, Pouton CW. Structure and function of gastro-intestinal lipases. *Advan Drug Delivery Rev* **25**: 15-32 (1997).

103) Hack A, Selenka F. Mobilization of PAH and PCB from contaminated soil using a digestive tract model. *Toxicol Lett* **88**: 199-210 (1996).

104) Rotard W, Christmann W, Knoth W, Mailahn W. Bestimmung der resorptionsverfügbaren PCDD/PCDF aus Kieselrot. *UWSF-Z Umweltchem Ökotox* **7**: 3-9 (1995).

105) Norris DA, Puri N, Sinko PJ. The effect of physical barriers and properties on the oral absorption of particulates. *Advan Drug Delivery Rev* **34**: 135-154 (1998).

106) Ghosh U, Weber AS, Jensen JN, Smith JR. Dissolved PCB congener distribution in generator column solutions. *Water Res* **32**: 1373-1382 (1998).

107) Denneman CAJ, Gestel van CAM. Bodemverontreiniging en bodemecosystemen: voorstel voor C-(toetsings)waarden op basis van ecotoxicologische risico's. Report no 725201001. National Institute of Public Health and the Environment, 1990.

108) Luthy RG, Aiken GR, Brusseau ML, Cunningham SD, Gschwend PM, Pignatello JJ, Reinhard M, Traina SJ, Weber WJJ, Westall JC. Sequestration of hydrophobic organic contaminants by geosorbents. *Environ Sci Technol* **31**: 3341-3347 (1997).

109) Sips AJAM. Article in preparation.

110) Sips AJAM, Bruil MA, Dobbe CJG, Klaassen R, Pereboom DPKH, Rompelberg CJM. Feasibility of an in vitro digestion model for determining bioaccessibility of contaminants from ingested soil. Report no 711701006. National Institute of Public Health and the Environment, 1998.

111) Oomen AG, Mayer P, Tolls J. Nonequilibrium solid phase microextraction (SPME) of the freely dissolved concentration of hydrophobic organic compounds: matrix effects and limitations. *Anal Chem* **72**: 2802-2808 (2000).

112) Paya-Perez AB, Riaz M, Larsen BR. Soil sorption of 20 PCB congeners and six chlorobenzenes. *Ecotoxicol Environ Safety* **21**: 1-17 (1991).

113) Weston DP, Mayer LM. In vitro digestive fluid extraction as a measure of the bioavailability of sediment-associated polycyclic aromatic hydrocarbons: sources of variation and implications for partitioning models. *Environ Toxicol Chem* **17**: 820-829 (1998).

114) Hervé F, Urien S, Albengres E, Duché J-C, Tillement J-P. Drug binding in plasma. A summary of recent trends in the study of drug and hormone binding. *Clin Pharmacokinet* **26**: 44-58 (1994).

115) Petty JD, Poulton BC, Charbonneau CS, Huckins JN, Jones SB, Cameron JT, Prest HF. Determination of bioavailable contaminants in the lower Missouri river following the flood of 1993. *Environ Sci Technol* **32**: 837-842 (1998).

116) Wang Y, Wang C, Wang Z. Uptake of moderately hydrophobic chlorophenols from water by semipermeable membrane devices (SPMDs) and by goldfish. *Chemosphere* **37**: 327-339 (1998).

117) Jeannot MA, Cantwell FF. Solvent microextraction as a speciation tool: determination of free progesterone in a protein solution. *Anal Chem* **69**: 2935-2940 (1997).

118) Poerschmann J, Kopinke F-D, Pawliszyn J. Solid phase microextraction to study the sorption of organotin compounds onto particulate and dissolved humic organic matter. *Environ Sci Technol* **31**: 3629-3636 (1997).

119) Poerschmann J, Zhang Z, Kopinke F-D, Pawliszyn J. Solid phase microextraction for determining the distribution of chemicals in aqueous matrices. *Anal Chem* **69**: 597-600 (1997).

120) Pörschmann J, Kopinke F-D, Pawliszyn J. Solid-phase microextraction for determining the binding state of organic pollutants in contaminated water rich in humic organic matter. *J Chromatogr A* **816**: 159-167 (1998).

121) Urrestarazu Ramos E, Meijer SN, Vaes WHJ, Verhaar HJM, Hermens JLM. Using solid-phase microextraction to determine partition coefficients to humic acids and bioavailable concentrations of hydrophobic chemicals. *Environ Sci Technol* **32**: 3430-3435 (1998).

122) Vaes WHJ, Urrestarazu Ramos E, Verhaar HJM, Seinen W, Hermens JLM. Measurement of the free concentration using solid-phase microextraction: binding to protein. *Anal Chem* **68**: 4463-4467 (1996).

123) Vaes WHJ, Hamwijk C, Urrestarazu Ramos E, Verhaar HJM, Hermens JLM. Partitioning of organic chemicals to polyacrylate-coated solid phase microextraction fibers: kinetic behavior and quantitative structure-property relationships. *Anal Chem* **68**: 4458-4462 (1996).

124) Yuan H, Ranatunga R, Carr PW, Pawliszyn J. Determination of equilibrium constant of alkylbenzenes binding to bovine serum albumin by solid phase microextraction. *Analyst* **124**: 1443-1448 (1999).

125) Arthur CL, Pawliszyn J. Solid phase microextraction with thermal desorption using fused silica optical fibers. *Anal Chem* **62**: 2145-2148 (1990).

126) Kopinke F-D, Pörschmann J, Georgi A. Application of SPME to study sorption phenomena on dissolved humic organic matter. Ed. Pawliszyn J. The Royal Society of Chemistry: Cambridge, 1999.

127) Oomen AG, Sips AJAM, Groten JP, Sijm DTHM, Tolls J. Mobilization of PCBs and lindane from soil during in vitro digestion and their distribution among bile salt micelles and proteins of human digestive fluid and the soil. *Environ Sci Technol* **34**: 297-303 (2000).

128) Mayer P, Vaes WHJ, Hermens JLM. Absorption of hydrophobic compounds into the poly(dimethylsiloxane) coating of solid-phase microextration fibers: high partition coefficients and fluorescence microscopy images. *Anal Chem* **72**: 459-464 (2000).

129) Gobas FAPC, Mackay D. Dynamics of hydrophobic organic chemical bioconcentration in fish. *Environ Toxicol Chem* **6**: 495-504 (1987).

130) Veith GD, Comstock VM. Apparatus for continuously saturating water with hydrophobic organic chemicals. *J Fish Res Board Can* **32**: 1849-1851 (1975).

131) Górecki T, Pawliszyn J. Effect of sample volume on quantitative analysis by solid-phase microextraction. Part 1. Theoretical considerations. *Analyst* **122**: 1079-1086 (1997).

132) Górecki T, Khaled A, Pawliszyn J. The effect of sample volume on quantitative analysis by solid phase microextraction. Part 2. Experimental verification. *Analyst* **123**: 2819-2824 (1998).

133) Ai J. Solid phase microextraction for quantitative analysis in nonequilibrium situations. *Anal Chem* **69**: 1230-1236 (1997).

134) Resendes J, Shiu WY, Mackay D. Sensing the fugacity of hydrophobic organic chemicals in aqueous systems. *Environ Sci Technol* **26**: 2381-2387 (1992).

135) Quach ML, Chen XD, Stevenson RJ. Headspace sampling of whey protein concentrate solutions using solid-phase microextraction. *Food Res Int* **31**: 371-379 (1999).

136) Poon K-F, Lam PKS, Lam MHW. Determination of polychlorinated biphenyls in human blood serum by SPME. *Chemosphere* **39**: 905-912 (1999).

137) Jansen RAG, Van Leeuwen HP, Cleven RFMJ, Van den Hoop MAGT. Speciation and lability of Zinc(II) in river waters. *Environ Sci Technol* **32**: 3882-3886 (1998).

138) Arnold CG, Ciani A, Müller SR, Amirbahman A, Schwarzenbach RP. Association of triorganotin compounds with dissolved humic acids. *Environ Sci Technol* **32**: 2976-2983 (1998).

139) Duizer E, Penninks AH, Stenhuis WH, Groten JP. Comparison of permeability characteristics of the human colonic Caco-2 and rat small intestinal IEC-18 cell lines. *J Contr Rel* **49**: 39-49 (1997).

140) Delie F, Rubas W. A human colonic cell line sharing similarities with enterocytes as a model to examine oral absorption: advantages and limitations of the Caco-2 model. *Crit Rev Ther Drug Carrier Syst* **14**: 221-286 (1997).

141) Artursson P. Cell cultures as models for drug absorption across the intestinal mucosa. *Crit Rev Ther Drug Carrier Syst* **8**: 305-330 (1991).

142) Levin MS, Talkad VD, Gordon JI, Stenson WF. Trafficking of exogenous fatty acids within Caco-2 cells. *J Lipid Res* **33**: 9-19 (1992).

143) Chijiiwa K, Linscheer WG. Effect of intraluminal pH on cholesterol and oleic acid absorption from micellar solutions in the rat. *Am J Physiol* **246**: G492-G499 (1984).

144) Ruby MV, Schoof R, Brattin W, Goldade M, Post G, Harnois M, Mosby DE, Casteel SW, Berti W, Carpenter M, Edwards D, Cragin D, Chappell W. Advances in evaluating the oral bioavailability of inorganics in soil for use in human health risk assessment. *Environ Sci Technol* **33**: 3697-3705 (1999).

145) Rabinowitz MB, Kopple JD, Wetherill GW. Effect of food intake and fasting on gastrointestinal lead absorption in humans. *Am J Clin Nutr* **33**: 1784-1788 (1980).

146) Campbell PGC. Metal speciation and bioavailability in aquatic systems. Eds. Tessier A, Turner DR. John Wiley: Chichester, 1995.

147) van Leeuwen HP. Metal speciation dynamics and bioavailability: inert and labile complexes. *Environ Sci Technol* **33**: 3743-3748 (1999).

148) Altman PL, Dittmer DS. Metabolism. Federation of American Societies for Experimental Biology: Bethesda, Maryland, USA, 1968.

149) Alexander F. The concentration of electrolytes in the alimentary tract of the rabbit, guinea pig, dog and cat. *Res Vet Sci* **6**: 238-244 (1965).

150) Davidson W. Defining the electroanalytically measured species in a natural water sample. *J Electroanal Chem* **87**: 395-404 (1978).

151) van den Hoop MAGT, van Leeuwen HP. Stripping voltammetry of heavy-metal-(bio)polyelectrolyte complexes. Part 1. Influence of supporting electrolyte. *Analytical Chimica Acta* **273**: 275-287 (1993).

152) van den Hoop MAGT, Díaz-Cruz JM, van Leeuwen HP. Voltammetry of metal complexes with macromolecules. *Curr Top Electrochem* **3**: 77-91 (1994).

153) Ma YQ, Traina SJ, Logan TJ. In situ lead immobilization by apatite. *Environ Sci Technol* **27**: 1803-1810 (1993).

154) Zhang P, Ryan JA, Yang J. In vitro soil Pb solubility in the presence of hydroxyapatite. *Environ Sci Technol* **32**: 2763-2768 (1998).

155) Zhang P, Ryan JA. Transformation of Pb(II) from cerrusite to chloropyromorphite in the presence of hydroxyapatite under varying conditions of pH. *Environ Sci Technol* **33**: 625-630 (1999).

156) Harrison RM, Laxen DPH. Physicochemical speciation of lead in drinking water. *Nature* **286**: 791-793 (1980).

157) van den Hoop MAGT. Electrochemical metal speciation in natural and model polyelectrolyte systems. PhD thesis; Agricultural University of Wageningen: Wageningen, 1994.

158) Parveen Z, Edwards AC, Cresser MS. Redistribution of zinc from sewage sludge applied to a range of contrasting soils. *Sci Total Environ* **155**: 161-171 (1994).

159) Gasser UG, Walker WJ, Dahlgren RA, Borch RS, R.G. B. Lead release from smelter and mine waste impacted materials under simulated gastric conditions and relation to speciation. *Environ Sci Technol* **30**: 761-769 (1996).

160) Ruby MV, Davis A, Kempton JH, Drexler JW, Bergstrom PD. Lead bioavailability: dissolution kinetics under simulated gastric conditions. *Environ Sci Technol* **26**: 1242-1248 (1992).

161) Feroci G, Fini A, Fazio G. Interaction between dihydroxy bile salts and divalent heavy metal ions studied by polarography. *Anal Chem* **67**: 4077-4085 (1995).

162) Oomen AG, Sips AJAM, Tolls J, van den Hoop MAGT. Lead speciation in artificial human digestive fluid. (Provisionally accepted by *Environ Sci Technol*).

163) Duizer E, Gilde AJ, Versantvoort CHM, Groten JP. Effects of cadmium chloride on the paracellular barrier function of intestinal epithelial cell lines. *Toxicol Appl Pharmacol* **155**: 117-126 (1999).

164) Oomen AG, Tolls J, Kruidenier M, Bosgra S, Sips AJAM, Groten JP. Availability of polychlorinated biphenyls (PCBs) and lindane for uptake by intestinal Caco-2 cells. (Submitted).

165) Artursson P, Karlsson J. Correlation between oral drug absorption in humans and apparent drug permeability coefficients in human intestinal epithelial (Caco-2) cells. *Biochem Biophys Res Comm* **175**: 880-885 (1991).

166) Kakemi K, Sezaki H, Konishi R, Kimura T, Murakami M. Effect of bile salt on the gastrointestinal absorption of drugs. *Chem Pharm Bull* **18**: 275-280 (1970).

167) Quan Y, Hattori K, Lundborg E, Fujita T, Murakami M, Muranishi S, Yamamoto A. Effectiveness and toxicity screening of various absorption enhancers using Caco-2 cell monolayers. *Biol Pharm Bull* **21**: 615-620 (1998).

168) Nriagu JO. Lead orthophosphates-IV. Formation and stability in the environment. *Geochim Cosmochim Acta* **38**: 887-898 (1974).

169) Lebourg A, Sterckeman T, Ciesielski H, Proix N, Gomez A. Estimation of soil trace metal bioavailability using unbuffered salt solutions: degree of saturation of polluted soil extracts. *Environ Toxicol* **19**: 243-252 (1996).

170) Traina SJ, Laperche V. Contaminant bioavailability in soils, sediments, and aquatic environments. *Proc Natl Acad Sci USA* **96**: 3365-3371 (1999).

171) Hilburn ME, Coleman IPL, Blair JA. Factors influencing the transport of lead across the small intestine of the rat. *Environ Res* **23**: 301-308 (1980).

172) Davis A, Ruby MV, Goad P, Eberle S, Chryssoulis S. Mass balance on surface-bound, mineralogic, and total lead concentrations as related to industrial aggregate bioaccessibility. *Environ Sci Technol* **31**: 37-44 (1997).

173) Hamel SC, Buckley B, Lioy PJ. Bioaccessibility of metals in soils for different liquid to solid ratios in synthetic gastric fluid. *Environ Sci Technol* **32**: 358-362 (1998).

174) Artursson P, Borchardt RT. Intestinal drug absorption and metabolism in cell cultures: Caco-2 and beyond. *Pharm Res* **14**: 1655-1658 (1997).

175) Yazdanian M, Glynn SL, Wright JL, Hawi A. Correlating partitioning and Caco-2 cell permeability of structurally diverse small molecular weight compounds. *Pharm Res* **15**: 1490-1494 (1998).

176) Quaroni A, Hochman J. Development of intestinal cell culture models for drug transport and metabolism studies. *Advan Drug Delivery Rev* **22**: 3-52 (1996).

177) Barry PH, Diamond JM. Effects of Unstirred Layers on Membrane Phenomena. *Physiol Rev* **64**: 763-872 (1984).

178) Dulfer WJ, Govers HAJ, Groten JP. Kinetics and conductivity parameters of uptake and transport of polychlorinated biphenyls in the Caco-2 intestinal cell line model. *Environ Toxicol Chem* **17**: 493-501 (1998).

179) Ruby MV, Davis A, Schoof R, Eberle S, Sellstone CM. Estimation of lead and arsenic bioavailability using a physiologically based extraction test. *Environ Sci Technol* **30**: 422-430 (1996).

180) Benoit JM, Cilmour CC, Mason RP, Heyes A. Sulfide controls on mercury speciation and bioavailability to methylating bacteria in sediment pore waters. *Environ Sci Technol* **33**: 951-957 (1999).

181) Jonnalagadda SB, Rao PVVP. Toxicity, bioavailability and metal speciation. *Comp Biochem Physiol* **106C**: 585-595 (1993).

182) Ruby MV, Davis A, Link TE, Schoof R, Chaney RL, Freeman GB, Bergstrom P. Development of an in vitro screening test to evaluate the in vivo bioaccessibility of ingested mine-waste lead. *Environ Sci Technol* **27**: 2870-2877 (1993).

183) Dacre JC, Ter Haar GL. Lead levels in tissues from rats fed soils containing lead. *Arch Environ Contam Toxicol* **6**: 111-119 (1977).

184) Albro PW, Fishbein L. Intestinal absorption of polychlorinated biphenyls in rats. *Bull Environ Contam Toxicol* **8**: 26-31 (1972).

List of publications

1) Oomen, AG; Sips, AJAM; Groten, JP; Sijm, DTHM; Tolls, J. Mobilization of PCBs and lindane from soil during *in vitro* digestion and their distribution among bile salt micelles and proteins of human digestive fluid and the soil. *Environ Sci Technol* **34**: 297-303 (2000).

2) Oomen, AG; Mayer, P; Tolls, J. Nonequilibrium solid phase microextraction (SPME) of the freely dissolved concentration of hydrophobic organic compounds: matrix effects and limitations. *Anal Chem* **72**: 2802-2808 (2000).

3) Vaes, WHJ; Mayer, P; Oomen, AG; Hermens, JLM; Tolls, J. Comments on "Adsorption versus Absorption of Polychlorinated Biphenyls onto Solid-Phase Microextraction Coatings" (1998). *Anal Chem* **72**: 639-641 (2000).

4) Oomen, AG; Sips, AJAM; Tolls, J; van den Hoop, MAGT. Lead speciation in artificial human digestive fluid, provisionally accepted by *Environ Sci Technol*.

5) Oomen, AG; Tolls, J; Kruidenier, M; Bosgra, S; Sips, AJAM; Groten, JP. Availability of Polychlorinated biphenyls (PCBs) and lindane for uptake by *in vitro* intestinal Caco-2 cells, submitted.

6) Oomen, AG; Tolls, J; Sips, AJAM; Groten, JP. Lead uptake and transport by *in vitro* intestinal Caco-2 cells, submitted.

Nederlandse samenvatting - voor niet ingewijden

Blootstelling aan contaminanten kan gebeuren door het inslikken van verontreinigde grond. Grond kan samen met voedsel ingenomen worden. Daarnaast krijgen met name kinderen grond binnen d.m.v. hand-mond gedrag. Gronddeeltjes die aan vingers of andere voorwerpen zitten worden in de mond gestopt en de grond wordt vervolgens ingeslikt. Dit leidt tot een gemiddelde dagelijkse grondinname tussen de 50 en 200 mg. Naast dit normale gedrag vertonen sommige kinderen pica-gedrag, waarbij materie zoals grond wordt ingeslikt. Op deze manier kunnen vele grammen grond op een enkele dag worden ingenomen. Aangenomen wordt dat grondingestie een belangrijke blootstellingsroute is voor veel verontreinigingen in de grond. Kinderen zijn de risicogroep omdat zij over het algemeen meer grond binnen krijgen dan volwassenen, en omdat zij gevoeliger kunnen zijn voor contaminanten.

Contaminanten zijn veelal pas toxisch als ze de systemische circulatie, de bloedstroom, bereiken en daarmee op alle plekken van het lichaam kunnen komen. Daarom wordt de fractie van een ingeslikte contaminant die de systemische circulatie bereikt de biobeschikbare fractie genoemd. Voordat een contaminant in grond biobeschikbaar wordt moet het een aantal stappen doorlopen. Deze stappen zijn weergegeven in het volgende schema.

| grond ingestie | → | mobilisatie | → | absorptie | → | metabolisme en uitscheiding |
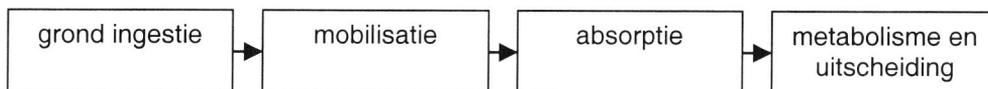
Ten eerste moet de grond worden ingeslikt. In het maagdarm-kanaal moeten vervolgens de contaminanten van de grond gemobiliseerd worden. De gemobiliseerde contaminanten kunnen daarna geabsorbeerd worden, d.w.z. getransporteerd over de darmwand. Absorptie vindt vrijwel uitsluitend plaats in de dunne darm. De contaminanten kunnen vervolgens in de darmen en lever gemetaboliseerd en weer uitgescheiden worden. Dat deel van de contaminant dat ingeslikt, gemobiliseerd, geabsorbeerd en *niet* gemetaboliseerd of uitgescheiden wordt, bereikt de systemische circulatie en is biobeschikbaar.

In het onderzoek dat is beschreven in dit proefschrift is gewerkt met twee verschillende typen contaminanten. Ten eerste, enkele hydrofobe, oftewel vetminnende, organische stoffen, gechloreerde bifenylen (PCBs) en lindaan, en ten tweede een zwaar metaal: lood. Lood en PCBs zijn stoffen die veel voorkomen in grond, en zij kunnen schadelijk kunnen zijn voor de gezondheid. Voor lindaan geldt dit ook, maar in mindere mate. Het is daarom van belang om nauwkeurig het niveau van contaminanten in de bodem te kunnen bepalen waarbij risico's voor de volksgezondheid op kunnen optreden, zodat hierop beleid gebaseerd kan worden.

De huidige Nederlandse interventiewaarden voor contaminanten zijn gebaseerd op toxiciteitsstudies waarbij de contaminant aan een proefdier wordt toegediend met voedsel of in een oplossing. Echter, toxiciteit kan beïnvloed worden door de matrix van ingestie. De biobeschikbaarheid kan bijvoorbeeld lager zijn als de contaminant wordt ingeslikt met grond i.p.v. met voedsel of in een oplossing, omdat bij voedsel in principe alle contaminanten worden gemobiliseerd en beschikbaar zijn voor absorptie. Ook de condities in het maagdarm-kanaal kunnen bepalend zijn voor de biobeschikbaarheid.

Het doel van dit proefschrift is inzicht krijgen in factoren die de biobeschikbaarheid bepalen van PCBs, lindaan en lood als ze met grond worden ingeslikt. Het onderzoek is primair gericht op de mobilisatie- en absorptiestap.

grond ingestie	→	mobilisatie	→	absorptie	→	metabolisme en uitscheiding
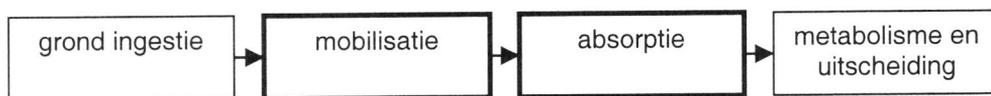
Mobilisatie van de contaminanten van standaardgrond, het zogenaamde OECD-medium, is bestudeerd met een *in vitro* digestiemodel dat het maagdarm-kanaal nabootst. Bovendien is bekeken in welke fysisch-chemische vormen de contaminanten voorkomen in het artificiele dunne darmsap, chyme genaamd. Dit is van belang omdat de speciatie van een stof, de verdeling van de stof over de fysisch-chemisch verschillende vormen, erg bepalend kan zijn voor de hoeveelheid stof die geabsorbeerd kan worden. In ieder geval kan de contaminant in vrij opgeloste vorm over de darmwand diffunderen. Intestinale absorptie is gesimuleerd m.b.v. *in vitro* Caco-2 darmcellen. Deze cellen groeien als een enkele laag op een filter en gedragen zich als humane darmcellen. De Caco-2 cellen zijn blootgesteld aan chyme-oplossingen, waarna is gemeten hoeveel contaminanten na verschillende blootstellingstijden in de cellen gaan zitten en over de cellaag getransporteerd worden.

Opbouw proefschrift

In het inleidende *Hoofdstuk 1* worden algemene aspecten van de contaminanten, de fysiologie van het maagdarm-kanaal en de verschillende stappen van biobeschikbaarheid behandeld. Het eerste deel van het proefschrift (*Hoofdstuk 2, 3* en *4*) betreft de PCBs en lindaan. Het tweede deel van het proefschrift (*Hoofdstuk 5* en *6*) betreft lood. In *Hoofdstuk 7* worden de resultaten in bredere zin besproken. Ook de verschillen en overeenkomsten tussen de PCBs, lindaan en lood, en implicaties voor risicobeoordeling worden bediscussiëerd.

Hieronder worden de experimentele resultaten en conclusies samengevat.

PCBs en lindaan

Hoofdstuk 2 beschrijft dat na *in vitro* digestie ongeveer 60% van de PCBs aan het OECD-medium is gesorbeerd. Ongeveer 25% is gesorbeerd aan micellen die worden gevormd door galzouten, en 15% aan eiwit. De respectivelijke percentages voor lindaan zijn 40%, 23% en 32%. Onder deze omstandigheden is dus een groot deel van de PCBs (60%) en lindaan (40%) niet gemobiliseerd, en dus niet beschikbaar voor absorptie, en zal dus niet biobeschikbaar worden. Als meer gal of eiwit wordt gebruikt tijdens de digestie stijgt het percentage contaminant dat van grond gemobiliseerd wordt. Het is daarom waarschijnlijk dat hydrofobe organische comtaminanten beter gemobiliseerd worden van de grond als de persoon in kwestie net heeft gegeten. Dan is namelijk veel gal, eiwit afkomstig van de digestie, en voedseldeeltjes aanwezig die de contaminanten kunnen sorberen.

Hoofdstuk 3 beschrijft het gebruik van de Solid Phase MicroExtraction (SPME) techniek om de PCBs en lindaan in een chyme-oplossing te analyseren. De hydrofobe stoffen concentreren zich in de SPME-fiber. De resultaten laten zien dat niet alleen contaminanten in de vrij opgeloste vorm bijdragen aan de flux naar de SPME-fiber, maar ook de gesorbeerde contaminantvormen, in ieder geval de contaminanten gesorbeerd aan eiwit, en mogelijk ook de fractie die gesorbeerd is aan de micellen. Het mechanisme van dit gedrag is dat waarschijnlijk de vrije contaminant concentratie in een waterlaagje rondom de SPME-fiber verlaagd wordt door de opname door de fiber. De gesorbeerde contaminanten kunnen dan dissociëren en de zo gevormde vrije stoffen kunnen ook in de SPME-fiber diffunderen. De netto flux naar de SPME-fiber bestaat dus uit vrije en gesorbeerde contaminanten, terwijl alleen vrije opgeloste contaminanten in de fiber coating diffunderen.

De vrije fractie van de PCBs en lindaan in chyme na een artificiele digestie met verontreinigd OECD-medium, geschat op basis van de SPME resultaten, is <1% en ±5%, respectievelijk.

In *Hoofdstuk 4* is intestinale absorptie van de PCBs en lindaan vanuit chyme onderzocht. Daartoe zijn monolagen van *in vitro* gedifferentieerde Caco-2 darmcellen blootgesteld aan oplossingen met gevarieerde concentraties chyme, gal en oliezuur. Binnen enkele uren was een evenwichtssituatie bereikt. Het grootste deel van de hydrofobe organische stoffen accumuleerde daarbij in de cellen, ondanks dat volgens *Hoofdstuk 2* en *3* slechts een klein deel van deze stoffen in chyme vrij opgelost was. Daarom kan worden geconcludeerd dat PCBs en lindaan gesorbeerd aan galzout micellen, eiwit en oliezuur hebben bijgedragen aan de contaminantaccumulatie in de Caco-2 cellen. Dit kan, vergelijkbaar met het mechanisme voor de SPME, verklaard worden door aanvulling van de vrije concentratie door dissociatie van de gesorbeerde vormen zodra de vrije concentratie daalt door opname door de cellen.

Lood

Hoofdstuk 5 beschrijft de mobilisatie en speciatie van lood na *in vitro* digestie van het OECD-medium. In aanwezigheid van gal tijdens de digestie werd ongeveer 23% van het lood gemobiliseerd, in afwezigheid ongeveer 11%. Er wordt waarschijnlijk meer lood uit grond gemobiliseerd bij een lage pH-waarde in de maag, d.w.z. als de persoon in kwestie lang niet heeft gegeten. Loodspeciatie in chyme is onderzocht met twee technieken. Ten eerste, de Ion Selectieve Electrode (ISE) waarmee de activiteit van het vrije metaalion (Pb^{2+}) gemeten wordt, en ten tweede, een voltammetrische techniek (DPASV) waarmee ook labiel, d.w.z. snel uitwisselbaar, lood gemeten wordt. De experimenten laten zien dat de fractie Pb^{2+} erg klein is, en loodfosfaat- en loodgal-complexen waarschijnlijk de belangrijke vormen zijn. De loodfosfaat-complexen zijn voltammetrisch labiel, d.w.z. ze kunnen dissociëren binnen de tijd van het voltammetrische experiment, binnen tienden van seconden. Hetzelfde geldt zeer waarschijnlijk voor de loodgal-complexen.

Intestinale absorptie van gemobiliseerd lood in een chyme-oplossing is onderzocht m.b.v. *in vitro* intestinale Caco-2 cellen en beschreven in *Hoofdstuk 6*. Ongeveer 27% van het lood accumuleerde in de cellen en 3% was over de cellaag getransporteerd na blootstelling van 24 uur. Het verloop in de tijd vertoonde geen tekenen van het bereiken van evenwicht. De loodflux over de monolaag kan geëxtrapoleerd worden naar *in vivo* loodabsorptie, en duidt op onvolledige loodabsorptie. Omdat de Pb^{2+} fractie verwaarloosbaar was (*Hoofdstuk 5*), moeten andere loodvormen hebben bijgedragen aan de loodflux naar de intestinale cellen. Een bijdrage aan de loodflux via pinocytose of via diffusie van hydrofobe loodcomplexen over het intestinale membraan is onwaarschijnlijk (*Hoofdstuk 6*). De hoge loodflux kan waarschijnlijk worden toegeschreven aan dissociatie van labiele loodcomplexen, waardoor vervolgens de geproduceerde Pb^{2+} ionen over het intestinale membraan kunnen diffunderen. De voltammetrisch labiele loodcomplexen zoals loodfosfaat en loodgal zijn hiervoor mogelijk verantwoordelijk.

Hydrofobe organische stoffen versus lood

Milieurelevante contaminantconcentraties, fysiologische componenten en tijden, en humane darmcellen zijn gebruikt bij de *in vitro* experimenten. Daarom vinden de processen, die bepalend zijn voor mobilisatie en absorptie van de contaminanten, waarschijnlijk ook plaats in een *in vivo* situatie. De *in vitro* resultaten moeten wel geëxtrapoleerd worden naar *in vivo* op basis van de blootstellingstijd en de capaciteit van het chyme en de cellen om contaminanten te binden en op te nemen.

Omdat een deel van de PCBs, lindaan en lood aan grond gebonden blijft tijdens de digestie, is ook *in vivo* een deel van de contaminanten waarschijnlijk niet beschikbaar voor absorptie. Dit in tegenstelling tot contaminanten die met voedsel worden ingeslikt, waar een volledige

mobilisatie wordt verwacht. Dit verschil in mobilisatie kan dus een aanzienlijk verschil veroorzaken tussen de biobeschikbaarheid van contaminanten die ingeslikt zijn met grond of met voedsel.

De experimenten met *in vitro* darmcellen laten zien dat *in vivo* waarschijnlijk alle gemobiliseerde PCBs en lindaan geabsorbeerd worden. Dit in tegenstelling tot lood, waar *in vivo* slechts een gedeeltelijke absorptie van het gemobiliseerde lood wordt verwacht. Dit veroorzaakt een verdere afname van de fractie lood dat biobeschikbaar wordt t.o.v. de ingeslikte hoeveelheid.

Een aanzienlijk deel van de contaminanten in grond blijkt biobeschikbaar te kunnen worden na ingestie, ondanks dat de contaminanten in grond minder biobeschikbaar zijn dan in voedsel of een oplossing. Daarom moet rekening worden gehouden met blootstelling aan contaminanten via grondingestie, met name voor kinderen. PCBs en lindaan, en hydrofobe organische stoffen in het algemeen, in grond zijn waarschijnlijk het meest biobeschikbaar als de grond wordt ingeslikt door iemand die net heeft gegeten. Lood in grond is daarentegen waarschijnlijk het meest biobeschikbaar als iemand lang niet heeft gegeten.

De vrije fracties van de PCBs, lindaan en lood in chyme waren klein. Desondanks accumuleerde een aanzienlijk deel in de darmcellen, en wordt een aanzienlijke *in vivo* absorptie verwacht. Van alle contaminanten hebben de gesorbeerde vormen waarschijnlijk bijgedragen aan de flux naar de darmcellen. De vrije concentratie blijft belangrijk, omdat het kan worden gezien als de drijvende kracht achter de flux naar de cellen. De labiele complexen kunnen worden gezien als de buffer van contaminanten die kunnen dissociëren en bijdragen aan de flux. De blootstellingstijd, en de capaciteit van de cellen om de contaminanten op te nemen, zijn bepalend voor de hoeveelheid labiele complexen die kunnen bijdragen aan de absorptie.

De SPME- en de DPASV-methoden vertonen gelijkenissen omdat met beide technieken de flux van de vrije en de snel uitwisselbare fractie kan worden gemeten. Daarom bieden deze technieken mogelijkheden om transport van stoffen in complexe media naar biologische systemen zoals Caco-2 cellen te onderzoeken.

Curriculum vitae

Ik, Agnes Guadalupe Oomen, ben geboren op 12 juni 1973 te Valles (SLP), Mexico. In 1991 behaalde ik het eindexamen VWO aan het Marnix college te Ede. In datzelfde jaar begon ik met de studie Moleculaire Wetenschappen aan de Landbouwuniversiteit Wageningen. Tijdens het eerste afstudeervak verrichtte ik onderzoek bij de vakgroep Fysische en Kolloïdchemie, onder begeleiding van Dr. Ir. Mieke Kleijn en Prof. Dr. Lyklema. Via Dr. Herman van Leeuwen van dezelfde vakgroep liep ik gedurende 4 maanden stage in Barcelona, Spanje, bij Dr. Miquel Esteban. Hier kwam ik voor het eerst in aanraking met metaalspeciatie en het begrip "biobeschikbaarheid". Daarna verrichtte ik onderzoek bij de vakgroep Toxicologie bij Ir. Juliette Legler en Prof. Dr. Koeman. De studie, met als oriëntatie milieuchemie, rondde ik af in het najaar van 1996. Aansluitend begon ik als promovenda, waarvoor ik het in dit proefschrift beschreven onderzoek uitvoerde. Het onderzoek werd gefinancieerd door het UTOX, een samenwerkingsverband tussen het Research Instituut voor Toxicologie (RITOX), TNO-Voeding en het Rijksinstituut voor Volksgezondheid en Milieu (RIVM). Begeleiding kwam van Dr. Adriënne Sips (Laboratorium voor blootstellingsonderzoek en milieu-epidemiologie (LBM), RIVM), Dr. Ir. John Groten (Afdeling verklarende toxicologie, TNO-Voeding) en Dr. Dick Sijm, wie later werd opgevolgd door Dr. Johannes Tolls (milieuchemie, RITOX), en prof. Dr. Willem Seinen (RITOX). Het onderzoek is verricht bij de drie betrokken instituten. In dezelfde periode nam ik deel aan diverse post-doctorale cursussen. Per december 2000 zal ik als onderzoeker werkzaam zijn bij het LBM van het RIVM.

Bedankt!

Ik begon vier jaar geleden met het onderzoek dat tot dit boekje heeft geleid. Ik vind dat zowel heel kort als heel lang geleden lijken, maar ik heb het vooral als een hele plezierige tijd ervaren. Ik wil iedereen bedanken die direct of indirect heeft bijgedragen aan het totstandkomen van het boekje. In het bijzonder wil ik noemen:

Mijn begeleiders

Tijdens mijn AIO-periode werd ik bijgestaan door een groot aantal begeleiders. Ieder heeft op zijn manier een belangrijke bijdrage geleverd aan het totstandkomen van dit boekje. Hoewel logistiek niet altijd even praktisch, ik heb ervan genoten om zowel bij RITOX, RIVM en TNO experimenten uit te voeren.

Dick, mede dankzij jou inspirerende begeleiding begon ik mijn promotie-onderzoek met het gevoel dat het allemaal wel goed zou komen.

Johannes, je nam de taak van Dick uitstekend over. Dank voor al je toewijding en inzet, voor de altijd open deur en het razend snel nakijken van de vele manuscripten.

Adrienne, bedankt voor je steun en interesse, het zorgvuldig doorlezen van de manuscripten, en voor de mogelijkheden om experimenten uit te (laten) voeren op het RIVM.

John, bedankt voor je enthousiasme. Na afloop van een gesprek met jou realiseerde ik me altijd veel beter met wat voor leuk onderzoek we bezig waren.

Willem, ik heb je pas op het einde beter leren kennen, maar ik heb je positieve houding erg gewaardeerd.

Marc, al was je geen directe begeleider, je stond altijd open voor vragen en discussie over loodspeciatie (en andere onderwerpen). Ik vond het erg leuk om met je samen te werken.

Op en rond de verschillende labs

Alle (ex)collega's van milieuchemie en -tox: bedankt voor de goede sfeer in het Kruyt en aan de overkant (dat later ook onze kant werd). Ik heb vele goede herinneringen aan de woensdagse taart, de jaarlijkse BBQ's en Kerstdiners, de regelmatige borrels. Werk en prive liepen vaak in elkaar over, waardoor goede vriendschappen zijn ontstaan. Bedankt: Andreas, voor de geweldige squashuurtjes. Femke, altijd gezellig als je er was. Gert-Jan, al weer lang vertrokken, maar gelukkig zie ik je nog regelmatig op feesten en congressen. Martine, ik vond het heel leuk om je goed te leren kennen (laten we dat zo houden). Ik kon altijd bij je terecht als er wat was, en ik vind het heel fijn dat je mijn paranimf bent. Philipp, ik je erg leren waarderen toen wij samen op een kamer werkte, we hebben heel wat bediscussieerd, en niet alleen over werk. Rik, jou opmerkingen hebben mij soms aangezet tot nadenken over zaken waar ik anders zomaar overheen zou stappen. Maar niet te vergeten: Else, Eñaut, Eric,

Frans, Hans-Christiaan, Heather, Ingrid, Joop, Judith, Karin, Leon, Manuela, Minne, Theo en Wouter. De overige Ritoxers wil ik bedanken voor de goede sfeer.

Verder zijn een aantal mensen in het Kruytgebouw belangrijk geweest voor een goede gang van zaken: Cor en Ton voor lab- en kantoorspulletjes. Ed & Gerard voor het regelmatig lospeuteren van het stopje in de luchtbrug (zie Figuur 2, Hoofdstuk 3), en voor het vele lenen van gereedschap. Femke en Frouke en de overige mensen van de afdeling Beeldverwerking & Vormgeving voor de mooie figuren, posters en omslag. Kees voor het squashen en het daarmee enigszins bouwen van een brug tussen de twee groepen (jammer dat we toen gingen verhuizen). En de mensen van de dierverzorging, bedankt voor het altijd vriendelijk groeten, ook in de weekenden.

Ook de LBM-groep van het RIVM wil ik bedanken. Ik kwam altijd met een goed gevoel langs, al werd ik regelmatig begroet met het Casperiaanse "Wat doe *jij* hier?". Erwin, Casper, Machteld en Diana, bedankt voor de hulp met het draaien van digesties en voor de altijd snelle reactie op mijn vragen om een andere datum, proefopzet e.d..

De afdeling Verklarende Toxicologie bij TNO-voeding: bedankt! Bij jullie was het altijd gezellig als ik weer een paar dagen kwam experimenteren. Nicole en Rob, bedankt voor de goede zorgen voor de celletjes en de hulp bij mijn zoektochten door het lab naar al dingetjes die ik nodig had voor de experimenten.

Mijn studenten, Jota, John, Maaike en Sieto, ik vond het leuk om jullie te begeleiden. Bovendien hebben jullie, met al dat labwerk, een belangrijke bijdrage geleverd aan dit proefschrift. Bedankt!

Thuis

De vele etentjes, goede gesprekken, wandelingen, fietstochten, feesten en nog veel meer met vrienden en vriendinnen zijn altijd erg belangrijk voor mij geweest. Eén iemand wil ik graag persoonlijk noemen: Denise, ik weet zeker dat jou boekje over een paar jaar ook af is.

Ik wil mijn familie en die van Antoine bedanken voor hun interesse in mij en in mijn onderzoek.

Opa, ik vind het heel bijzonder dat u één van mijn paranimfen bent.

Pieter & Françoise, dank voor jullie vertrouwen en onvoorwaardelijke steun. Françoise, ook bedankt voor het lezen van de Nederlandse samenvatting. Clasien en Gijsbert, jullie zijn al lang niet meer mijn kleine zusje en broertje, en dat is wel zo leuk. Clasien, ik ga helaas nog verder van het Kruyt werken, maar wie weet kunnen we nog regelmatig op het RIVM lunchen.

Antoine, je heerlijke relativerende houding, je mooie verhalen en plezier over alledaagse dingen, en je altijd aanwezige steun hebben mij veel goed gedaan. Bedankt!